PB 189 495

FLUID BED STUDIES OF THE LIMESTONE BASED FLUE GAS DESULFURIZATION PROCESS

Alvin Skopp, et al

Esso Research and Engineering Company
Linden, New Jersey

27 August 1969

Distributed ... 'to foster, serve and promote the nation's economic development and technological advancement.'

CLEARINGHOUSE
FOR FEDERAL SCIENTIFIC AND TECHNICAL INFORMATION

U.S. DEPARTMENT OF COMMERCE/National Bureau of Standards

This document has been approved for public release and sale.

PB189495

FLUID BED STUDIES OF THE LIMESTONE BASED FLUE GAS DESULFURIZATION PROCESS

BY

A. SKOPP
J.T. SEARS
R.R. BERTRAND

FINAL REPORT

MAY 15, 1967 - AUGUST 27, 1969

Prepared under Contract No. PH 86-67-130 for

National Air Pollution Control Administration
Division of Process Control Engineering

ESSO RESEARCH AND ENGINEERING COMPANY
Government Research Division
Linden, New Jersey

GR-9-FGS-69

Reproduced by the
CLEARINGHOUSE
for Federal Scientific & Technical
Information Springfield Va. 22151

119

BLANK PAGE

FOREWORD

This report describes studies carried out by the Esso Research and Engineering Company for the National Air Pollution Control Administration under Contract No. PH 86-67-130. The studies examined the feasibility of desulfurizing flue gas in a fluidized bed with limestone materials, both when discarding the sorbent and when regenerating the sulfated stones and reusing the material in a cyclic process. The work was performed over the period May 15, 1967 to August 27, 1969 at the Esso Research Center in Linden, New Jersey. Mr. Allen Potter was the contract monitor for the National Air Pollution Control Administration.

The authors wish to express their appreciation to Thomas Coughlin and Henry Silakowski for performing the laboratory experiments. We would like to thank Dr. A. C. Frost for his work during the initial phases of the program.

TABLE OF CONTENTS

Page

FOREWORD i

1. SUMMARY 1

2. INTRODUCTION 5

3. DESULFURIZATION WITH LIMESTONE AND DOLOMITES 6

  3.1. Apparatus 6

    3.1.1. Gas Manifold System 6
    3.1.2. Fluid Bed and Fines Recovery System 6
    3.1.3. SO_2 Detection System 6

  3.2. Experimental Procedures 9

  3.3. Data Analysis 10

  3.4. Measured Fluid Bed Reactivity of Coarse Sorbents 12

4. IMPROVING SORBENT UTILIZATION 19

  4.1. Effect of Bed Attrition on Sorbent Utilization 19

  4.2. Effect of Physical and Chemical Modifications on Sorbent Reactivity 23

    4.2.1. Effect of Calcining Conditions on Oxide Utilization 23
    4.2.2. Reactivity of the Hydroxide 27
    4.2.3. Studies with Uncalcined Limestones and Half Calcined Dolomites 28
    4.2.4. Reactivity of Metal-Oxide Modified Stones 31
      4.2.4.1. Metal Oxide Modification of N-1359 Lime 31
      4.2.4.2. Copper Oxide Doped, Half-Calcined Dolomite 32

  4.3. Reactivity and Use of Finely Sized Sorbent 33

    4.3.1. Small Particle Reactivity 33
    4.3.2. Residence Time Required for Small Particles in Fluid Bed Result in Uneconomical Design 34

  4.4. Miscellaneous Studies of Coarse Sorbent Fluid Bed Desulfurization 36

    4.4.1. Sorbent Attrition Rate 36
    4.4.2. Calcination in a Continuously Operated Bed 37
    4.4.3. Effect of Fly-Ash 38

TABLE OF CONTENTS (Cont'd)

Page

5. REGENERATION STUDIES 39
    - 5.1. Thermodynamic Considerations in Sorbent Regeneration 39
    - 5.2. Experimental Apparatus 42
    - 5.3. Experimental Procedures 45
    - 5.4. Regeneration-Definition Studies 45
        - 5.4.1. Reduction of $CaSO_4$ 45
        - 5.4.2. Sorbent Reactivity After First Reduction 49
        - 5.4.3. Agglomeration 50
            - 5.4.3.1. Fly Ash Effects 50
            - 5.4.3.2. Self-Agglomeration Without Fly-Ash 50
        - 5.4.4. Possible Sulfite Formation and Thermal Regeneration 51
    - 5.5. Cyclic Performance 51
        - 5.5.1. Reactivity of Cycled Sorbents 51
        - 5.5.2. Reduction Efficiency of Cycled Sorbents 53
        - 5.5.3. Attrition of Cycled Sorbents 55

6. PROCESS DESIGN CONSIDERATIONS 58
    - 6.1. Desulfurizer: Conventional Power Plant 58
        - 6.1.1. Sizing Reactor 58
        - 6.1.2. Sizing: Limestone Particles 59
        - 6.1.3. Fluidization Requirements 60
        - 6.1.4. Sorbent Selection 61
    - 6.2. Regenerator 62
        - 6.2.1. By-Product Processing 62
    - 6.3. Schematic Design: Conventional Power Plant 62
    - 6.4. Future Process Variation: Fluidized Bed Combustion 64
    - 6.5. Possible Process Innovations: Sulfur Production 65

7. ECONOMICS OF FLUID BED LIMESTONE DESULFURIZATION 66
    - 7.1. Basis for Cost Estimates 66
    - 7.2. Process Installation in Existing Power Plant 67
    - 7.3. Future Conventional Power-Plant Process Installation 68
        - 7.3.1. Single Pass Desulfurization - 200 MW Plant 68
        - 7.3.2. The Regenerative Process - 200 MW Plant 70

TABLE OF CONTENTS (Cont'd)

Page

7.3.3. The Regenerative Process - 1000 MW Plant 73

7.4. Direct Injection - 200 MW Plant 77

7.5. Regenerative Desulfurization in a Fluidized-Bed-Combustion, 1000 MW Plant 78

7.6. Economics Summary 79

8. STATUS AND RECOMMENDATIONS 81

8.1. Present Status 81

8.2. Technical Problem Areas 81

8.3. Other Process Considerations 82

8.4. Commercialization Lead Time 83

8.5. Recommendations 83

NOMENCLATURE 84

REFERENCES 85

APPENDICES 87

I. DESULFURIZATION KINETICS, BASIC DATA 88

II. REDUCTIVE REGENERATION BASIC DATA 91

III. ERROR ANALYSIS - DESULFURIZATION TO $CaSO_4$ FORMATION 94

IV. EQUILIBRIUM PREDICTIONS OF POSSIBLE REACTIONS IN DESULFURIZATION 96

V. GIBBS FREE ENERGY OF FORMATION OF RELEVANT SPECIES 104

VI. RESIDENCE TIME AVERAGING FOR THE EFFECTIVE RATE CONSTANT IN A FLUIDIZED BED 105

VII. ECONOMIC EVALUATION FOR A ONCE-THROUGH FLUID BED LIMESTONE DESULFURIZATION PROCESS USING SMALL PARTICLES 109

VIII. FLUIDIZED BED REGENERATIVE DESULFURIZATION PROCESS DETAILS 111

1. SUMMARY

A study has been completed to determine the technical and economic potential of removing sulfur dioxide from the flue gas of fossil fuel-burning power plants by using inexpensive limestones or dolomites as SO_2 sorbents in a fluid bed. The fluid bed desulfurization process involves the reaction of SO_2 with CaO and oxygen at about 1600°F.

$$CaO + SO_2 + 1/2\ O_2 \longrightarrow CaSO_4$$

Initial experiments were made to define the kinetics of the above reaction with precalcined sorbent. Five different limestones and dolomites were studied in an externally heated, 3" diameter, fluid bed reactor using a simulated flue gas. The data obtained showed that the fluid bed reactivity depended on the sorbent used and on the degree of sorbent utilization. For example, the rate constant determined for the above reaction at 1600°F for 2.8 mm diameter particles of a high CaO limestone was found to drop from about 3000 min^{-1} to 700 min^{-1} as the CaO utilization changed from 5 to 20%. Over this same range of CaO utilization, the reactivity of a calcite dolomite that was investigated varied from 7000 min^{-1} to 3000 min^{-1}. These rapid declines in reactivity are due to the formation of $CaSO_4$ product shells which reduce the diffusivity of SO_2 and O_2 into the interior of the particles.

The rate of the desulfurization reaction is important in determining efficiency of desulfurization and sorbent utilization. Thus, for the limestone cited above, with a nominal gas-solids contact time of 0.1 sec., 100% SO_2 removal will occur with fresh limestone while a maximum removal of only 48% will be achieved when the stone is 25% reacted.

In an attempt to improve the fluid bed reaction rates, a number of sorbent and process modifications were investigated. These consisted of:

- Trying to remove the surface sulfate shell by operating the fluid bed under particle-attriting conditions.
- Modifying the physical and chemical form of the sorbents
- Using finely sized sorbents
- Regenerating the sorbent by reducing the $CaSO_4$ to CaO.

Both an increase in bed height and in fluidizing velocity were found to increase the amount of particle attrition in the fluid bed. The dolomite tested attrited more readily than the limestone which was investigated but in neither case was the attrition selective to the surface sulfates, nor was it able to give increased sorbent utilization.

Improving the calcination, using hydrated lime, using half-calcined dolomites, and doping the sorbents with catalytic metal oxides were all investigated as ways of increasing the reactivity. Pressure induced calcinations, carried out at temperatures where the equilibrium dissociation pressure of the limestone was greater than atmospheric pressure, gave some improvement in sorbent reactivity over that obtained with diffusion controlled calcination where the equilibrium dissociation pressure was less than atmospheric. However, the small improvement was not judged to merit any special calcining procedure. Hydration of lime gave very small particles which were no more reactive than similarly sized particles of calcined limestone. Metal oxide-doped stones and half-calcined dolomites also gave no improvement in reactivity.

An increase in sorbent reactivity was found with decreasing particle size but reasonably long fluid bed residence times were still required to give good sorbent utilization. Thus, for example, it was estimated that 60μ particles of one of the limestones which was studied would have to spend an average of about 40 minutes in the reaction zone to provide 90% flue gas desulfurization with stoichiometric addition rates of the stone. The high-recycle, transfer-line reactor system needed for such an operation would result in desulfurization costs estimated to be above $2.20/ton coal. The concept of operating a "hetero-reactor system" in which recycle requirements are reduced by using a bed of coarse particles to prevent rapid entrainment of the much finer reactive particles, was found to offer little or no advantage to the use of coarse particles alone.

Reductive regeneration of coarse sulfated sorbents was felt to offer the potential of both decreasing sorbent requirements and producing a concentrated SO_2 stream with by-product value. As a first step in studying the regenerative fluid bed desulfurization process, the equilibrium relationships involved in the reduction of $CaSO_4$ to CaO and SO_2 were analyzed to define conditions for the reduction. Temperatures above 1900°F were found to be needed to reduce $CaSO_4$ and produce an effluent gas containing SO_2. With CO or H_2 as reductant, the reduction reaction is:

$$CaSO_4 + CO(H_2) \xrightarrow{\Delta} CaO + CO_2(H_2O) + SO_2$$

Under highly reducing conditions, considerable CaS is formed instead of CaO. Experimentally, a 2:1 ratio of CO_2/CO was chosen to keep sulfide formation in the particles at 1-2%.

Using an externally-heated, 2-1/2" ID ceramic fluidized-bed reactor, a gas containing 10% CO or H_2 was found to reduce $CaSO_4$ at 2000°F to yield an effluent containing nearly 9% SO_2, the reaction apparently proceeding to equilibrium. The oxide produced was capable of reacting with SO_2. Cycling of stones between desulfurization and reductive regeneration demonstrated continued reactivity for SO_2 by regenerated particles. Continued exposure to high temperature caused a decrease in reactivity, presumably due to porosity loss. However, desulfurization activity was maintained at or above initial levels for 10 cycles lasting about 110 hours with a calcined limestone. A nine percent

SO_2 effluent from the regenerator was produced in each of these regeneration cycles. The limestone had a very low breakdown-elutriation rate, less than 0.025%/hr at 2 ft/sec. fluidizing velocity.

Although fly ash (from the combustion of coal) was found to have no effect on the adsorption, data obtained at the higher temperature corresponding to regeneration showed that the hot fly ash could cause agglomeration of sorbent particles. Self-agglomeration of the sulfated lime particles was also found to be possible at regeneration temperatures.

The data obtained in this program provided the basis for the conceptual design of once-through and regenerative fluid bed desulfurization processes for use in conventional power plants. Both the once-through and regenerative processes would use a coarse limestone fluid bed reactor operating at about 1600°F. A temperature near 1600°F is needed to obtain sufficient reaction rates and this means locating the desulfurization reactor somewhere in the superheater region of a modified boiler. Current fluid bed technology and process design limits desulfurization reactor diameter to about 50 feet. For a 200 MW plant, one such reactor would be required while larger power plants would use multiple reactors of this size.

Using 1100 to 5000μ limestone particles, the once-through design calls for a 24" deep settled bed operating at a superficial velocity of 15 ft/sec. Assuming ideal gas-solids contacting, 87% gas desulfurization is calculated with three times stoichiometric sorbent addition rates. The make-up sorbent could be uncalcined limestone since experiments have shown it to calcine rapidly in the 1600°F fluid bed.

The regenerative design assumes the same sized sorbent and superficial velocity with a settled bed depth of 15". Ninety percent flue gas desulfurization is calculated at a sorbent makeup rate equivalent to one-third that required for stoichiometric reaction with the SO_2 in the flue gas. The regenerator would be relatively small with a cross-sectional area about 1/30 that of the desulfurizer. Partial combustion of fuel would provide the high temperature gas needed to reduce the sulfated sorbent and maintain the regenerator temperature at about 2000°F. The expected effluent stream of 9% SO_2 could be prepared for use in a contact sulfuric acid plant or could be reduced further to yield sulfur.

Both the once-through and the regenerative designs are based on extrapolation of the activity data obtained on a low activity limestone (i.e., the lowest activity of the five sorbents evaluated in this program). Therefore, these designs are felt to be conservative with respect to most other potential sorbents.

Economic evaluations, based on the above design consideration, predicts the costs shown on the next page. A positive feature of these processes is that the costs are relatively insensitive to the price of the sorbent assumed in this study, i.e., $2.05/ton.

Estimated Costs of Limestone Fluidized Bed Desulfurization Processes

Process	Plant Size MW	Plant Investment	Operating Costs, $/Ton Coal Burned @ 90% Plant Load Factor	60% Plant Load Factor
Once-Through Limestone Process	200	$3,030,000	2.35	3.18
Regenerative Limestone Process	200	$4,585,000	1.02	2.01
	1000	$16,950,000	.44	1.14

The predicted costs for the regenerative process compare favorably with those of other proposed desulfurization techniques when applied to new pulverized coal boilers. The cost and time involved in modifying existing boilers to accomodate a fluid bed desulfurizer, however, rules out its use in such equipment.

Technical problems, such as gas solids contacting, passage of fly-ash through the fluid bed grid, and agglomeration in the regenerator remain to be investigated. Poor contacting in the adsorbing bed would lead to lower than predicted gas desulfurization. In the designs used for the economic evaluations, a grid containing many small gas inlet holes was assumed in order to limit gas bubble size and provide good contacting. With such a design, it would have to be demonstrated that fly ash would not compact and clog the grid. In the regenerator, poor contacting could result from agglomeration of fly-ash and sorbent. This could give incomplete regeneration, lower than predicted SO_2 concentrations, and less efficient use of reductant. If these problems cannot be avoided by changes in regenerator design or operating conditions, then it would be necessary to use a gas or liquid fuel to supply the reducing gas. This would not have much effect on process economics since the fuel requirements for sorbent regeneration are only about 3 or 4% those of the power plant boiler.

The major effort in this study was devoted to the application of fluidized bed desulfurization in conventional power plant boilers. However, limited consideration was also given to its application in fluidized bed combustion (FBC) boilers. In FBC, the fuel would be burned in a fluidized bed of solids which contained a part or all of the steam raising surface. These solids could then be limestone for an in situ desulfurization system. As coal is burned above the grid in FBC boilers, the problem of passing fly ash through a grid encountered with the conventional boiler is eliminated. Achieving good gas-solid contacting would be much easier as gas velocities are expected to be much lower in an FBC plant.

Fluid bed combustion itself is still only in the research stage. Nevertheless, desulfurization in an FBC system employing sorbent regeneration appears potentially attractive from both a technical and economic standpoint. It is therefore recommended that future development of limestone-based fluid bed desulfurization be directed at adapting the process to fluidized bed combustion schemes.

2. INTRODUCTION

Among the many proposed processes being investigated to remove SO_2 from power plant flue gas, the direct injection of pulverized limestone or dolomite into the boiler has the advantage of low initial capital cost and moderate operating cost because of the use of inexpensive reactants. The use of powdered limestone and dolomite as reactants to reduce the sulfur dioxide content in flue gases is based on the reaction of SO_2 with the CaO formed on calcination of the raw stone. Unless coupled with a wet scrubbing system, direct injection of limestone does not achieve high desulfurization efficiency or high sorbent utilization.

As part of the National Air Pollution Control Administration's program to investigate the use of limestone and dolomites for flue gas desulfurization, Esso Research and Engineering Company was granted a contract to study the feasibility of using limestone and dolomite sorbents in a fluid bed reactor system. The commercial application of such a fluid bed desulfurization process would involve delivering the hot flue gases (1600°F) to a separate reactor and subsequently returning them to the boiler. The advantages of this process appear to reside in the potential for good sorbent utilization, high desulfurization efficiencies, easy continuous material handling, and the possibility for cyclic use of the sorbent.

3. DESULFURIZATION WITH LIMESTONES AND DOLOMITES

3.1. Apparatus

The high temperature fluidized bed unit built for the limestone desulfurization studies described in this report is shown in Figures 1 & 2. The unit consists of three major components, a gas manifold system for blending a simulated flue gas, a high temperature fluid bed and fines recovery system, and an infrared analyzer for monitoring the SO_2 content of the effluent gas.

3.1.1. Gas Manifold System

The simulated flue gas used in these studies was formed in three blending steps. N_2, CO_2, and air were first mixed at room temperature in a common carrier line. This mixture was then heated to over 200°F and injected with steam in a 300-350°F furnace. Transport lines heated to above 150°F prevented water vapor from condensing out as the N_2-CO_2-air-H_2O mixture proceeded either directly to a 25 foot long preheat coil below the fluid bed, or to the by-pass stream used for calibration of the SO_2 detector. SO_3 formation was minimized by the addition of SO_2 to the mixture just before it left the preheat coils and entered the fluid bed.

3.1.2. Fluid Bed and Fines Recovery System

The inlet gas leaving the 25-foot preheat coil entered the 3" I.D. 5-foot long Incoloy 800 fluid bed reactor through a 100μ opening screen placed over a plate perforated with 3/32" diameter holes spaced 1/4" apart. A 3/8" I.D. sample withdrawal port and a thermocouple well extended down from the grid through the interior of the preheat coil windings. The fluid bed reactor and the preheat coil were heated by a 6-foot long, 18 KW furnace manufactured by Electro Applications Incorporated, Houston, Pa.

The top of the reactor was coupled to an insulated, 7" I.D., 18" high expanded section which returned high climbing slugs of particles to the fluid bed. The gases leaving the bed passed through a heated line at 400°F into a glass cyclone separator, then to a porous stainless steel filter to remove the entrained fines. The cyclone filter-system was located in a small oven kept at 400°F to prevent possible sulfuric acid condensation.

3.1.3. SO_2 Detection System

The gases leaving the cyclone-filter unit passed through an air-cooled condensing coil and a water-cooled condenser. The condensed water was then separated from the gas stream in a cyclone separator. Most of the gases then proceeded directly to the vent. However, up to 2 CFM was side-tracked to a refrigerating unit which lowered the gas temperature to 35°F and condensed out more water. This minimized interference from H_2O absorption in the SO_2 IR analyzer.

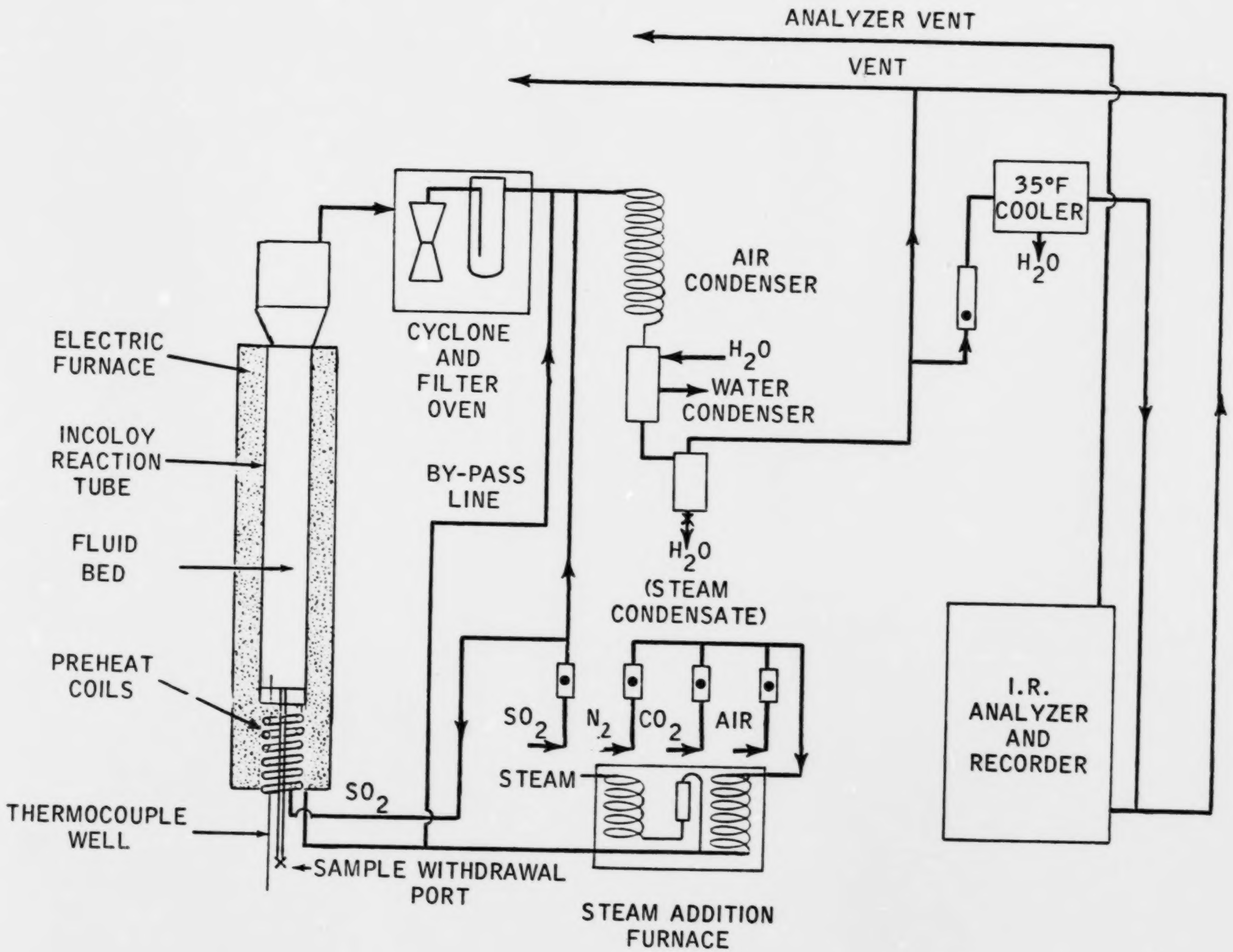
ANALYZER VENT
VENT
35°F COOLER
H_2O
AIR CONDENSER
H_2O
WATER CONDENSER
ELECTRIC FURNACE
CYCLONE AND FILTER OVEN
INCOLOY REACTION TUBE
BY-PASS LINE
FLUID BED
H_2O
(STEAM CONDENSATE)
I.R. ANALYZER AND RECORDER
PREHEAT COILS
SO_2
N_2
CO_2
AIR
STEAM
SO_2
THERMOCOUPLE WELL
SAMPLE WITHDRAWAL PORT
STEAM ADDITION FURNACE

Figure 1

Flow Diagram for the High Temperature Fluid Bed Desulfurization Unit

Figure 2

High Temperature Fluid Bed Desulfurization Unit

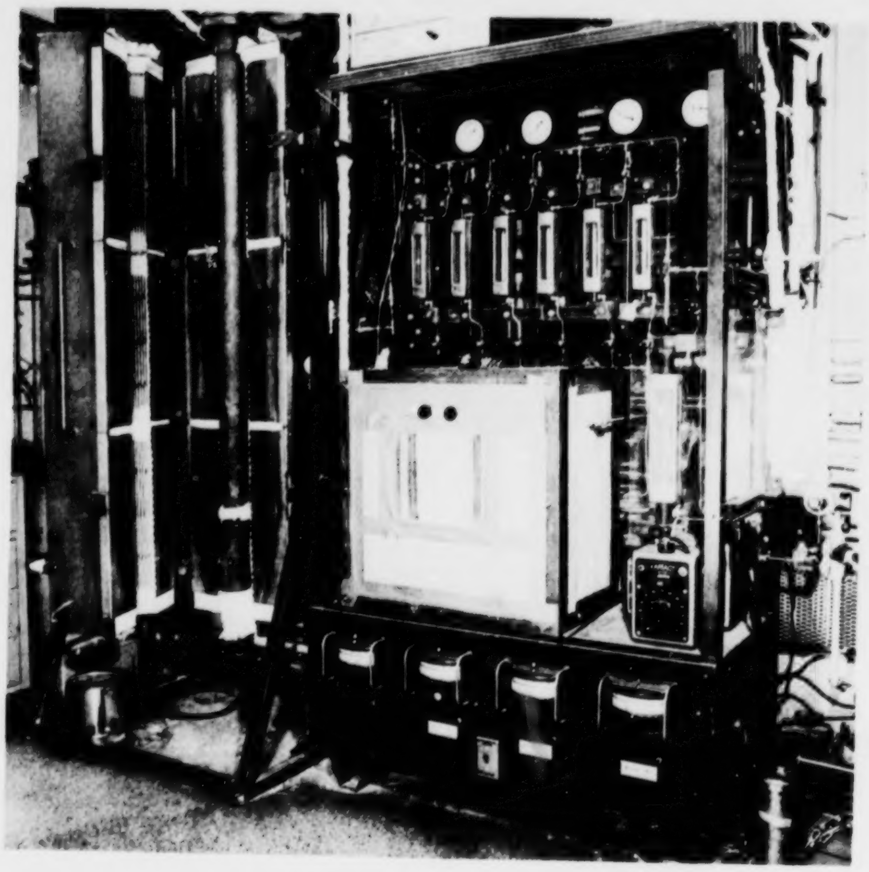

A Beckman I.R. analyzer model #IR315, used for determining the SO_2 content of the effluent gas, was calibrated before and after each run by passing the simulated flue gas through the by-pass line going directly from the steam addition box to the condensing coils. This arrangement gave a calibration curve which was not only quick and easy to prepare, but representative of the actual gases being used in the experimental work. It took into account the solubility and consequential removal of SO_2 and CO_2 in any water condensed out of the gas, as well as the interference of H_2O and CO_2 in the I.R. analyzer.

3.2. Experimental Procedures

The experiments were made by charging the reactor with a known amount of adsorbent, fluidizing the adsorbent with nitrogen while heating it to the desired temperature, and then introducing other gases to produce a simulated flue gas. The simulated flue gas used for most of the experimental program had a composition corresponding to about that obtained from combusting a heavy fuel oil containing 4% sulfur with 5% excess air.

Table I

Simulated Flue Gas Composition

Gas	Constituent Mole %
N_2	74.73
CO_2	14.00
H_2O	10.00
O_2	1.00
SO_2	0.27

Six different stone types were investigated in this program, a dolomite (N-1337), a calcite dolomite (N-1351), a limestone (N-1359), a dolomitic limestone (N-1360), an algal limestone (N-1363), and a ferrous limestone (N-1343), with primary emphasis given to the N-1337 and N-1359 stones.

Table 2

Descriptions of Limestones and Dolomites Investigated

Designation	Quarry Source	Type Stone (1)	Weight Percent, Calcined (2)				
			CaO	MgO	SiO_2	Fe_2O_3	Al_2O_3
N-1337	Chas Pfizer Co. (Gibsonburg, O.)	Dolomite	54	44	0.92	0.33	0.15
N-1343	Hopper Bros. Quarries (Ashland, Neb.)	Fossili, ferrous limestone	94	.85	2.98	0.66	0.73
N-1351	Jeffery Limestone Co. (Parma, Mich.)	Calcite dolomite	54	28.5	8.2	7.0	1.55
N-1359	Grove Lime Co. (Stephen City, Va.)	Limestone	97	1.16	1.07	0.22	0.29
N-1360	Monmouth Stone Co. (Monmouth, Ill.)	Dolomite, limestone	81	13.0	3.65	1.25	0.27
N-1363	Casey Stone Co. (Casey, Ill.)	Algal	66	1.42	21.0	2.50	6.60

3.3. Data Analysis

Figure 3 shows the type of SO_2 adsorption data that were obtained in the program. Conversion of CaO to $CaSO_4$ (i.e., sorbent utilization) was calculated by integrating the area between the SO_2 breakthrough curve and the feed concentration line to obtain the amount of SO_2 adsorbed. The difference in weight of the batch of particles before and after a run provided an independent check on the total utilization of limestone. On the average, the chart records gave a calculated $CaSO_4$ formation 3.2% (±1.7% at 95% confidence limits) greater than the actual weight gain for the sorbent (see Appendix III). This is well within possible errors from rotameter calibrations or decreased weight gain from possible disproportionation of adsorbed $CaO-SO_2$ into CaS and $CaSO_4$.

Figure 3

Typical SO_2 Adsorption-Breakthrough Curve

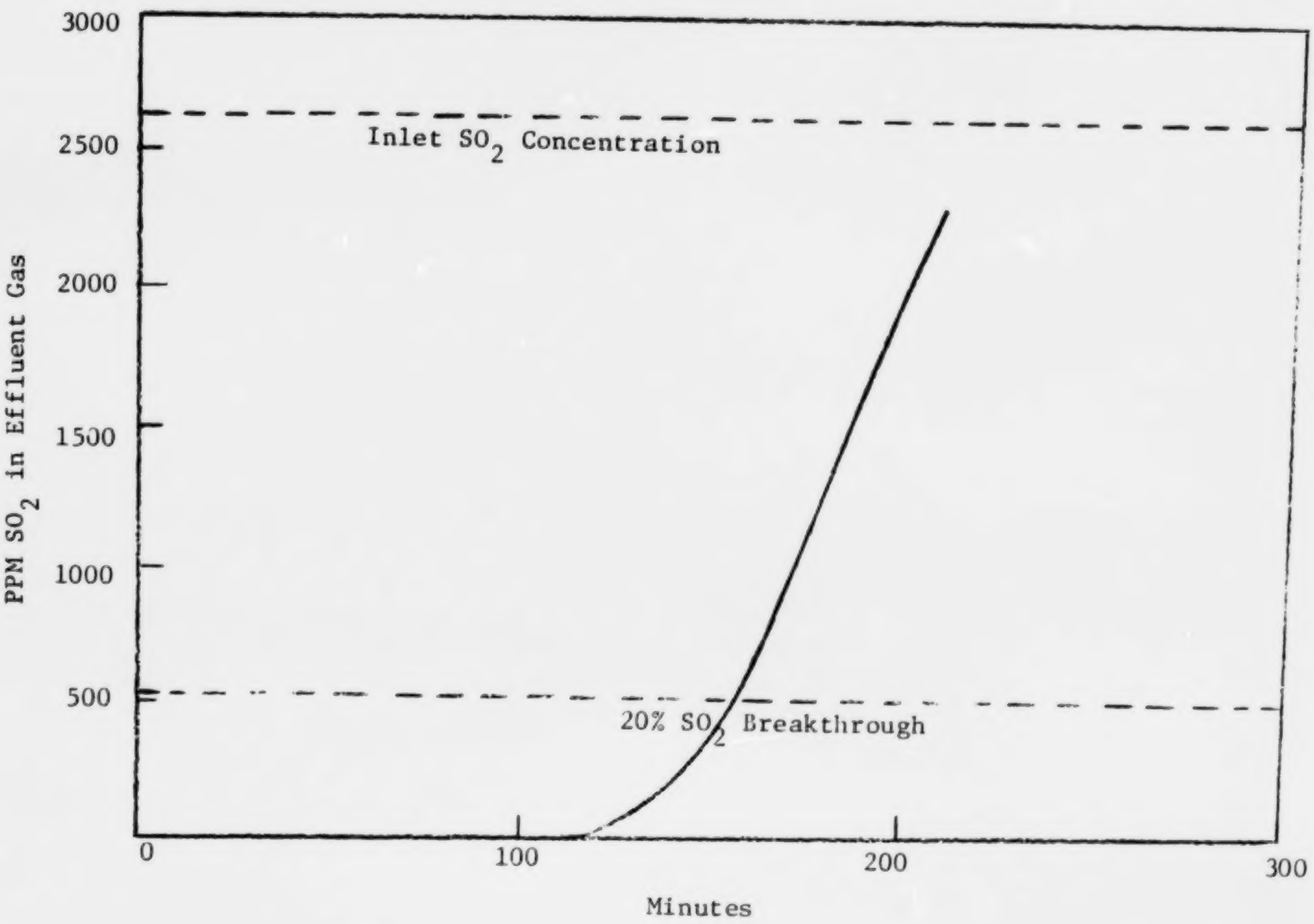

The sorbent utilization at 20% SO_2 breakthrough was used in this program as a relative measure of sorption rates. Actual adsorption rates were also determined. The equation used to obtain these rates was derived assuming complete backmixing of the sorbent and plug flow of the gas. Based on these assumptions, a kinetic reaction model was developed to provide a relationship between a reaction rate coefficient, R(X), and the following experimentally measurable quantities: the inlet SO_2 gas phase concentration, C_o; the outlet SO_2 concentration, C_H; the settled bed height, H_o; the superficial velocity, U; and the fraction CaO utilized in the sorbent, X. The reaction rate coefficient, R(X), is the rate of SO_2 removal from a volume of gas per unit time, per unit volume of particulate bulk phase. The reaction rate coefficient is written as a function of the sorbent CaO utilization, X, to show that it is dependent on the degree of sorbent utilization. Thermodynamic analysis indicates that MgO in calcined dolomites and limestones cannot react near 1600°F to effect desulfurization, for both $MgSO_4$ and $MgSO_3$ are unstable at this temperature (see Appendix V for details). As shown in Section 4.2.3. of the report, even at lower temperatures where it can theoretically react, MgO still does not form $MgSO_4$ to any appreciable degree. Thus, only CaO should react to form the sulfate and permanently remove SO_2 from flue gas.

Considering the reaction of SO_2 with the sorbent on passing through the lamella shown in the following figure we can write the material balance over a differential height, dz:

Figure 4

Material Balance Diagram

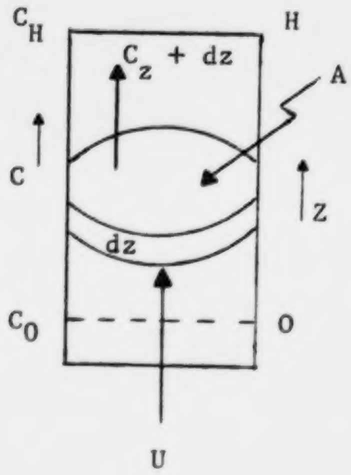

SO_2 removed from gas = SO_2 absorbed by sorbent

$$-U\cdot A\cdot(C_z-C_{z+dz}) = A\cdot dz\cdot(1-\epsilon)\cdot R(X)\cdot C_z = -U\cdot A\cdot dC_z \qquad (1)$$

where A is the reactor cross-sectional area, ϵ is the void fraction in the bed, and C_z is the SO_2 concentration at the point Z. R(X) is the reaction rate coefficient per unit volume of particulate phase. On rearrangement and integration over the boundary conditions of the fluid bed one obtains:

$$\int_{C_o}^{C_H} U \frac{dC_z}{C_z} = \int_{0}^{H} R(X)\ (1-\epsilon)\,dz \qquad (2)$$

$$\ln \frac{C_H}{C_o} = -\frac{R(X)\cdot(1-\epsilon)}{U}\cdot H \qquad (3)$$

where H is the expanded bed height.

Assuming $H = H_o/(1-\epsilon)$, equation (3) was derived to yield the final rate equation (4) from which R(X), the reaction rate coefficient could be determined from experimentally measured parameters.

$$\ln\frac{C_H}{C_o} = -R(X)\cdot\frac{H_o}{U} \qquad (4)$$

3.4. Measured Fluid Bed Reactivity of Coarse Sorbents

The initial fluid bed experiments were made using coarse, 16 to 18 mesh, pre-calcined particles of the dolomite N-1337 and the limestone N-1359. Temperature was maintained constant at 1600°F, superficial gas velocity was varied from 2 to 6 ft/sec, and settled bed height from 1 to 8 inches. The calculated reaction rate coefficients are shown in Figures 5 and 6 as a function of sorbent CaO utilization (X). Analyses of the data contained in these figures showed that the reactor model (Eq. 4) fit the experimental data over a wide range of superficial velocities at different fixed bed heights. However, as the settled bed height was increased, the calculated reaction rate decreased. This is attributed to gas distribution and contacting variations in the laboratory unit. Slugging and channeling in a fluid bed are a function of the bed height. Slugs of gas bubbles form at high gas velocities and extend across the entire reaction area, causing inefficiences in desulfurization. However, they are not fully formed upon entrance to the fluid bed and only form as the gas travels through the bed. At low bed heights, insufficient time is available before the gas leaves the bed to form these slugs. Preferred routes of gas passage through the bed may also exist and such channeling also decreases gas contacting. Different bed heights and reactor grid configurations will result in different modes of channeling through the particles. These different variations are difficult to predict and analyze, and are generally empirically correlated, as was done in this study.

Figure 5

Reaction Rate Coefficient, Dolomite 1337

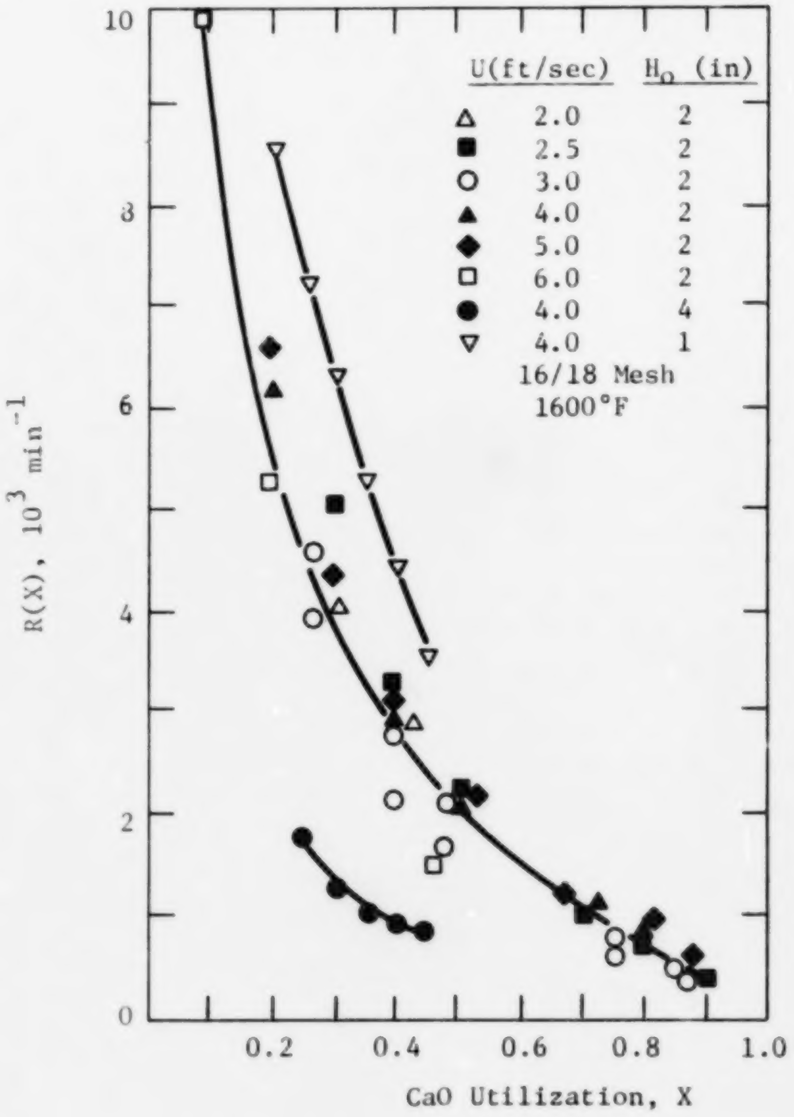

Figure 6

Reaction Rate Coefficient, Limestone 1359

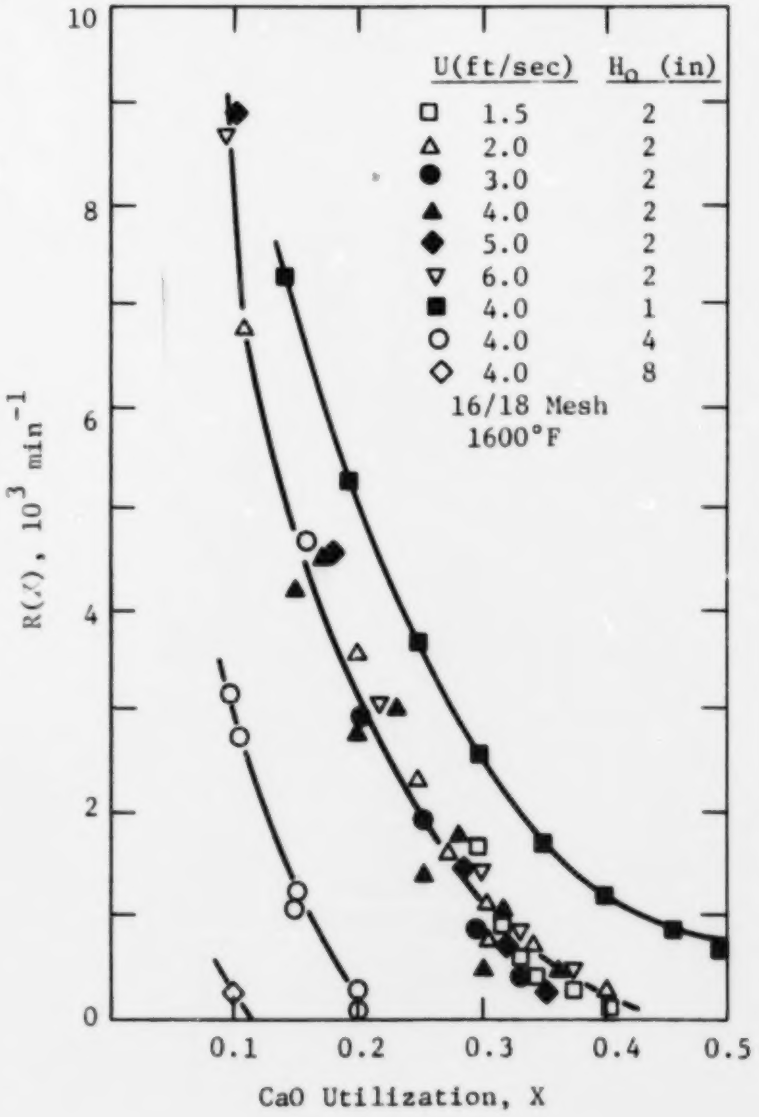

The reaction rate obtained for 6/8 mesh sorbent is shown in Figure 7 for N-1359. For this particular sorbent and particle size distribution, no effect of bed height was observed; however, the limited data available prevent drawing any valid conclusions as to the presence or magnitude of a bed height effect.

Figure 7

Reaction Rate Coefficient, Lime (1359)

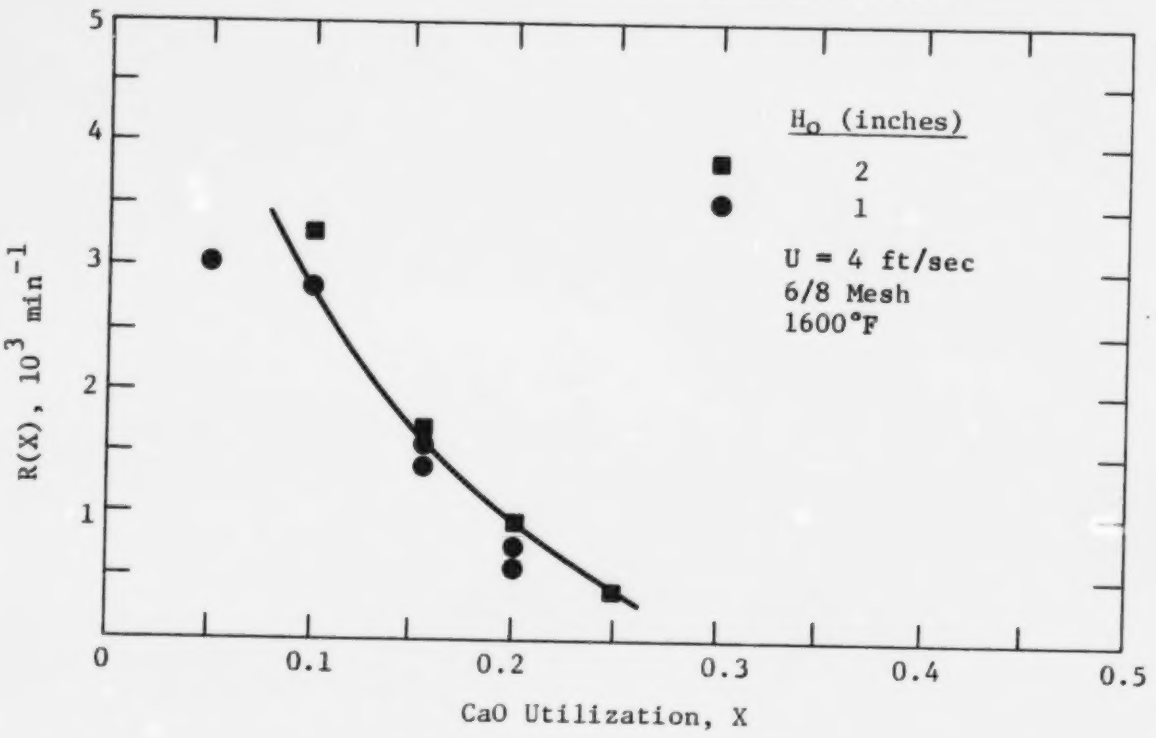

The reaction rate coefficient, R(X), can be related to k(X), the reaction rate constant, in the following manner:

$$R(X) = k(X) \cdot Y(k, H_o) \qquad (5)$$

where the term Y, the contacting factor, is obtained in the actual laboratory reactor used to study the reaction. The contacting factor, Y, is essentially the efficiency of gas-solid contacting. It is a function of the reaction rate constant, k, and the settled bed height, H_o. The magnitude of the contacting factor depends on contacting efficiency in the actual laboratory reactor used to study the reaction and is determined in part by the gas distribution provided by the grid system used, the ratio of bed diameter to bed height, and the particle diameter employed. Various models have been proposed for calculating contacting efficiency in fluidized bed systems (3) and under conditions of slugging bed operation (4,5). These models are based on the use of relatively small diameter particles.

In the coarse particle systems used in this work we have determined k(X) for two different sorbents by using equation (5) in a correlation of the reaction, R(X), with H_o. This correlation is based on a simplified linear model which assumes that the contacting efficiency, Y, can be expressed as follows:

$$Y(H_o) = 1-m(k)\ H_o \quad (0 < Y < 1) \qquad (6)$$

where m = experimentally determined constant,

H_o = settled bed height.

This model implies a contacting factor of 1.0 at zero (0) bed height only. While this boundary is probably correct, it is possible that the contacting efficiency remains at 1.0 for small finite bed heights. If this is true, it would slightly effect the value of k finally obtained. The simple linear model presented should be replaced in more refined calculations by a more general exponential model as $Y \longrightarrow 0$.

By plotting values of R from figures 4 and 5 vs H_o at values of X, and extrapolating to zero bed height, k(X) was obtained for both the N-1337 and N-1359 stones at various values of X. The ratio, $R/\kappa = Y$, was found to be nearly the same at a given value of k, which showed that the efficiency factor was indeed primarily dependent on H_o and k with negligible variation due to stone composition and density differences. Figure 8 presents the contacting factors so obtained and illustrates the marked dependence of contacting efficiency on H_o and k in the laboratory reactor. It is important to realize that similar contacting efficiencies would not be expected for a commercial reactor having a different grid design and a vastly different ratio of bed diameter to bed height.

Figure 8

Contacting Factor - Rate Constant Dependance in Laboratory Reactor

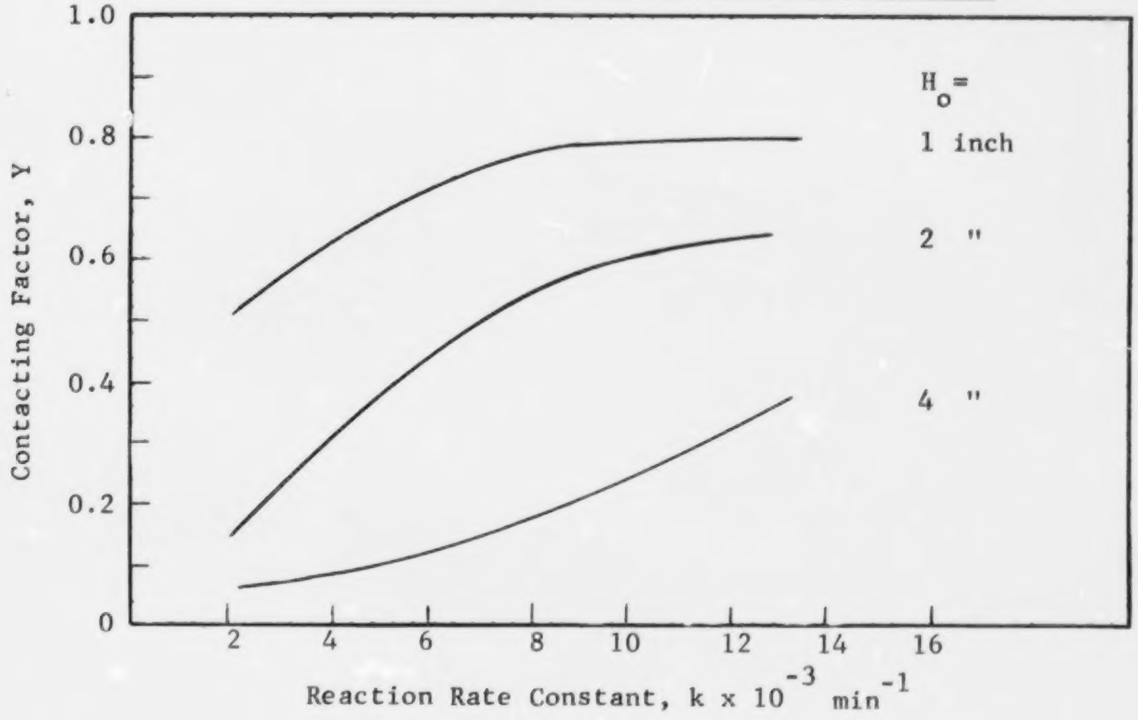

The reaction rate constants for the 16/18 mesh dolomite (N-1337) and lime (N-1359) have been calculated and are shown in Figure 9. Thus, all the experimental data have been reduced to universal, simple reaction rate results from which ultimate sorbent performance in good contacting fluid beds can be predicted. In Figure 10, the desulfurization rate constants for the three other stones, N-1351, N-1363, N-1360, are presented along with N-1359 desulfurization data for 6/8 mesh particles. The rate constants for the two dolomitic stones (N-1337, N-1351) are seen to be substantially higher than those of the high CaO limestones. Lime particles (N-1359) appear to have the lowest reaction rate of any stone tested.

Figure 9

Reaction Rate Constants for
Lime and Dolomite (1359, 1337)

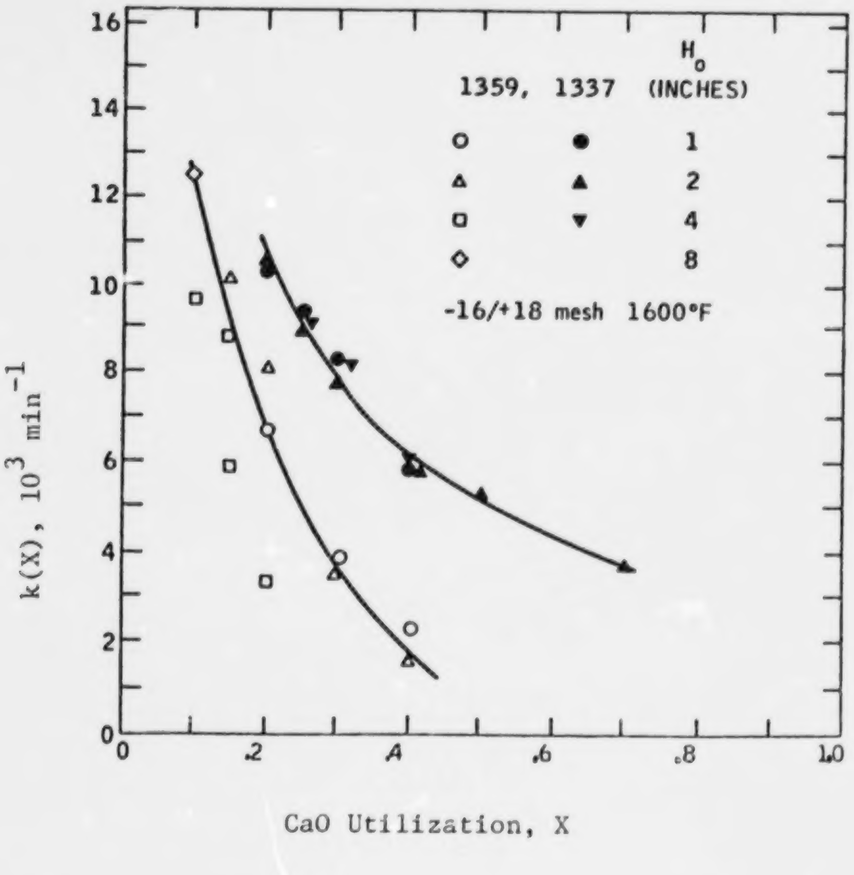

Figure 10

Reaction Rate Constants for Various Stones (See Table 2 for Compositions)

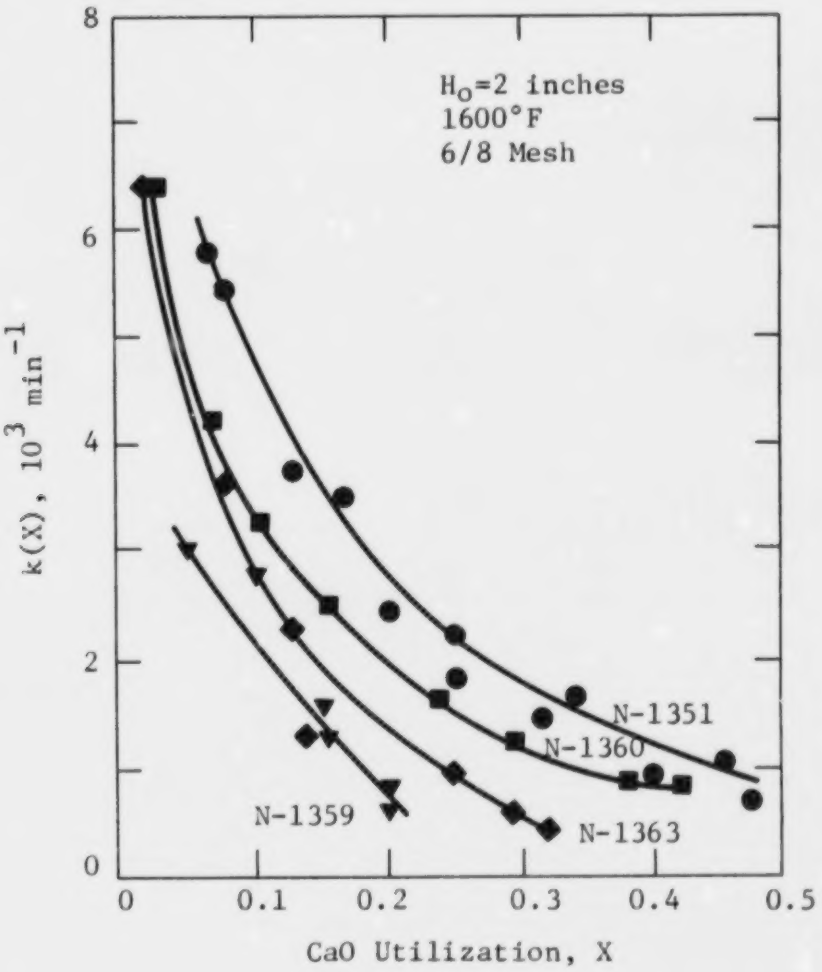

An indication of the change of the rate constant for N-1359 lime particles as a function of temperature. The ratio of the rate constant, k, at temperature T to the rate constant at 1600°F was calculated by assuming contacting efficiency characteristics similar to those in Figure 8 for particles other than 16/18 mesh size.

In Figure 11, $k_T/k_{1600°F}$ is shown as a function of temperature. This represents an outline of the decrease in the desulfurization reaction rate as the temperature is lowered to 1200°F from 1600°F. The present data are consistent with the 28 kcal/mole activation energy found by Battelle (6) in the range 1500-2150°F for simultaneous calcination - desulfurization. It might be noted that weight gain due to CO_2 pick-up was found at the lowest temperatures; however, recarbonation was only of the order of magnitude of the SO_2 reaction rate.

Figure 11

Rate Constant Temperature Dependence for N-1359 Lime

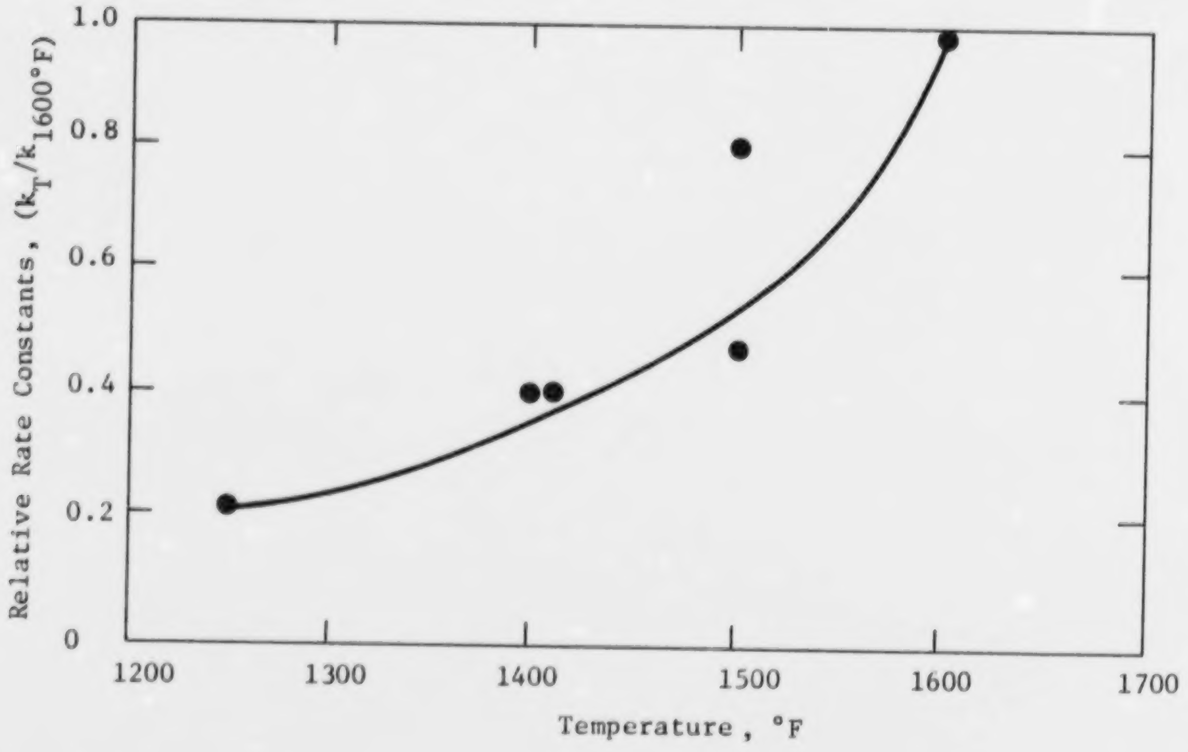

4. IMPROVING SORBENT UTILIZATION

The rapid decrease in reactivity, shown in Figures 9 and 10 for the different partially reacted sorbents, indicates that the attainment of high sorbent utilization (e.g., $>$50%) in a commercial flue gas desulfurization process would require long sorbent residence times if coarse particles were used. Consequently, fluid bed reactors would have to be designed for large solids hold-up. In order to improve sorbent utilization and so decrease this hold-up, four different process variations were investigated in our experimental program. These process variations consisted of the following:

- inducing surface attrition of the sorbent in the fluid bed in order to continuously remove sulfated material.
- making inexpensive physical or chemical modifications of the sorbent to increase its reactivity.
- using finely sized sorbent.
- using coarse sorbent with continuous reductive regeneration to the oxide and recovery of the SO_2 for conversion to a salable product.

4.1. Effect of Bed Attrition on Sorbent Utilization

Natural surface attrition, resulting from particle to particle contact within the fluid bed, was investigated as a means of continuously removing the $CaSO_4$ formed at the surface of the sorbent.

Attrition in a bed of given sized particles can be increased in two ways. Either an increased superficial velocity or an increased bed height should increase the degree of grinding of the particles with one another. An increased bed height has the added advantage of decreasing the competing shell formation rate, since more particles receive an equal amount of SO_2 for a given period of time.

Table 3 and Figure 12 show the effect of these variables on the overall attrition rate for N-1359 and on oxide utilization at the 20% breakthrough point. A comparison of two runs made at a bed height of approximately six inches, one at a superficial fluidizing velocity of 3.5 ft/sec, the other at a superficial velocity of 7.0 ft/sec, shows that a doubling of the superficial velocity more than quadruples the overall attrition rate. However, the increased attrition rate (0.33 gms/min) is only about one-quarter of the formation rate of fresh oxide surface required for stoichiometric reaction with the now doubled rate of SO_2 passing through the bed, and the oxide utilization drops slightly from 6.7 wt. % to 5.0 wt. %.

Table 3

EFFECT OF ATTRITION ON OXIDE UTILIZATIONS FOR -12 +14 MESH PARTICLES OF CALCINED N-1359

Bed Charge - Grams (Approximate Height - inches)	Superficial Gas Velocity ft/sec	Amount of Attrition before 20% Break-through - Grams	Overall Attrition Rate gm/min	Formation Rate of fresh oxide required-gm/min	Total Oxide (CaO + MgO) Utilization at 20% Breakthrough Point
580 grams (∼6 inches)	3.5	5	.07	0.6	6.7%
580 grams (∼6 inches)	7.0	11	.33	1.2	5.0%
1175 grams (∼12 inches)	7.0	71	1.2	1.2	2.6%
2345 grams (∼24 inches)	5*-7.0	703**	2.3	1.2	14.8%

* Operating difficulties necessitated higher bed pressures with correspondingly lower superficial velocities.

** Operating difficulties gave a poor material balance; amount of attrition was a value calculated from the differences between the before and after bed weights and the SO_2 flowrate.

Figure 12

Effect of Bed Height on Attrition Rate of N-1359

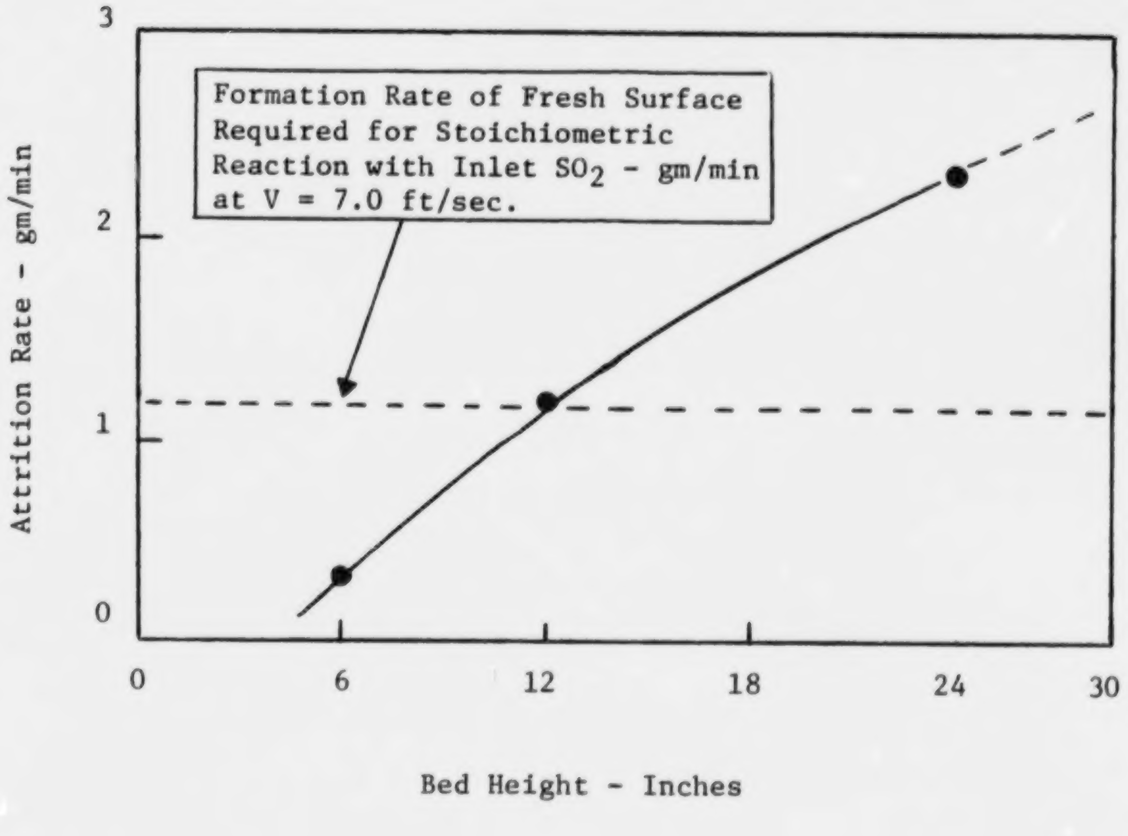

In the expectation that an increase in the bed height would increase the degree of internal grinding of the particles and promote attrition of the sulfate shell, additional runs were made at bed heights of twelve and twenty-four inches at a superficial fluidizing velocity of 7.0 ft/sec (Figure 12).

Increasing the bed height to twelve inches greatly increased the overall attrition rate to 1.2 gm/min, equal to the 1.2 gm/min formation rate of fresh oxide surface required for stoichiometric reaction with the SO_2. However, the oxide utilization dropped to 2.6%. Such loss of oxide utilization was also observed in some of the later studies. One possible explanation for this behavior is that since the sulfated surface is slightly "sticky", and hence possibly malleable at these temperatures (as indicated by the difficulty in dumping a fixed or settled bed), a moderate degree of attrition may actually have deformed and sealed surface pores of the sulfated shell.

With the expectation that an even higher degree of attrition could overcome this possible sealing effect of attrition, the bed height was again doubled to 24". The resulting 2.3 gm/min attrition rate was nearly twice the formation rate of fresh oxide surface required for stoichiometric reaction with SO_2, but only 14.8 mole % oxide utilization was obtained. This low utilization suggested that the attrition was not selectively removing sulfated surface to expose reactive oxide but was breaking down the particles in their entirety. This was confirmed in studies with the dolomite, N-1337. Using 6" to 24" deep beds of calcined 12 to 14 mesh N-1337, with superficial gas velocities up to 7.0 ft/sec, it was found that unreacted dolomite broke up more readily than the limestone to produce fines in the 50 to 100 mesh range. Under similar conditions, the same sorbent but having 30% of its CaO sulfated, attrited as readily as the unreacted dolomite and produced fines of about the same composition as the remaining sorbent. If the surface were being selectively attrited, the fines would have had a higher sulfate content than that of the bulk adsorbent.

4.2. Effect of Physical and Chemical Modifications on Sorbent Reactivity

A number of physical and chemical modifications of the limestone (N-1359) and the dolomite (N-1337) were tested to determine if these could provide more reactive sorbents whose decreased requirements would more than offset the costs of modifying the sorbents. Improving the calcination, using the hydroxide form of the sorbent, using half calcined dolomites, and doping the sorbents with catalytic metal oxides were all investigated as ways of improving reactivity.

4.2.1. Effect of Calcining Conditions on Oxide Utilization

The following two types of calcination were studied in detail for the limestone N-1359: one which removed the CO_2 from the carbonate sites by diffusion (i.e., the equilibrium dissociation pressure remained below 1 atm.), and one where the CO_2 left the carbonate sites at a dissociation pressure above atmospheric pressure. Table 4 and Figures 13 and 14 summarize the results obtained from this study. The diffusion controlled calcination gave oxide utilization in the 1.5 to 3.5% range and the pressure induced calcination gave utilizations in the range of 6 to 8%.

The pressure-induced calcinations were carried out in a 1' x 1' x 2' stainless steel box whose walls and top were maintained at 1800-1850°F in a large Lindberg furnace (see Figure 15). Small quantities of particles were dropped through a pipe into the box, where they were rapidly heated by radiation to 1665°F. They then proceeded to evolve CO_2 at atmospheric pressure. The high surface heat flux probably permitted small entrapped pockets of carbonate to overheat, overpressure, and finally rupture to form needed voids in a popcorn manner near the particle surface. Uncalcined stone situated further away from the outside surface was insulated by the layer of calcined stone, and so the absence of a high heat flux probably minimized pore formation towards the center of the particle. Higher box wall temperatures to induce higher particle surface temperatures were avoided to minimize the dead-burning of completely calcined particles. Total calcination time was governed by the time it took a previously added batch of particles to calcine and reach 1800-1850°F before they were covered with a new batch of carbonate. 1100 grams of N-1359 could be calcined in one hour.

Some additional conclusions regarding the selection of calcinating conditions can be drawn from the data in Table 4. Glasson (7) found that dead burning with the consequential loss of specific surface area increased with temperature and the CO_2 concentration above the calcined oxide. This same effect is apparent in our data. Thus, Runs 6, 7, and 12 using material calcined at temperatures between 1450 and 1625°F gave higher utilizations than Runs 9, 10, and 11 which used material calcined at 1750°F, where both the temperature and CO_2 concentrations (itself a function of temperature) were relatively high. This trend is shown by the dashed line in Figure 13. The series of runs made with material

Table 4

Effect of Calcining Conditions on Oxide Utilizations for -12 +14 Mesh BCR-1359

Run #	% CaO Utilized (at 20% B.T.)	Calcining Conditions	SO_2 Reacting Conditions
		Fluidized Bed Calcinations (Diffusion Controlled) - Fluid Bed Run	
6	3.49%	Gently fluidized bed, 2 1/2 hrs up to 1450°F, held at 1450°F for 1/2 hr	580 gm bed, 1600°F, V = 3.5 ft/sec 2 gms fines*
7	3.52%	Fluidized bed, up to 1600°F in 1 hr, dumped	580 gm bed, 1600°F, V = 3.5 ft/sec 1 gm fines
9	2.81%	Fluidized bed, up to 1750°F in 1/2 hr, dumped	580 gm bed, 1600°F, V = 3.5 ft/sec 0.5 gm fines
10	2.04%	Fluidized bed, up to 1750°F in 1/2 hr, held at 1750°F for 1 hr	580 gm bed, 1600°F, V = 3.5 ft/sec 0.3 gm fines
11	2.30%	Fluidized bed, up to 1750°F in 1 hr held at 1750°F for 1/2 hr	580 gm bed, 1600°F, V = 3.5 ft/sec 0.8 gm fines
13	2.56%	Fluidized bed, up to 1400°F for 8 hr, some attrition	580 gm bed, 1600°F, V = 3.5 ft/sec 8.3 gms fines
16	1.50%	Violently fluidized bed, up to 1300°F for 12 hours - high attrition	580 gm bed, 1600°F, V - 3.5 ft/sec no fines
		Fixed Bed Calcination (Diffusion Controlled) - Fluid Bed Run	
12	3.25%	Fixed bed calcination, V = 1.2 ft/sec, top of bed at 1625°F in 7 hrs - difficult to dump	580 gm bed, 1600°F, V = 1.2 ft/sec fixed bed - very difficult to dump. No fines
19	6.66%	Particles exposed to 1800°F walls-heated for 1 - 2 hours from radiation - no purge gas	580 gm bed, 1600°F, V = 3.5 ft/sec 5 gm of fines
4	5.43%	Fixed bed with purge-walls to 1700°F, partially pressure-induced, partially diffusion controlled calcination	580 gm bed, 1600°F, V = 3.5 ft/sec 1 gm fines

Note: All runs had breakthrough curves of the type shown in Figure 4.

---

* Amount of material collected in the cyclone separator.

Figure 13

Effect of Calcining Conditions on Oxide Utilization for N-1359

Particle Size: - 12 + 14 Mesh
Reactor Conditions: 580 gm bed, 1600°F, V = 3.5 ft/sec
Time at Calcination Temperature: Variable

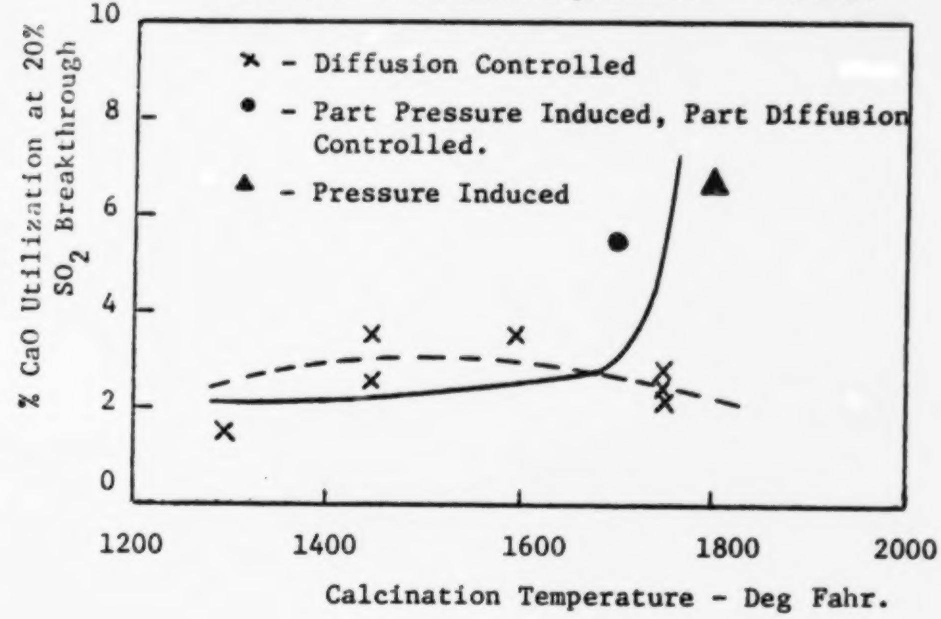

Figure 14

Effect of Time at Calcination Temperature on Oxide Utilization for N-1359

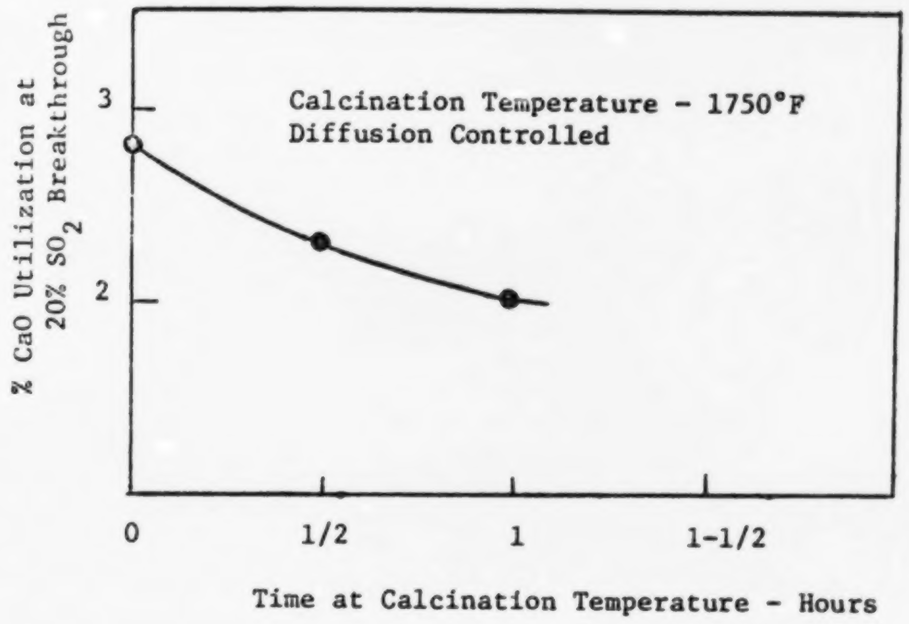

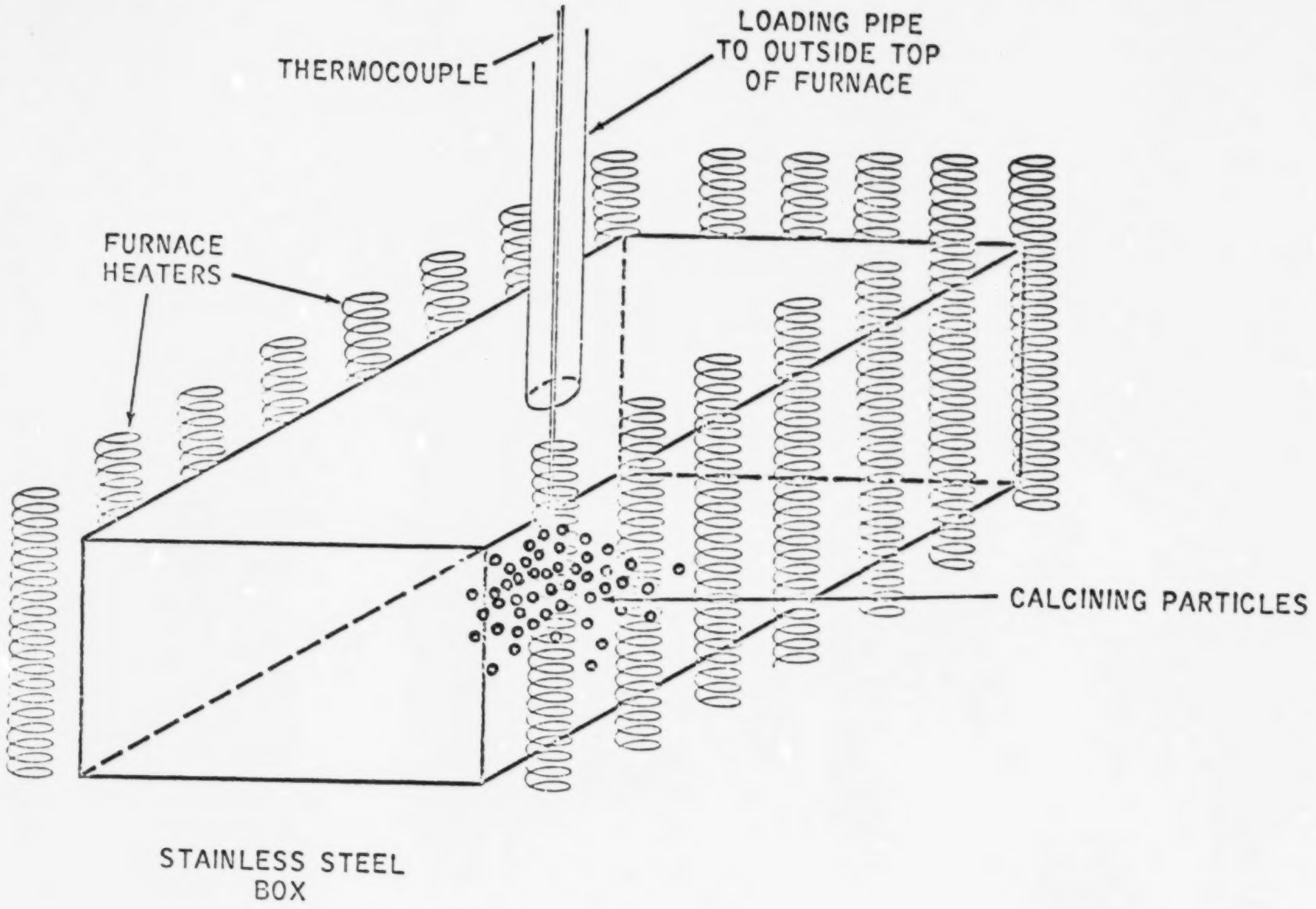
THERMOCOUPLE
LOADING PIPE TO OUTSIDE TOP OF FURNACE
FURNACE HEATERS
CALCINING PARTICLES
STAINLESS STEEL BOX

Figure 15

Radiant Heat Calciner for Pressure-Induced Calcinations calcined at 1750°F, but maintained at calcination temperature for varying lengths of time. also showed the decrease in oxide utilization resulting from an increase in dead burning as exposure time was lengthened. This is shown in Figure 14. Undoubtedly the pressure-induced calcinations carried out in a pure CO_2 atmosphere at higher temperatures had an even higher degree of dead-burning. In these cases, however, the resultant pore formations evidently offset this deleterious effect.

All runs referred to in Table 4 had sharp breakthrough curves implying that further diffusion-controlled reaction would be slow. Although some increase in sorbent reactivity can thus be obtained by operating under pressure induced conditions, large improvements in sorbent utilization are judged to be unlikely.

4.2.2. Reactivity of the Hydroxide

To determine if the hydroxide would be the preferred form of the sorbent for fluid bed desulfurization, experiments were carried out with the hydroxide made from N-1359 limestone. The hydroxide was made by calcining the carbonate, slowly adding the stoichiometric amount of ice water needed to form the hydroxide, and then drying the hydroxide for five hours at 100°F.

A 325 cm^3 bed of 25 to 50 mesh hydroxide made in this way was tested with simulated flue gas at a superficial velocity of 1.2 ft/sec and a 600°F temperature. This temperature was selected because it is below the thermodynamic dissociation temperature of $Ca(OH)_2$ in the flue gas atmosphere (see Appendix IV, Section IV-2).

Total SO_2 removal occurred until 3.5 wt% of the $Ca(OH)_2$ had been consumed and then there was a very sharp SO_2 breakthrough. The discharge bed material was found to contain 30% CO_2. Evidently, the carbonation proceeded at a sufficiently high rate to hinder sulfation, probably through pore blockage.

Recarbonation is thermodynamically unfavorable at temperatures above about 1450°F (see Appendix IV, Section IV-2), but at such temperatures, the hydroxide reconverts to the oxide. To determine if the oxide made from such an intermediate hydroxide was more reactive than that made directly from the carbonate, the following experiment was made. 250 cm^3 of the 25 to 50 mesh hydroxide was run in the fluid bed at a velocity of 1.2 ft/sec and a temperature of 1600°F. Under these conditions, 41.9 wt% of the CaO reacted at the 20% SO_2 breakthrough point. A comparable run with just the calcined N-1359 sorbent (i.e., no intermediate hydroxide formation) yielded only 22.2% CaO utilization at the 20% breakthrough point.

The increased oxide utilization of the hydroxide-treated material might be explained in two ways. The hydroxide formation-calcination steps could conceivably "activate" a hitherto unreactive material through crystal rearrangements. A more likely explanation, however, is an increased porosity, which might be caused from the agglomeration of very small particles to form the -25 + 50 U.S. mesh bed particles. During the hydration step, severe decrepitation was noted with the formation of a high percentage of very small particles. In a commercial process, if these particles were not retained in the bed for a sufficient time to insure good particle utilization, there would be no advantage to using intermediate hydroxide. On the other hand, a fluid bed designed to retain such particles would also retain small particles of normally calcined N-1359 which later experiments showed to be about as active as the more difficult to prepare hydroxide. Therefore, no advantage is seen for using the hydroxide.

4.2.3. Studies With Uncalcined Limestones and Half Calcined Dolomites

At temperatures above approximately 1500°F, both $MgSO_3$ and $MgSO_4$ are thermodynamically unstable in a typical flue gas environment (see Appendix IV). At temperatures below about 1450°F, on the other hand, $CaCO_3$ is thermodynamically stable at the 14% CO_2 concentration of flue gas (Figure A-1, Appendix IV). Consequently, the only way that both the calcium and magnesium portions of a dolomite can be utilized for SO_2 adsorption is for the process to be operated at a temperature where the $CaCO_3$ remains uncalcined but where SO_2/O_2 is able to displace CO_2 from the carbonate

In an attempt to evaluate this displacement reaction, 12 to 14 mesh of the uncalcined limestone N-1359 was used in a one foot bed at 600° and 1200°F. At the lower temperature, there was no noticeable reaction while at 1200°F, the calculated rate coefficient was less than 2% of the coefficient for calcined material at 1600°F.

In contrast to the limestone, the half calcined dolomites were found able to adsorb SO_2 at temperatures down to 1000°F. Three dolomites, N-1337, 1351 and 1360, were calcined at 1200 to 1300°F in a SO_2-free flue gas atmosphere. Under these conditions, the $MgCO_3$ was converted to the oxide while the $CaCO_3$ remained unchanged.

$$CaCO_3 \cdot MgCO_3 \longrightarrow CaCO_3 \cdot MgO + CO_2 \qquad (7)$$

Weight losses sustained during calcination corresponded to those expected from the above reaction as Table 5 shows.

The reactivity of half-calcined materials at low temperatures was much lower than the fully calcined stones at 1600°F and appeared to be less dependent on utilization (see Figure 16). Comparative results for the three stones are summarized in Table 5 for reaction at 1300°F.

Table 5

Sulfur Dioxide Capture by Half-Calcined Dolomites at 1300°F

Sorbent	Mol. % of CaO in CaO + MgO	Half Calc'n. Wt. Loss Theor.	Half Calc'n. Wt. Loss Actual	% CaO Utilization at constant k ($k \doteq 100\ min^{-1}$)
N-1337	46.7	25.4	26.9	87
N-1351	57.5	18.0	18.1	52
N-1360	81.9	8.0	9.6	11.5

Theoretically, the half-calcined dolomites can remove SO_2 by reaction with $CaCO_3$, MgO or both. The failure of the MgO to react to any meaningful degree was confirmed in these studies by analysis made of sulfated stones, Table 6. The sorbent weight increase, and the percent sulfur and CO_2, determined by analyzing the final product, agreed most closely with those values calculated on the basis of no MgO reaction.

Table 6

Analysis of Sulfated Half-Calcined Dolomites

	Observed	Calculated Assuming % of MgO Sulfated Is: 0%	10%	20%
N-1351				
Wt. % Sulfur	10.9	11.0	10.8	10.5
Wt. % CO_2	10.0	11.0	12.6	14.2
Weight Gain, %	11.5	14.5	16.8	18.9
N-1337				
Wt. % Sulfur	15.9	15.5	14.9	14.5
Wt. % CO_2	4.8	3.5	6.0	8.5
Weight Gain, %	17.2	17.8	24.2	27.4

Figure 16

Reaction Rate Coefficient for Calcined Dolomite (1337)

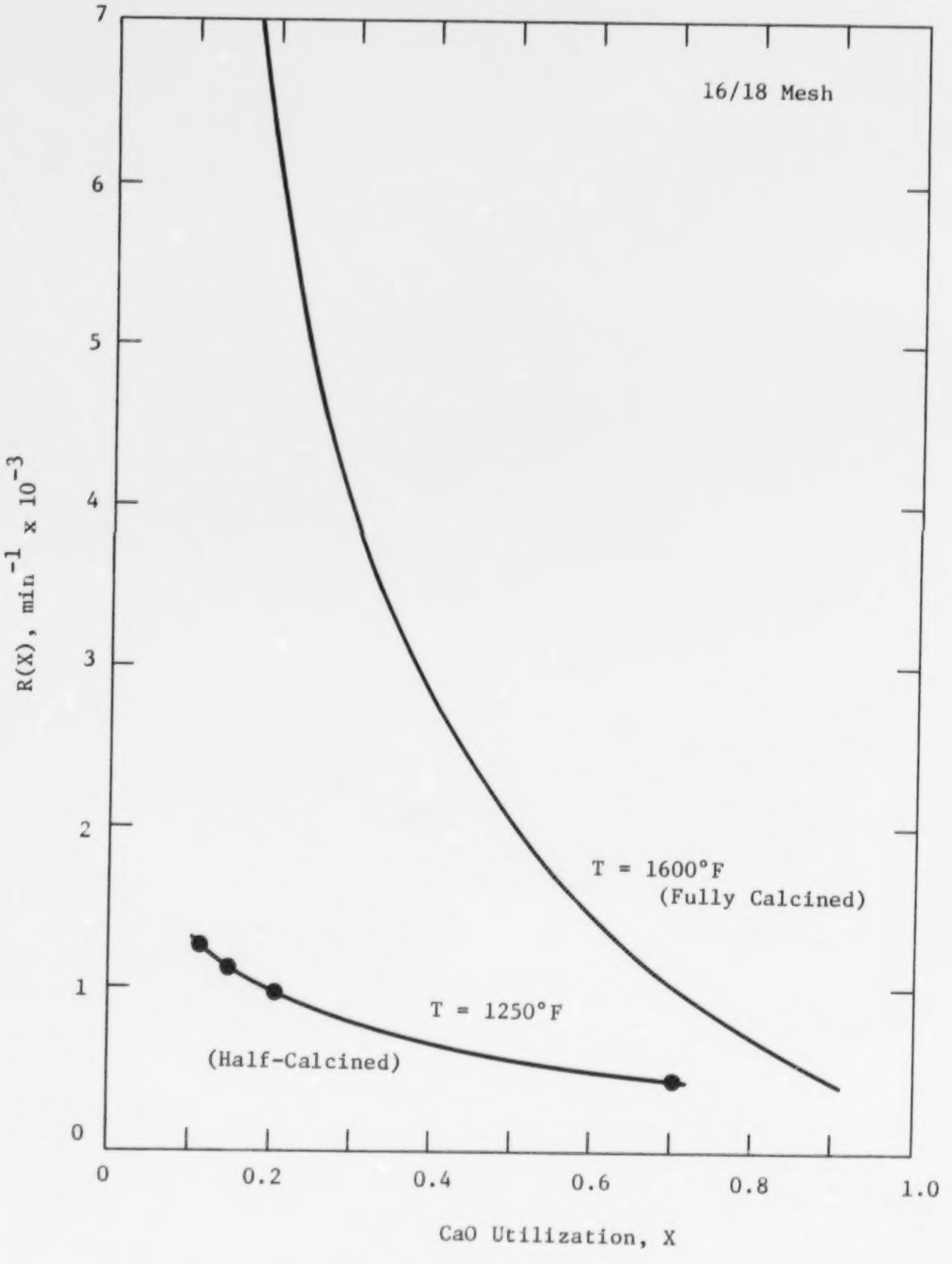

As Figure 16 shows, however, its activity was much lower than that of the fully calcined dolomite. Consequently, the use of half calcined dolomites is not judged to be attractive, even though they can be used at lower temperatures than fully calcined dolomites or limestones.

4.2.4. Reactivity of Metal-Oxide Modified Stones

The modification of sorbent by doping with metal oxides was also investigated as a means of increasing reactivity. Doping was carried out by contacting the uncalcined sorbent with a solution of metal nitrate, washing the doped sorbent, followed by drying and calcination. Treatment of the sorbent with nitrate solutions of copper (II), aluminum and iron (III) resulted in considerable evolution of CO_2 suggesting reaction with $CaCO_3$. The treatment with the copper solution produced a hard copper oxide shell around the sorbent. Treatment with the aluminum and ferric solutions resulted in the formation of gelantinous aluminum and ferric hydroxide.

4.2.4.1. Metal Oxide Modification of N-1359 Lime

As shown in the following table no improvement in CaO utilization was observed when the calcined, doped N-1359 lime was used for desulfurization. In most cases, a definite deterioration of sorbent performance was observed. All the breakthrough curves with exception of the copper-treated sample were similar to that obtained with untreated sorbent, but were displaced toward lower utilizations. The sorbent treated with the copper solution had a gentler breakthrough curve, but did not give an increase in oxide utilization.

Table 7

Modification of 1359 Lime - Doping With Metal Oxides

Treatment	Calcium Oxide Utilization at % SO_2 BT		
	1	20	50
None	.18	.20	.21
None	.18	.20	.21
Nickel	.17	.20	.21
Copper (II)	.14	.19	.22
Copper (II)	.09	.16	.20
Aluminum	.07	.10	.12
Cobalt	.12	.14	.16
Cobalt	.07	.09	.12
Ferric	.11	.14	.16

The effect of modifying the sorbent with copper oxide was further investigated by measuring the rate of SO_2/O_2 reaction using treated and untreated sorbent calcined under identical conditions. The following table shows that no major change in reactivity occurred on modifying the sorbent.

Table 8

Reaction Rate of SO_2/O_2 With Modified N-1359 Lime at 1600°F

Fraction CaO Utilized	Reaction Rate Coefficient (Min^{-1})			
	16/18 Mesh		12/14 Mesh	
	Copper Oxide	Control	Copper Oxide	Control
0.05			7430	6400
0.10	2770	3500	3180	3950
0.20	530	100		

A copper modified sample of uncalcined N-1359 limestone was used for desulfurization at 1300°F. Effective desulfurization under these conditions was not successful. A measurement of the rate of SO_2/O_2 reaction resulted in a rate coefficient of only 156 min^{-1} at 5% CaO utilization - a factor of at least 50 less than with calcined sorbent at 1600°F.

4.2.4.2. Copper Oxide Doped, Half-Calcined Dolomite

Dolomite (N-1337) was treated with an aqueous cupric salt followed by calcination at 1200°F to deposit a film of copper oxide on the sorbent. A comparison of the rate of SO_2/O_2 reaction at 1200°F using the modified dolomite and a normal half-calcined dolomite showed a slight decrease in sorbent reactivity on modification with copper. This effect is illustrated in Table 9.

Table 9

Rate of SO_2/O_2 Reaction With Modified Half-Calcined Dolomites at 1200°F

Dolomite (1337), 14/16 Mesh Particles

Fraction CaO Utilized	Normal Half-Calcined Dolomite	Copper Modified Half-Calcined Dolomite
0.1	1000 min^{-1}	860 min^{-1}
0.2	790 min^{-1}	470 min^{-1}
0.3	640 min^{-1}	205 min^{-1}

4.3. Reactivity and Use of Finely Sized Sorbent

The use of finely sized sorbent, alone and in combination with coarser material, was investigated as a way of achieving both good SO_2 removal efficiency and high sorbent utilization in a fluid bed flue gas desulfurization process.

4.3.1. Small Particle Reactivity

The rate constant data presented in Figures 9 and 10 and the less detailed results on intermediates and small particle sizes available in Appendix I were analyzed for a dependence of rate constants on particle size. Using assumptions of similar contacting efficiency characteristics and CaO utilization-rate constant characteristics for different particle sizes, rough dependence of rate constants on particle size were obtained.

For 1337 dolomite, 60% utilization, the following dependency was found in the diameter range 100-3000 μ,

$$k_{1337} \propto d^{-0.5} \qquad (8)$$

For 1359 lime, 20% utilization, a different dependency was found,

$$k_{1359} \propto d^{-1.3} \qquad (9)$$

Although the power coefficiencies may easily be in error by 1/3, it does appear from these first approximations that 1359 lime has a much more marked dependence on particle mesh size than 1337 dolomite.

If only gaseous diffusion into the porous particle were the limiting mechanism, one would expect a d^{-2} proportionality on the rate constant, assuming a constant diffusion coefficient in a continuously reacting outer shell (8). Thus, our experiments showed that a simple diffusion model does not adequately represent the data.

The uneven powers determined for the effects of particle diameter could be explained by many different reaction mechanisms. Among the possibilities are the following: (a) a mixture of chemical reaction and diffusion control, (b) a variation in the diffusion constant with particle size if Knudsen diffusion is important, (i.e., change in pore size distribution from calcination), and (c) the necessity of molecular reorientation of the solid with chemical reaction. With such a number of unresolved possible reaction mechanisms, it would seem advisable to base engineering predictions only on experimental, empirical correlations and not on mechanistic schemes.

4.3.2. Residence Time Required for Small Particles in Fluid Bed Result in Uneconomical Design

The results of Section 4.3.1. relating the reaction rate constant to particle size have been combined with the detailed kinetic data on 16 to 18 mesh N-1337 presented in Section 3.4. to predict utilization versus residence time for individual 60μ and 1100μ particles at 1600°F. The results obtained are shown in Figure 17. The analysis is based on 90% desulfurization of a 2700 ppm SO_2 containing flue gas. Individual particle residence time required to achieve 50% utilization with the small particles is calculated to be about 8 minutes compared to one hour for the large particles. At 90% sorbent utilization, the small particles require about 40 minutes, down from the 5 hours required for the large particles.

Figure 17

CaO Utilization for Single Particle N-1337 Sorbent

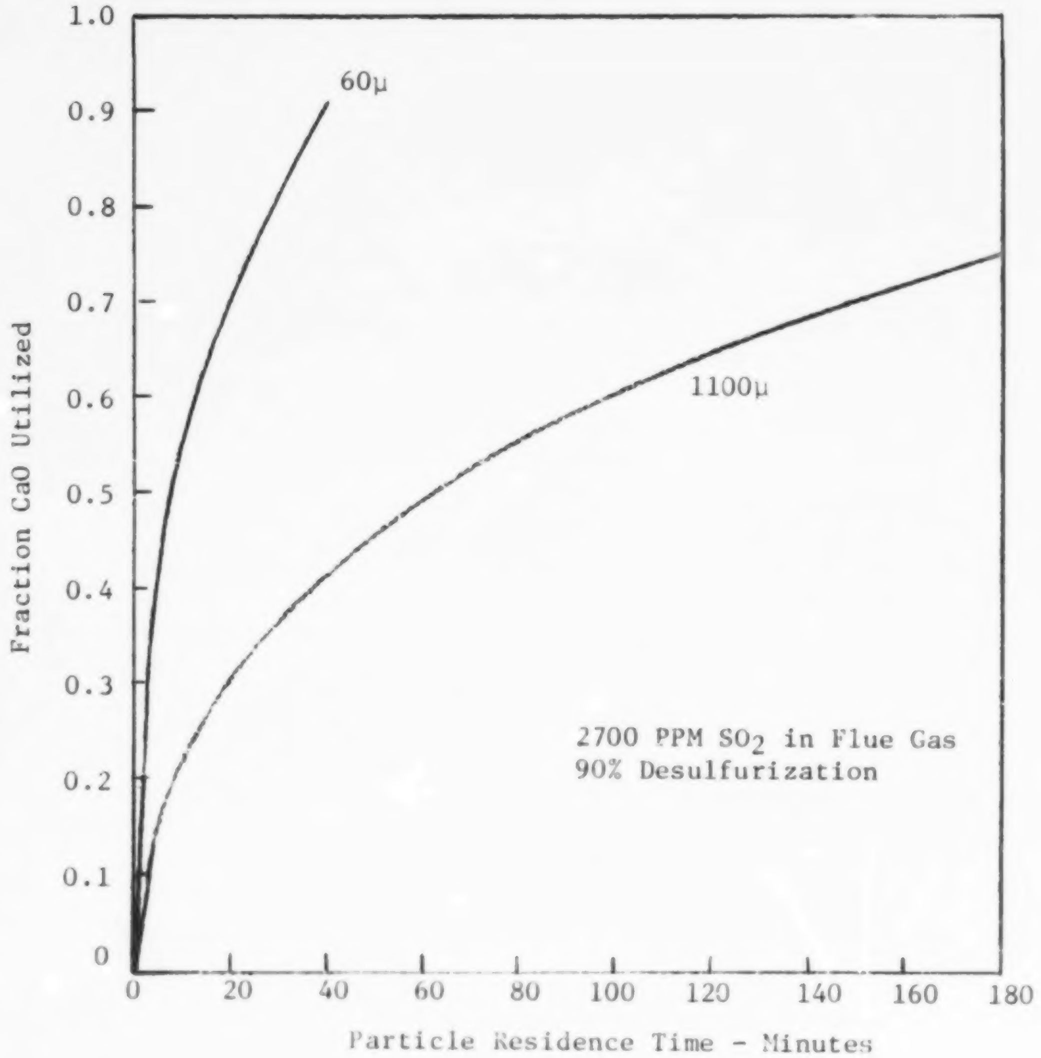

These residence time requirements for small particles would not result in a conventional fluid bed design for desulfurization but rather in the design of a high dust-loaded transfer line reactor using many stages of very large cyclones for solids recycle. An analysis of such a design, detailed in Appendix VII, indicates the process to be economically unattractive and of questionable technical feasibility.

In an attempt to reduce costs by decreasing cyclone requirements and designing a more conventional fluid bed, the "hetero-reactor concept" was investigated. The hetero-reactor concept involves the use of coarse particles in conjunction with fine particles to prevent the immediate entrainment of the latter, while still obtaining the benefit of its high reactivity. An analysis was made of the expected performance of a hetero-fluid bed reactor assuming that a settled bed height of 2 ft. would be required to obtain the necessary gas-solids contacting for removing 90% of the SO_2 from the flue gas. With this bed height, stoichiometric addition of 1100μ fresh sorbent would provide an average residence time of about 8 hours. Calculations based on Figure 17 and the model developed in Appendix VI indicate that the particle utilization would be 90% without any fine particles present so there would be no advantage in using them. The situation changes somewhat if suitable gas-solids contacting can be obtained with a bed height of only 1 ft. In this case, the average particle residence time is reduced to about 4 hours. At stoichiometric addition, this is unable to provide 90% desulfurization with only the coarse particles present. If reactor operation at a one-foot settled bed height can be achieved, then it is necessary to consider the cost savings from use of a lower bed height as compared to the cost of using both coarse and fine particles in a hetero-reactor operation. For a one-foot settled bed height, the operating cost savings for a fluid-bed desulfurizer sufficient to treat the flue gas from a 800 MW power plant are estimated to be about \$195,000/yr or 8¢/ton coal burned (Appendix VII). Based on an annual N-1337 dolomite requirement of 548 tons/year for a 1.0 stoichiometric feed rate, this operating cost savings can support an expenditure of about \$0.36 per ton of sorbent for operation of the hetero-reactor system. This cost savings assumes no treatment of the coarse sorbent is necessary to prevent immediate entrainment of the fines. In experiments we have made with a hetero reactor, this has not been found to be the case. Observed fine particle residence times have been about the same as gas residence times indicating almost immediate entrainment. In a one foot bed, such low residence times would give an even lower utilization to the fine particles than to the coarse ones. It is likely therefore that some treatment of the coarse sorbent would be required to provide a surface capable of holding the fine particles. Such treatment would undoubtedly cost more than \$.36/ton limestone. Coupled with the improbability of a one foot bed being able to provide sufficiently good gas-solids contacting, the hetero-reactor concept is judged to offer no advantage over a coarse particle system.

4.4. Miscellaneous Studies of Coarse Sorbent Fluid Bed Desulfurization

Three additional factors were studied that could effect the use of coarse limestone or dolomitic sorbent in a fluid bed flue gas desulfurization process. These factors are sorbent attrition, calcination and interaction with hot fly-ash.

4.4.1. Sorbent Attrition Rate

Attrition, followed by elutriation, is important in a coarse-particle bed, since it causes sorbent to be transported out of the reactor before full utilization has occurred. By measuring the amount of material entrained overhead in a run, a measure of stone stability can be obtained. Particles entrained out of the bed will be those fragments whose terminal velocities are less than the gas velocity through the disengaging section of the laboratory reactor.

A systematic study of the attrition of calcined dolomite N-1337 was made to ascertain the effect of gas velocity on particle break-up. Figure 18 shows the increase in attrition plotted against ($U-U_o$), the actual minus the minimum fluidizing velocity. $U-U_o$ is used since no attrition would be expected below the minimum fluidization velocity, the transition point from a static bed to the fluidized attriting stage.

Although the number of stones tested was limited, a comparison of calcined particles' attrition rates showed the dolomite to have less physical integrity than high CaO lime particles.

Table 10

Relative Attrition of Limestones

Measured from overhead loss of calcined materials in initial desulfurization

Stone No., N-	Relative Attrition Rates
1337 (dolomite)	1
1343 (ferrous limestone)	0.125
1359 (limestone)	0.185

The data from Figure 18 and Table 10 were used for an approximation of the expected attrition in a high velocity, large fluidized bed in Section 6. where the design of a commercial-size reactor is described.

Figure 18

Effect of Velocity on Particle Attrition

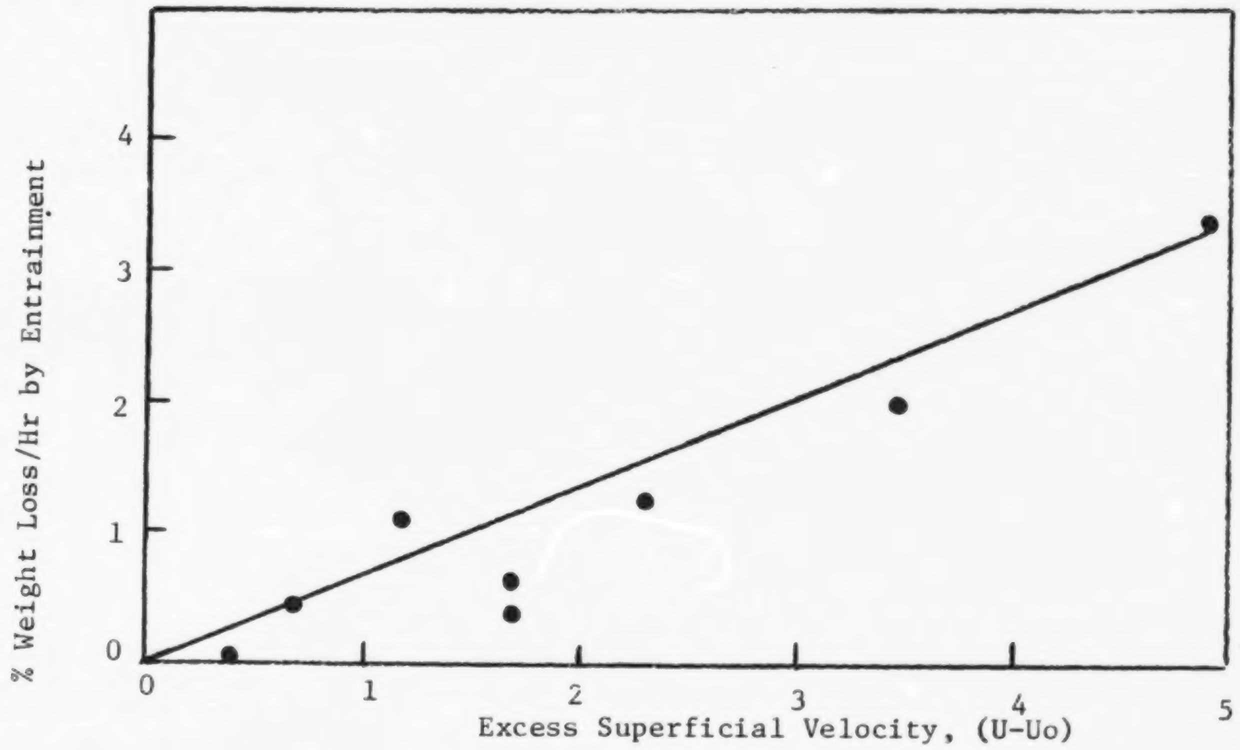

4.4.2. Calcination in a Continuously Operated Bed

The use of uncalcined limestone as sorbent make-up to the fluid bed is naturally preferred to the use of the more expensive precalcined stone. To confirm that uncalcined sorbent could be charged to a fluid bed desulfurization process, parallel runs were made in which the stoichiometric quantities of calcined and uncalcined 70 to 100 mesh N-1337 particles needed to react with 85% of the incoming SO_2, were added at 5 minute intervals to a gently fluidizing (V = 1.6 ft/sec) 200 cm^3 bed of 70 to 100 mesh glass particles. The measured outlet SO_2 concentration plots were almost exactly identical, indicating that the reaction characteristics of prior-calcined and bed-calcined particles were the same.

In view of these runs it is apparent that raw carbonate stone, previously ground to proper size, can be used as a feed material to a large, continuously operating unit.

4.4.3. Effect of Fly-Ash

The effect of fly ash was evaluated by adding about 3-5% fly ash to the bed of sorbent prior to an experimental run. The bed could then be brought to temperature with either a trickle flow of gas or gas flowing at full velocity.

The following two points were demonstrated in the fly-ash studies: (1) coal fly-ash does not stick or agglomerate with lime particles in the desulfurization reactor at 1600°F, and (2) fly-ash elutriates out of the bed at fluidizing velocities equal to or greater than 2 ft/sec. Thus, fly-ash should have no detrimental effect on the adsorption of SO_2 in the proposed fluidized bed reactor.

5. REGENERATION STUDIES

The regeneration of sulfated sorbent was investigated as a way of reducing fresh stone requirements, and as a way of producing a saleable by-product to reduce processing costs.

5.1. Thermodynamic Considerations in Sorbent Regeneration

The limestone regeneration technique investigated in this program involves the reaction of partially sulfated sorbent with reducing gas at high temperatures. Under appropriate reducing conditions, reactions (10) and (11) shown below can be made to predominate. They yield regenerated CaO and a concentrated SO_2 stream. Competing with these two reactions are reactions (12), (13) and (14) which can also take place under reducing conditions.

$$(10)\ CaSO_4 + CO \longrightarrow CaO + SO_2 + CO_2$$

$$(11)\ CaSO_4 + H_2 \longrightarrow CaO + SO_2 + H_2O$$

$$(12)\ CaSO_4 + 4CO \longrightarrow CaS + 4CO_2$$

$$(13)\ CaSO_4 + 4H_2 \longrightarrow CaS + 4H_2O$$

$$(14)\ 3CaSO_4 + CaS \longrightarrow 4CaO + 4SO_2$$

Reactions (12) and (13) are undesirable since they convert sulfate to sulfide without liberation of SO_2, and they consume large amounts of reductant.

To study conditions under which the desired reaction would be predominant, analyses were made of the equilibrium relationships of the system represented by the above equation. Equilibrium data calculated by Wheelock & Boylan (9) were used initially to provide a qualitative picture of the $CaSO_4$ reduction system. These data showed that reactions (10), (11) and (14) were favored by high temperatures while the other reactions were favored at lower temperatures. Gas composition had an effect through the CO/CO_2 and H_2/H_2O ratios. High ratios promoted a high SO_2 concentration via reaction (10) and (11) but also promoted reactions (12) and (13) to an even greater extent (i.e., the equilibrium for these reactions depends on the fourth power of the CO/CO_2 and H_2/H_2O ratios). A ratio of 1/2 produced mostly CaO and SO_2 in preference to CaS at most temperatures.

In order to quantify these effects of temperature and gas composition, equilibrium compositions for both the solid and gas phases were calculated for a series of hypothetical regeneration systems. These calculations were made by a high speed digital IBM 7090 Computer using a program developed by the Rand Corporation (10,11). The Rand program calculates the equilibrium composition of a system - subject to material balance restraints - by minimizing the free energy of the system. A partial summary of the results obtained using this program are given in Table 11. It can be seen that temperatures above 1300°K (1880°F) are required for regeneration by CO or H_2 of the sulfate to the oxide. At lower temperatures, the reaction proceeds to the sulfide, while temperatures above 1400°K (2060°F) offer no advantage in terms of equilibrium conversion. It should be noted that complete conversion of $CaSO_4$ to CaS, without SO_2 formation, is predicted for reduction with pure methane at 2240°F.

Table 11

Equilibrium Reduction of $CaSO_4$

	Inlet Gas Composition, Mole %					Outlet Gas Composition Mole %				% of Reacted $CaSO_4$ Converted to	
Temp, °F	CO	H_2	CO_2	H_2O	N_2	SO_2	CO_2	H_2O	N_2	CaO	CaS
1880	5	0	10	0	85	0	15	0	85	0	100
1880	0	5	0	10	85	0	0	15	85	0	100
1880	10	0	20	0	70	0	30	0	70	0	100
1880	0	10	0	20	70	0	0	30	70	0	100
1880	15	0	30	0	55	0	45	0	55	0	100
1880	0	15	0	30	55	0	0	45	50	0	100
2060	5	0	10	0	85	4.0	14.4	0	81.6	95	5
2060	0	5	0	10	85	4.0	0	14.4	81.6	95	5
2060	10	0	20	0	70	7.7	27.7	0	64.6	95	5
2060	0	10	0	20	70	7.7	0	27.7	64.6	95	5
2060	15	0	30	0	55	11.1	40	0	48.8	95	5
2240	5	0	10	0	85	3.9	14.4	0	81.7	94	6
2240	0	5	0	10	85	3.9	0	14.4	81.7	94	6
2240	0	10	0	20	70	7.5	0	27.7	64.8	94	6
2240	15	0	30	0	55	10.7	40.2	0	49.1	94	6
2240	10	15	0	30	55	10.8	0	40.2	49.0	94	6
2240	---- 100% CH_4 ------					0	33.3	66.7	0	0	100

Table 11 shows SO_2 concentrations ranging up to about 11 mole %. Higher SO_2 concentrations would have been predicted had reducing gases been specified with CO plus H_2 concentrations in excess of 15%. The problem, however, with using a more strongly reducing gas is one of maintaining the regenerator in thermal balance. This problem is more easily explained with reference to Figure 19 which shows a material and thermal balance for the regenerator. Entering the regenerator is partially-sulfated sorbent at the temperature existing in the desulfurizing bed; i.e., 1600°F. The sorbent's temperature is raised to about 2000°F, and after regeneration is returned to the absorbing bed. The fluidizing gas is a high temperature reducing gas produced by the partial combustion of a fuel. At the outlet of the reactor, the gas temperature has fallen to approximately that of the bed, while its composition has changed as shown in Table 11.

The predominant reactions (10) and (11) occurring in the regenerator at 2000°F are endothermic and remove a considerable amount of

	Reaction	Heat of Reaction, ΔH Cal/g-mole @ 2060°F
(10)	$CaSO_4 + CO \longrightarrow CaO + SO_2 + CO_2$	43,400
(11)	$CaSO_4 + H_2 \longrightarrow CaO + SO_2 + H_2O$	50,800

Figure 19

Thermal Balance Diagram-Regeneration

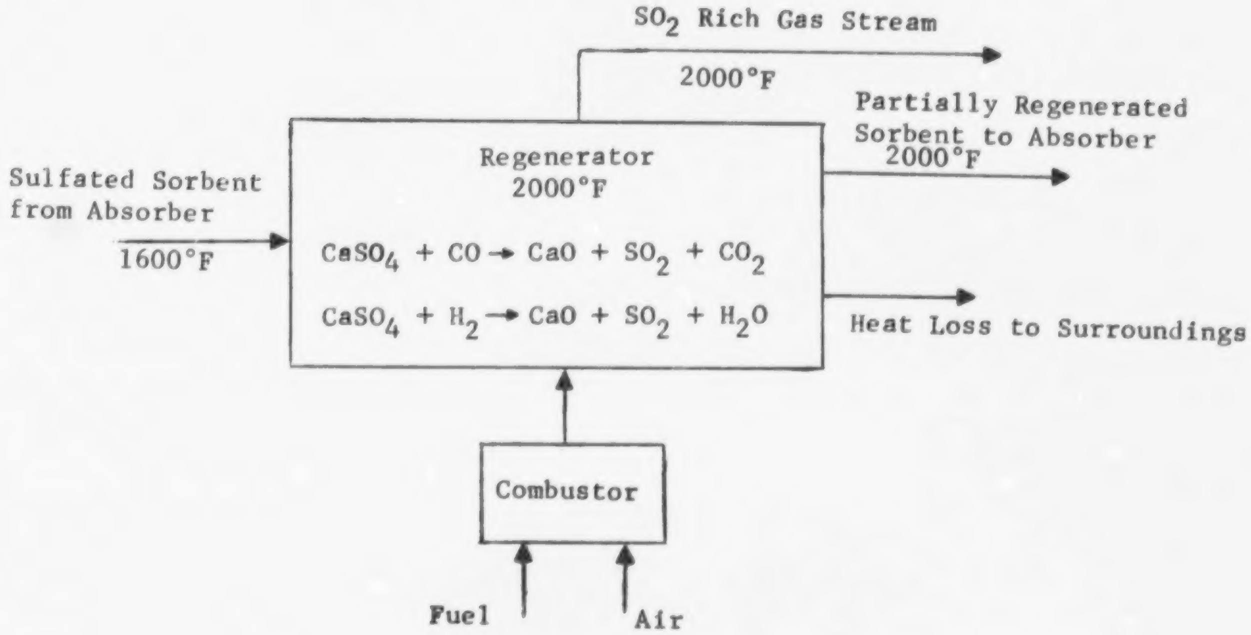
SO_2 Rich Gas Stream
2000°F
Partially Regenerated Sorbent to Absorber
2000°F
Regenerator
2000°F
$CaSO_4 + CO \rightarrow CaO + SO_2 + CO_2$
$CaSO_4 + H_2 \rightarrow CaO + SO_2 + H_2O$
Sulfated Sorbent from Absorber
1600°F
Heat Loss to Surroundings
Combustor
Fuel
Air

Figure 20

Thermal Balance of the Regenerator

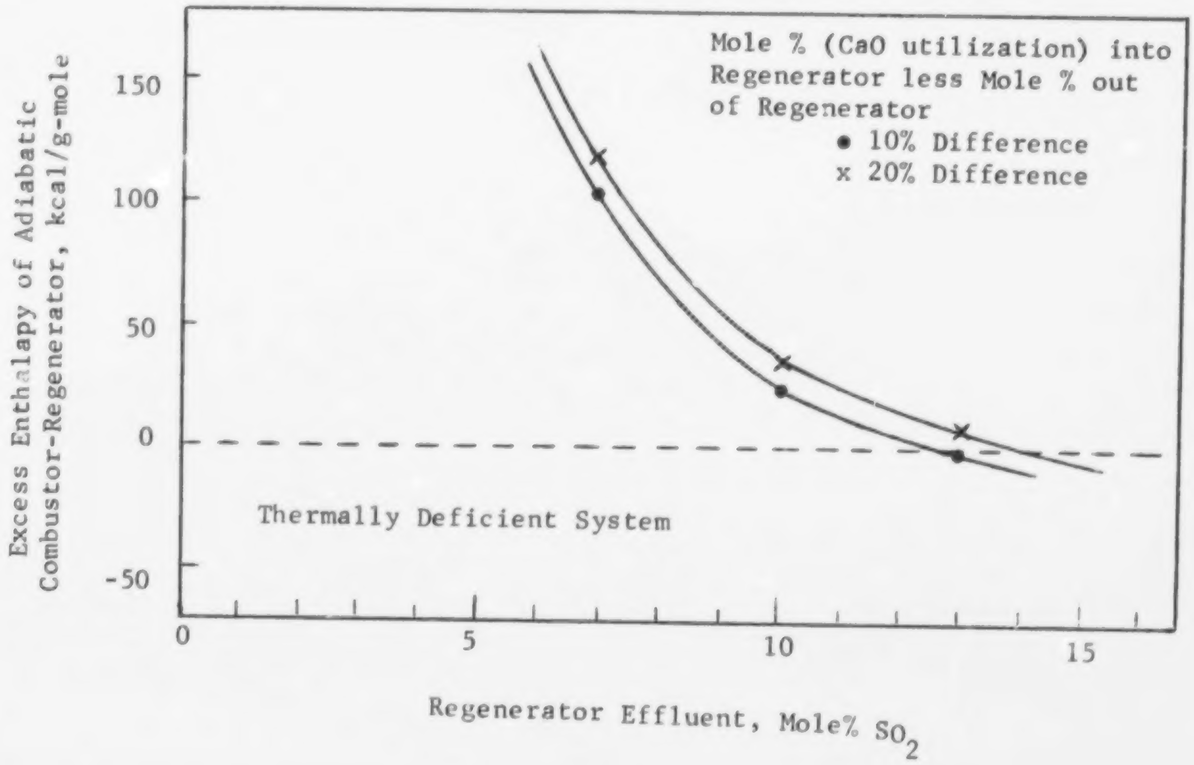

heat from the system. In addition, sensible heat is removed from the regenerator by the circulating sorbent which exits at a higher temperature than it enters. The amount of heat so removed depends on the solids circulation rate. Finally, even with a well insulated regenerator, some heat will leak to the surroundings. To maintain the regenerator temperature, these thermal requirements must be satisfied by a change in the enthalpy of the gas flowing through the system. Assuming equilibrium conditions, the inlet gas composition determines the outlet composition and therefore its enthalpy at the specific temperature (i.e., 2000°F). The composition and enthalpy of the inlet gas depend only upon the fuel used, the air to fuel ratio, and the air and fuel temperatures. In effect then, the change in enthalpy that will occur in the gas passing through the system will depend only on the inlet conditions at the combustor.

These considerations are what limit the maximum SO_2 concentration in a commercial system to about 13%. Figure 20 shows the thermal balance of a system, using coke as fuel, as a function of the SO_2 concentration in the regenerator effluent (and thus on the $CO + H_2$ concentration in the inlet gas). Curves are presented for variations in per-pass conversion of the circulating solids (mole % $CaSO_4$ in entering solids - mole % $CaSO_4$ in existing solids). Above about 13% SO_2 in the outlet gas, not enough heat from the fuel is available for endothermic reduction and the system is thermally deficient. In a real system where there is some heat loss from the regenerator to the surroundings, the tolerable SO_2 limit will actually be somewhat below this value.

5.2. Experimental Apparatus

The regeneration studies of sulfated particles were carried out in an alumina-ceramic fluidized bed unit. The equipment is pictured in Figure 21 and a schematic of the unit is shown in Figure 22. Reducing gas was made by blending H_2, CO, H_2O, CO_2 and N_2 in the desired proportions. Methane could also be used if desired and SO_2 was available for calibrating the SO_2 analyzer.

Additional provision was made for the introduction of oxygen to the reactor effluent to combust any sulfur, H_2S or COS formed during the reductiun. The reactor itself was a 2 inch i.d. alumina tube. An earlier stainless steel reactor was found to corrode badly at the 2000°F operating temperature. An inlet section of packed alumina cylinders, 1/8" x 1/8", served as a dispersing grid. The gasketed reactor tube ends were placed outside of a small Lindberg furnace. This kept the rubber gaskets at low temperatures so that they could perform through numerous duty cycles. The outlet from the fluid bed fed into an oxygen combustion chamber where any H_2S, COS, or S that might be formed could be combusted, and then into a cyclone filter and water condenser.

As in the absorption experiments, sulfur dioxide measurement was performed by an infra-red Beckman analyzer (IR 315A). The range of the instrument was selected for 0-15M% SO_2 in the effluent. It was calibrated as outlined in the desulfurization kinetic studies (Section 3.1.3).

Figure 21

Fluidized Bed
Regeneration Unit

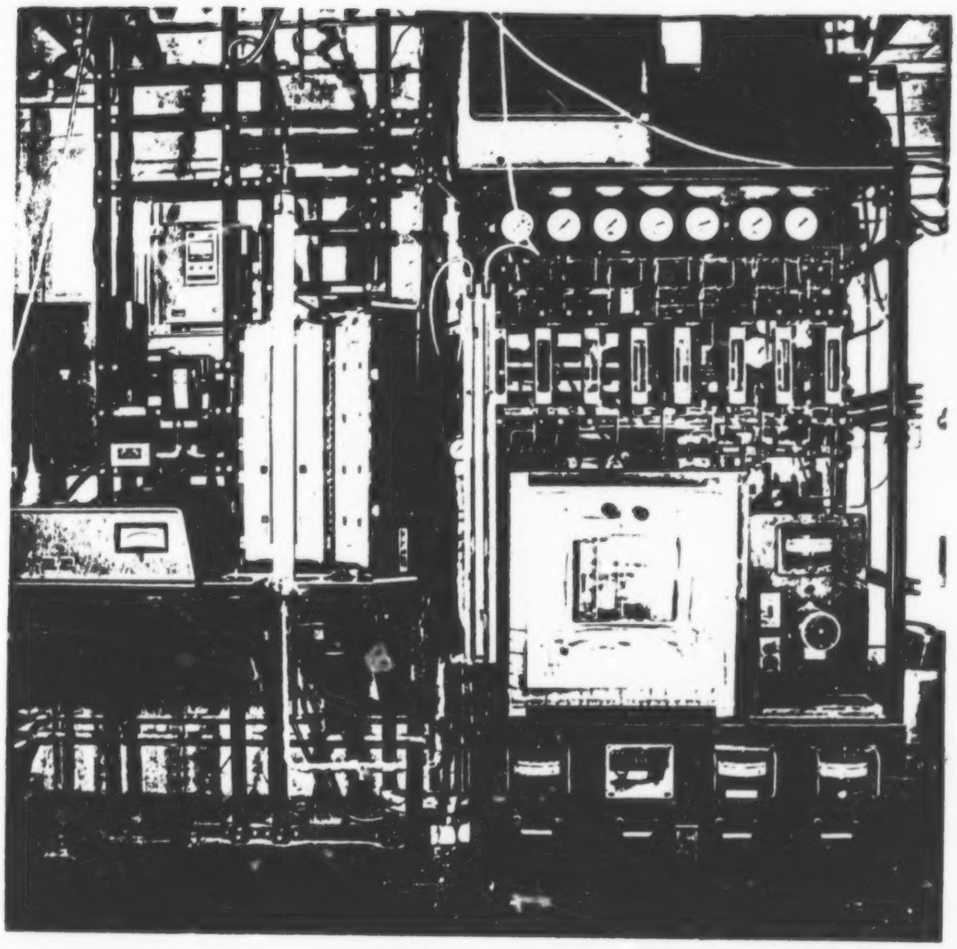

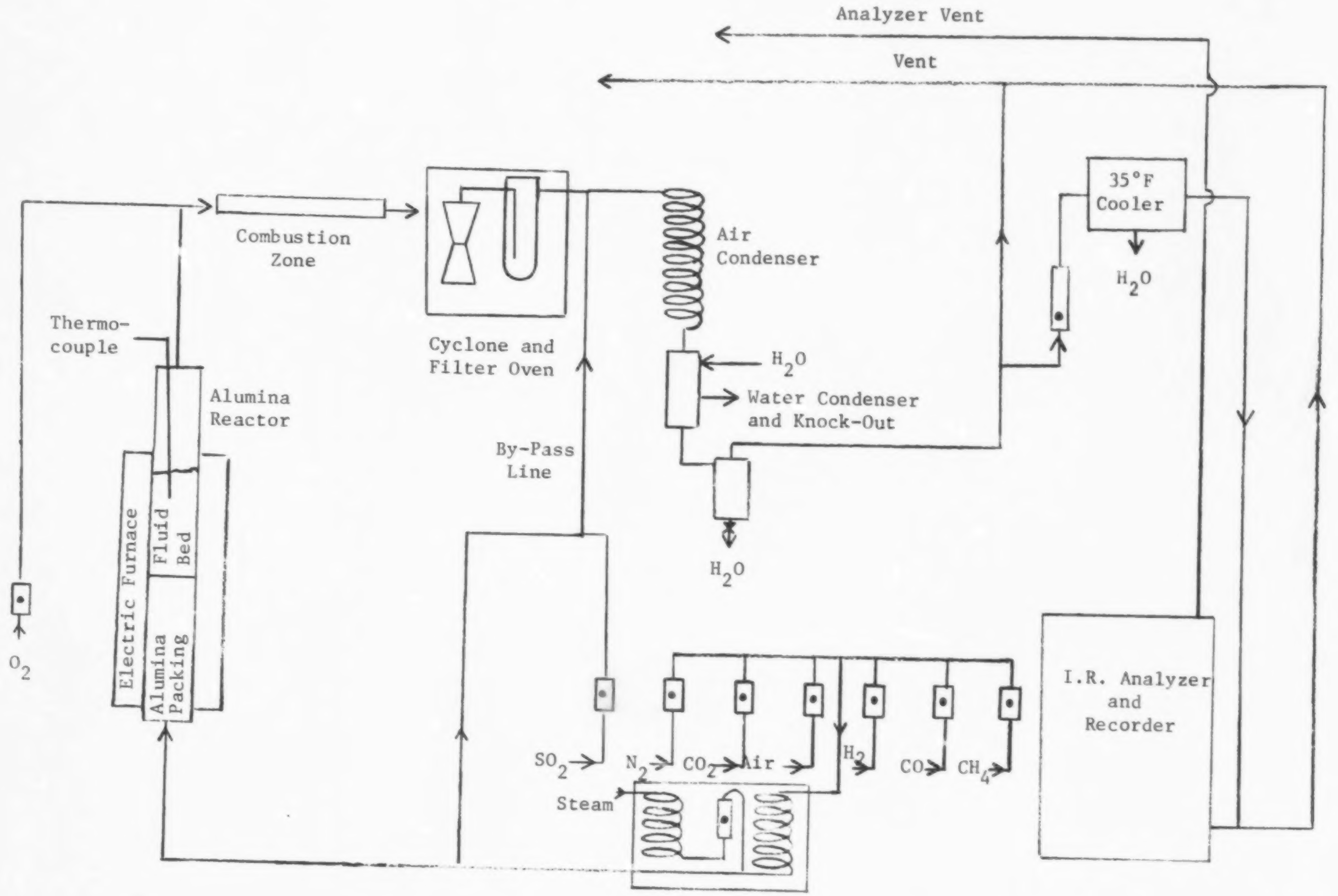
Analyzer Vent
Vent
Combustion Zone
Cyclone and Filter Oven
Air Condenser
35°F Cooler
H_2O
Thermo-couple
Alumina Reactor
H_2O
Water Condenser and Knock-Out
By-Pass Line
Electric Furnace
Fluid Bed
Alumina Packing
H_2O
O_2
I.R. Analyzer and Recorder
SO_2
N_2
CO_2
Air
H_2
CO
CH_4
Steam

Figure 22. Flow Diagram for the Fluidized Bed Regeneration Unit

5.3. Experimental Procedures

In the regeneration studies, different reducing conditions were first employed to determine operating conditions for achieving high SO_2 effluent concentrations. Reductants were CO, H_2 and CH_4, as obtained from commercial gas cylinders. Limestone particles were first sulfated by reaction with simulated flue gas. Direct reduction on commercial calcium and magnesium sulfates was also carried out in these preliminary studies.

To determine the cyclic capacities of regenerated sorbents, a batch of material would be subjected to repeated cycles of adsorption and regeneration. In these cyclic experiments, both the adsorption and the regeneration were run in the regenerator unit so as not to expose the particles to unnecessary temperature variations or air. Adsorption was performed first, following the desulfurization procedures outlined in Section 3.2. Upon termination of the absorption phase, nitrogen alone was passed through the bed to keep it fluidized while the temperature was raised for regeneration. The reductant mixture was then intorduced and maintained until regeneration was complete. The SO_2 effluent concentration was continuously monitored during a cycle. Regeneration yielded a reactive material for reuse as a desulfurizer. Weighings of the discharge were performed after each complete cycle as a check on loss of material through attrition and of actual sulfation changes as obtained from recorder charts. Differences of only 1-2% were recorded on average, well within experimental error, which indicates that no systematic error was occurring.

5.4. Regeneration-Definition Studies

5.4.1. Reduction of $CaSO_4$

Initial experiments with $CaSO_4$ (i.e., anhydrite) demonstrated that SO_2 was generated by a reducing gas containing CO or H_2. The SO_2 effluent concentrations obtained for 10 and 15 mole % reducing gas at various temperatures are compared to equilibrium predictions in Figure 23. Hydrogen appeared to produce higher SO_2 concentrations than CO, but not enough data were obtained to reach a definite conclusion on this. In the partial combustion of coal or hydrocarbons to produce the reducing gas , normally a 2/1 ratio of $(CO/CO_2)/(H_2/H_2O)$ is dictated by equilibrium for $(CH_2)_n$ fuel. Thus, mostly CO would be present in a commercial reducing gas and any small difference in reactivity between CO and H_2 can be neglected.

Figure 23

Sulfur Dioxide in Regeneration Effluent

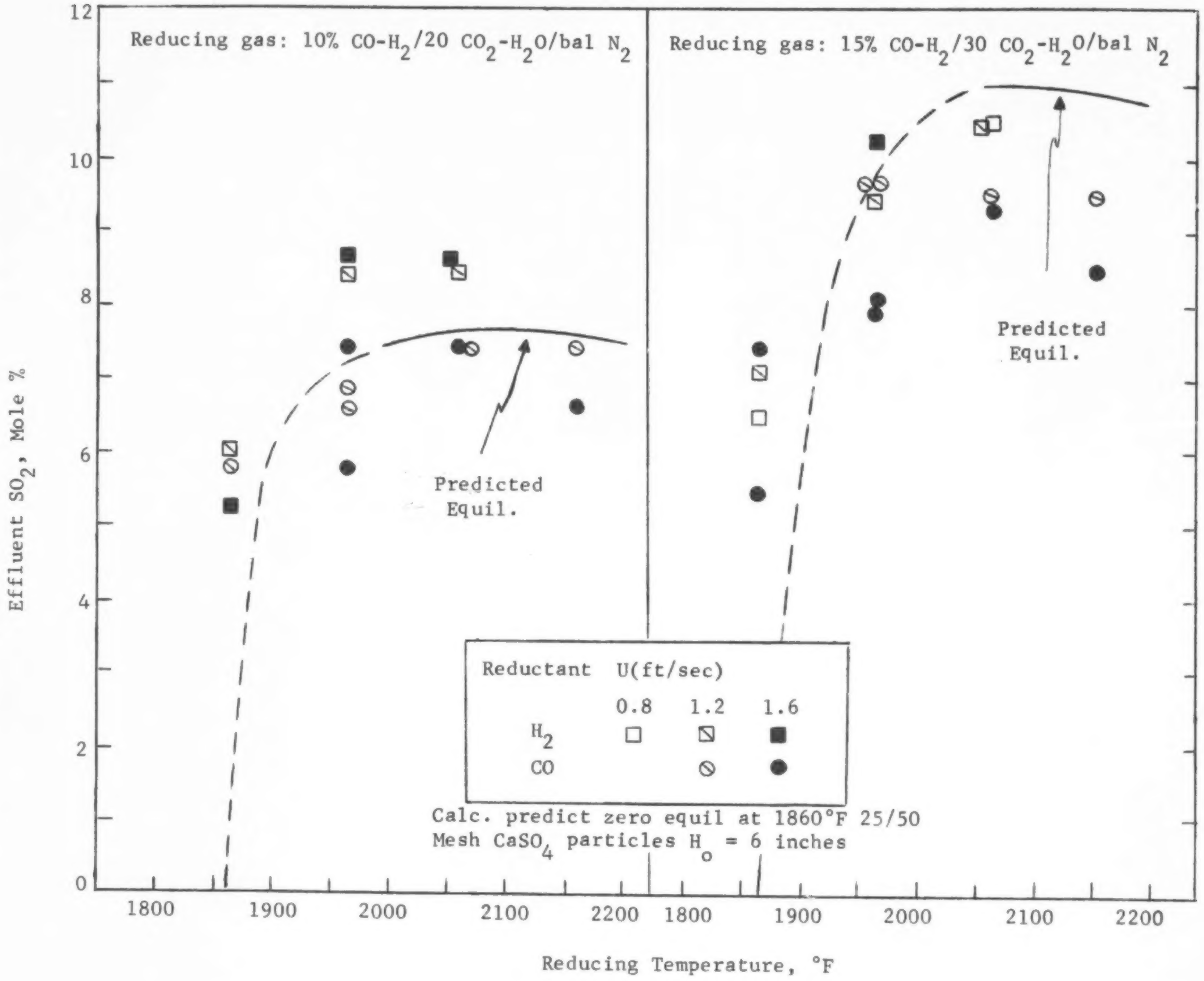

Calc. predict zero equil at 1860°F 25/50 Mesh CaSO$_4$ particles H$_o$ = 6 inches

Reducing conditions were kept mild by the use of a 1:2 ratio of reductant to its oxidized species in order to inhibit calcium sulfide formation during reduction.

Reduction of partially sulfated limestone and dolomites also was accomplished readily with CO/CO_2 mixtures. A typical chart record obtained of a batch reduction of a fluid bed of sulfated limestone is presented in Figure 24. With good gas-solids contacting, the SO_2 level in the effluent was found to depend on reductant concentration, as in the case of anhydrite reduction. The maximum level was quite independent of the amount of SO_2 absorbed by the different stones.

Figure 24

Typical Record of Regeneration Effluent

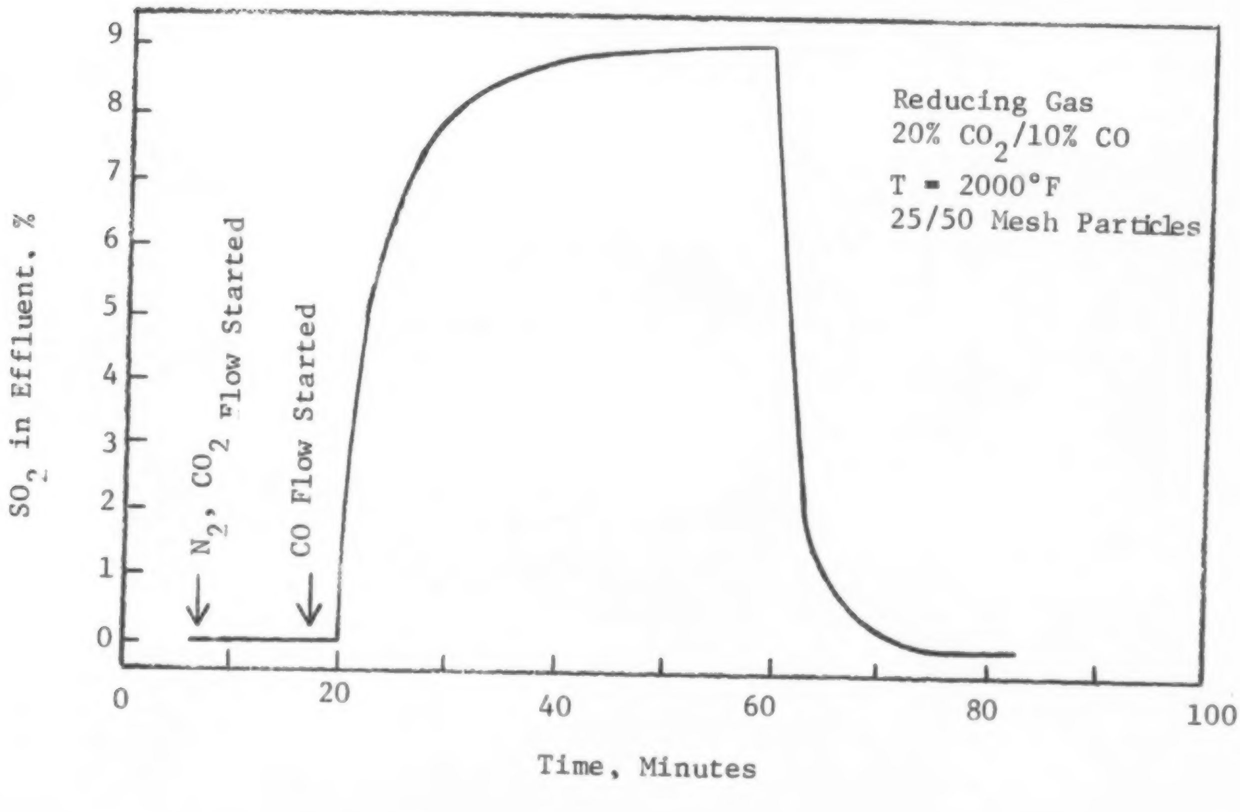

It is worth mentioning that the time lag, t_h, for holdup in the system from feed to recorder was about 1.5 minutes at U=2 ft/sec. However, on given occasions, it was noticed that if the reductant flow were stopped, SO_2 was observed in the effluent at the plateau level up to $7 \cdot t_h$ times before falling to zero concentration, which indicates a mixing or desorption control mechanism.

An increase in the ratio of CO_2/CO or H_2O/H_2 from 2:1 did not increase the SO_2 effluent concentrations. However, it should be pointed out that approximately 90% efficiency of the reducing species to produce SO_2 was already occurring. Lowering the CO_2/CO or H_2O/H_2 ratio, on the other hand, did decrease the SO_2 level. With pure H_2 plus inert N_2, only 25-30% efficiency of reductant to produce SO_2 was achieved. CaS formed, as well as H_2S. The ratio of $CaS/(CaO + SO_2)$ in the effluent was determined to be about 5:2.

With particles larger than 25/50 mesh, difficulties encountered with fluidization agglomeration (discussed in Section 5.4.3.) produced low SO_2 concentrations and caused uncertainties in the analysis of regeneration of these sized particles. However, experiments were made in a 5/8" i.d. packed bed and these indicated that regeneration rates with particles up to 2.5 mm in size are comparable to rates with the small diameter stones.

Reduction with methane did not proceed readily. Methane, in the presence of CO_2 and H_2O did react with sulfates material to evolve some SO_2, but the SO_2 concentration was significantly lower than that obtained with CO or H_2 (Table 12). The results with a CH_4/N_2 feed produced about one SO_2 molecule per methane molecule, in contradiction to thermodynamic analysis which predicts no SO_2 at equilibrium, but this is still unsatisfactory for sulfated sorbent regeneration.

Table 12

Sulfur Dioxide Concentration From Methane Reduction of Calcium Sulfate

Gas Flow = 2 ft/sec
Mole Ratio = 2:1, Balance N_2

	% SO_2 in Effluent			
% Methane	1900°F	1950°F	2000°F	2050°F
5	1.5	2.3	2.5	--
10	2.5	4.5	4.3-5.0	6.0

With all reductants, the SO_2 concentration in the reactor effluent was found to have about a first order dependence on the inlet reductant concentration in the range 5-15%. With CO or H_2, reduction appears to be equilibrium limited, as may be deduced from the equilibrium comparisons of Figure 23 and the fact that a SO_2 concentration plateau is maintained until exhaustion of the sulfate in the stone (Figure 24).

The low SO_2 effluent concentrations with CH_4 reduction are too low for practical use as feed to a sulfuric acid plant. However, the 8 to 10% sulfur dioxide effluent levels that are obtained with CO/H_2 reduction are high enough to serve as a feedstock for by-product processing in a H_2SO_4 plant.

5.4.2. Sorbent Reactivity After First Reduction

As shown in Section 4.2.3., magnesium oxide does not react with sulfur dioxide in a flue gas to any appreciable extent. This is true even of MgO formed by reducing $MgSO_4$. Thus, the fact that magnesium sulfate can be reduced at temperatures as low as 1400°F cannot be profitably utilized in a regenerative desulfurization system.

However, calcium oxide does exhibit reactivity for sulfur dioxide after its formation by the reduction of calcium sulfate. In fact, flue gas desulfurization by once-regenerated particles proceeded at greater rates than that obtained with freshly calcined limestone. A comparison is presented in Table 13.

Table 13

Reaction Rate Coefficient of Once Regenerated Materials

Desulfurization, 1600°F; U = 2 ft/sec; 25/50 Mesh Particles
Regeneration Temp., 2000°F; Desulfurization in ceramic unit
X = Fraction of CaO utilized

Material	Reaction Rate Coefficient (sec^{-1}) Unregenerated	Regenerated
$CaSO_4$ Anhydrite		
X = 0.50	--	9-22
Dolomite (1337)		
X = 0.52	8	45-50
X = 0.56	1-2	41.5
X = 0.72	~ 0	16
Limestone (1359)		
X = 0.25	4.5	30
X = 0.47	~0	3.5

5.4.3. Agglomeration

5.4.3.1. Fly Ash Effects

Experiments were made to determine the effect of fly ash and sorbent agglomeration during high temperature regeneration. Experimentally, the procedure was to add about 3-5% fly ash to a bed patch prior to an experimental run. The bed was then brought to temperature, about 2000°F, with either a trickle flow of gas, or gas flowing at full velocity.

Agglomerated lumps of sorbent and fly ash (and fly ash alone) were found and these caused uneven fluidization and thus subsequent uneven, lower SO_2 concentrations in the regenerator effluent. The lumps clogged the reactor, as found by examination at the conclusion of a run. The lumps were fragile to physical shock at room temperature, but their strength characteristics at high temperature are unknown.

The discovery of high temperature particle-fly ash agglomeration might create problems in an actual commercial regenerator. If the fly-ash is transported out of the reactor before temperature (and agglomeration) can be reached and is not returned by the cyclones, no serious consequences would develop. If partial combustion of coal is used to produce the reducing gas, the fly ash will already be at temperature and agglomeration difficulties could occur.

5.4.3.2. Self-Agglomeration Without Fly-Ash

It has been definitely established that self-agglomeration of sorbent particles can occur at temperatures near 2000-2100°F. This phenomenon appears possible without the necessity of iron or silica agents as fluxing materials (i.e., fly-ash), although the presence of ferrous materials enhances agglomeration. During one experiment investigating reduction characteristics, calcium sulfate particles (pure material) formed a semi-solid cylinder from the great majority of particles in the batch. Other experiments produced smaller agglomerated lumps. These lumps are very fragile at room temperature and fall apart at touch, similar to the fly-ash agglomerated lumps. It appears that this agglomeration problem becomes more acute as the temperature is raised.

Some problems could occur in fluidization in the regenerator, based on this evidence, which would result in gas by-passing, low reductant utilization, and low SO_2 concentrations in the effluent gas. However, providing sufficient fluid bed agitation, whether by mechanical stirring or preferably by better fluidization, should alleviate the type of agglomeration as a potential problem.

5.4.4. Possible Sulfite Formation and Thermal Regeneration

Thermodynamic analysis indicated that thermal decomposition of calcium sulfate begins near 2450°F while the sulfite begins to decompose near 1200°F. Apparently, however, either a molecular form of $CaSO_3$ or a strongly sorbed SO_2 species can exist to much higher temperatures in lime. This was shown by passing a gas of SO_2 (1%)/N_2/CO_2 (but without oxygen) through a fluidized bed of lime at 1600°F. The gas was desulfurized efficiently until about 40% of the stone was utilized. Undoubtedly some disproportionation of $CaSO_3$ to CaS and $CaSO_4$ also occurred. At 2000°F, a feed stream of pure N_2 produced an effluent stream of about 14% SO_2. About two thirds of the sorbed sulfur compounds were stripped by this procedure, indicating that a sulfur dioxide/sulfite specie was present in large amounts.

Although formation of $CaSO_3$ is preferred from the standpoint of regeneration, this phenomenon would be difficult to utilize. Efficient combustion demands that excess oxygen be present since sub-stoichiometric (and near-stoichiometric) combustion produces H_2S, COS and unburned carbon. Under excess oxygen conditions, the formation of $CaSO_4$ would predominate.

5.5. Cyclic Performance

5.5.1. Reactivity of Cycled Sorbents

Particles of limestone N-1359, dolomite N-1337, and calcium sulfate anhydrite were used in a cyclic sequence series of experiments on flue gas desulfurization and regeneration. All three materials were found to retain sorption reactivity upon cycling. The data for lime N-1359, for absorption are presented in Figures 25 and 26. Small correction factors have been applied to the data in Figure 26 for variations in bed height and gas velocity so that all the data refer to the same initial conditions. Note that the reactivity first increases with cycling, then decreases with further use, but even after 8 cycles (approximately 115 hours in the hot fluid bed) the capacity of the stone was still equal to the initial capacity. In contrast, the desulfurization reactivity of anhydrite dropped from the first cycle towards 30-50% of the initial activity after 4-5 cycles.

The good maintenance of reactivity upon cycling of the limestone suggests the use of such material in a continuous recycle system. As expected, continued cycling did eventually cause a decline in capacity as "dead-burning" of the stones presumably occurred from exposure to the regenerator temperature of 2000°F. It is known that dead-burning begins to occur at about 1900°F (12). Dead-burning decreases reactivity by decreasing the porosity of the particle as it rearranges into a more packed material. This limits diffusion paths into the particle and provides a limit to the reaction rate.

Figure 25

Breakthrough Curves on Cycling

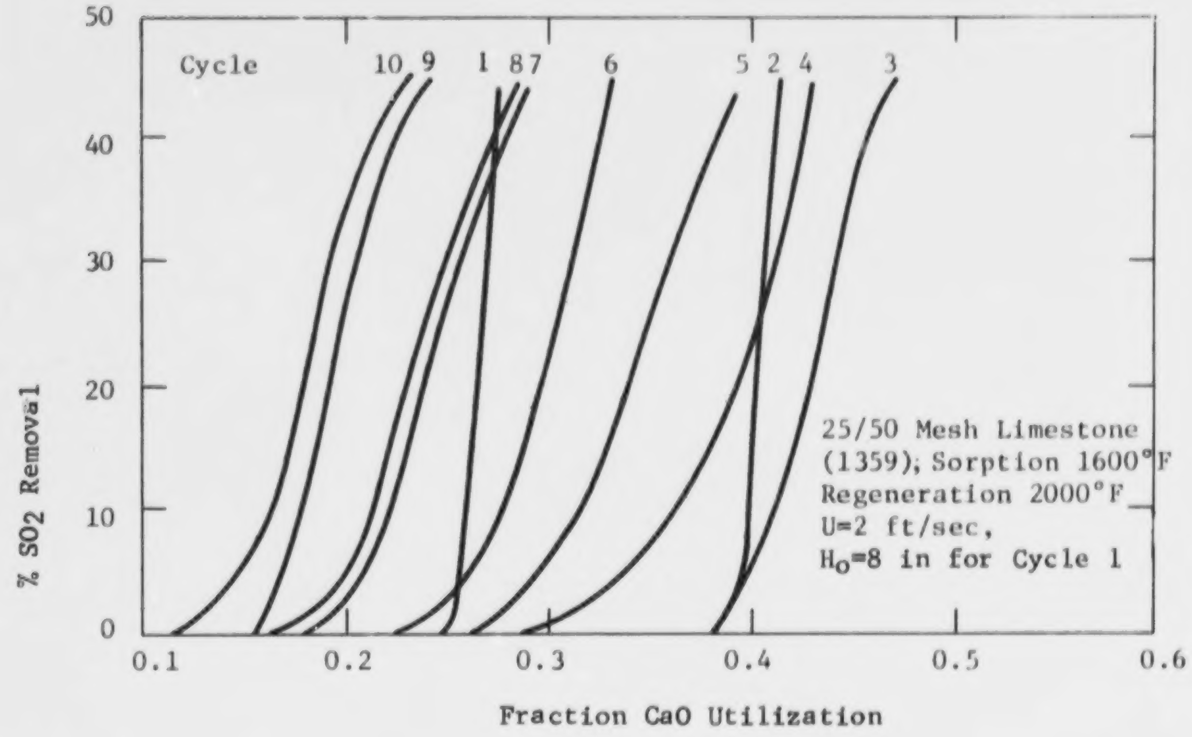

Figure 26

Desulfurization Reactivity Upon Cycling

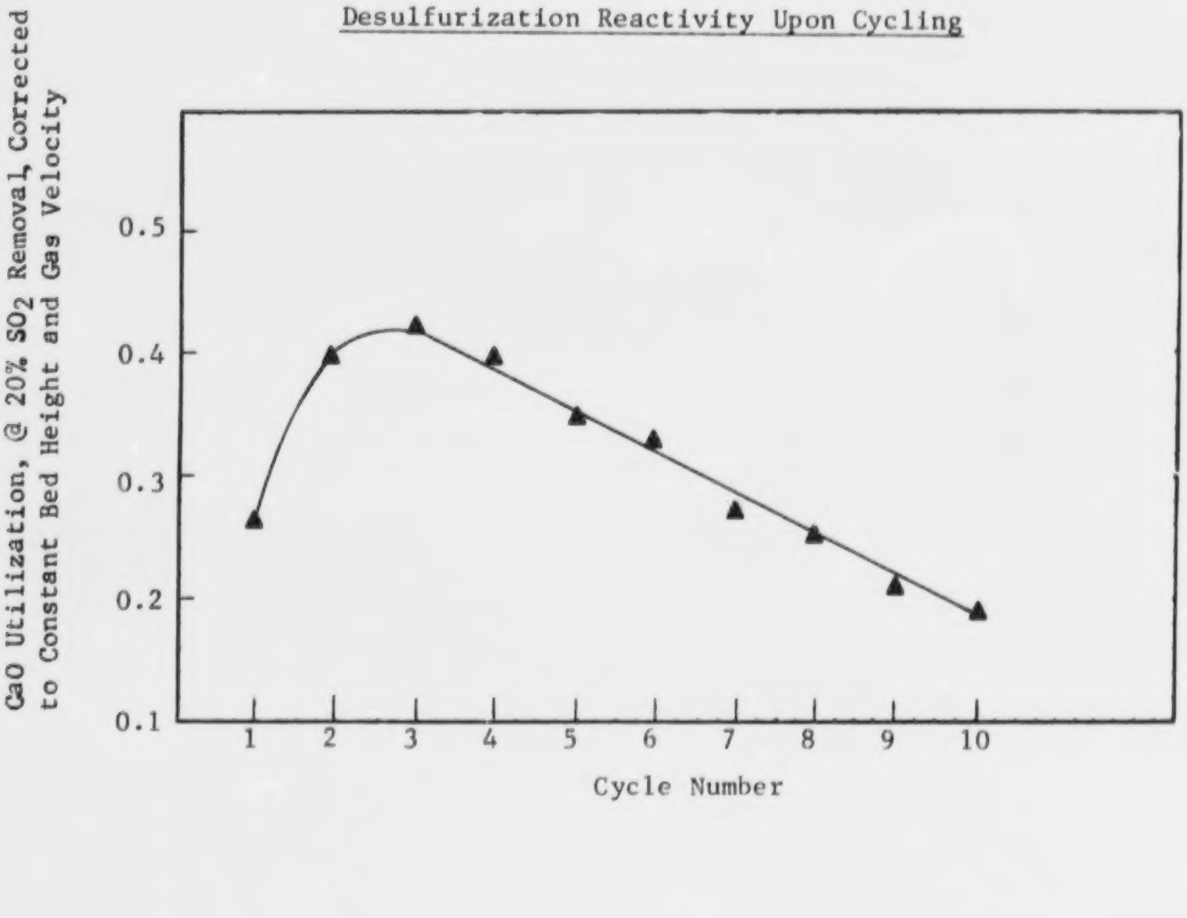

The initial increase in reactivity upon cycling is speculated to be due to a change in the physical structure of the particle. Upon calcination, a porous macroscopic structure is formed, while molecular vacancies are formed by evolution of CO_2 from the carbonate. Time is required for reorientation-expansion of the molecular spacing, presumed necessary in order to accommodate a sulfate group. However, upon regeneration and evolution of SO_2, the molecular spacing remains as reoriented to provide a more reactive, accommodating particle. The opposite phenomenon of dead-burning soon overshadows molecular reorientation, however, and the capacity begins to decrease. Calcined dolomite also exhibited this phenomenon of initial activity increase (Table 13). On the other hand, calcium oxide generated from anhydrite had an initial large reactivity which decreased rapidly with cycling as dead-burning occurred. In this case geometric accommodation already was present and no molecular reorientation was possible or necessary.

From this speculation, one would predict that the important parameter limiting cyclic capacity is exposure time to the high (2000°F) regeneration temperatures, rather than cycle number per se. In the experiments with the lime (1359), the sorbent received exposures of 15-20 hours to dead-burning temperatures, including experimental adjustments, etc., but only 4-6 hours of actual reduction time were used. In an efficient closed-circulation system, it would thus seem that the number of cycles equivalent to 15 hours of high temperature exposure should be possible before there is a loss in sorbent reactivity below the initial rate.

Anhydrite, as well as limestone, might be suitable for use in a recycle, regenerative system. The desulfurization rate for the anhydrite is high enough initially that the faster activity decrease can be tolerated, and still the average sorbent utilization would be as high or higher than lime (1359). This would need to be verified more fully, however, if anhydrite or gypsum were to be used as a sorbent.

5.5.2. Reduction Efficiency of Cycled Sorbents

The time dependence of the effluent SO_2 concentration from batch reduction had a typical history, depicted earlier in Figure 24, for all the runs of a series of cycle experiments. The maximum SO_2 plateau level was maintained near 9% for each cycle as Figure 27 indicates.

Figure 27

Effluent From Regenerator-Cyclic Performance

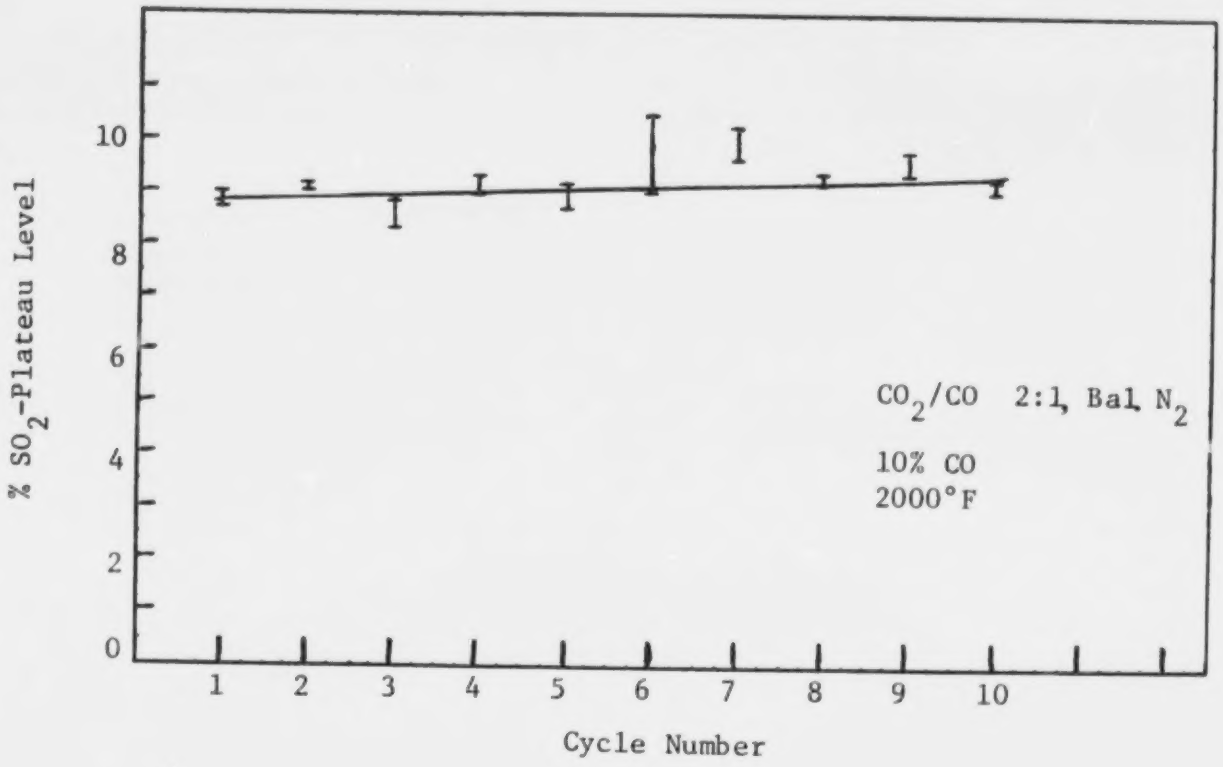

Regeneration was complete each cycle. Graphical integration of time records of SO_2 in effluent streams found fair-to-good calculated material balance between absorption and regeneration (1-10% difference in total SO_2 between the two integrations). Weight balances at the conclusion of a cycle were always good (0-1% variation) and provided a check on completeness of regeneration. Calcium sulfide did not build up in the particles and remained low at the 1-2% level (Table 14). This might be expected as O_2 will oxidize any sulfide to SO_2 and $CaSO_4$ during the desulfurization cycle.

Table 14

Sulfide Content in Limestone From Cyclic Regeneration

Reg. Temp = 2000°F, CO_2/CO = 2:1, CO% = 10%, Bal. N_2

% Sulfide	Cycle Concluded
0	Start
0.75	1
1.7	5
1.45	10

5.5.3. Attrition of Cycled Sorbents

Attrition of lime 1359 was found to be small upon cycling as Figure 28 illustrates. Attrition of dolomite 1337, however, was quite large on the first cycle (50%), and was still quite large on the succeeding cycle as seen in Table 15.

Figure 28

Physical Integrity of Lime (1359)

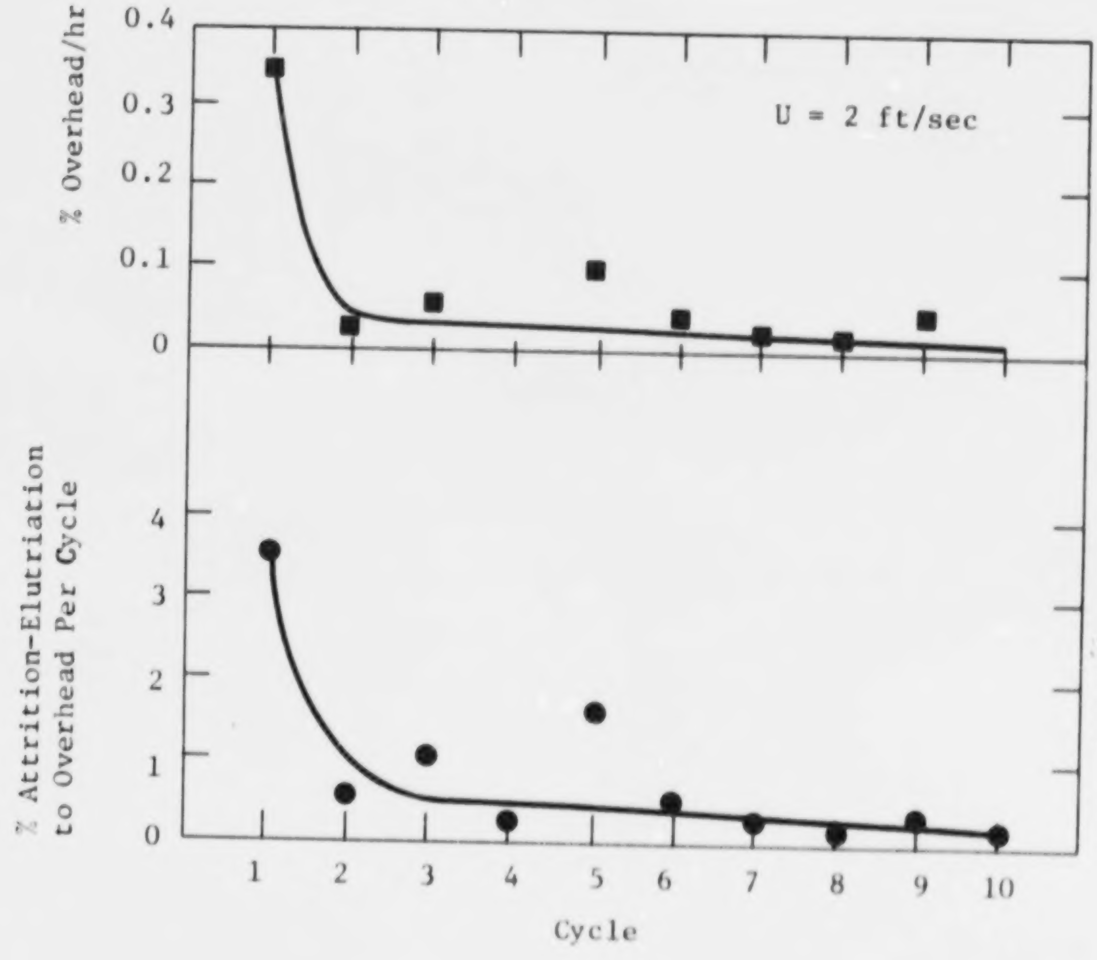

Table 15

Attrition During Cyclic Use of Sorbents

25/50 Mesh Particles, Sorption at 1600°F, Regeneration at 2000°F, in-situ regeneration unless otherwise noted.

Stone	Cycle Time (hr)	% CaO Utiliz. @ SO_2 Out/In=0.2	Gas Vel. (ft/sec)	Loss Overhead,(%)	Initial Bed Height (cm)
Dolomite 1337					
Cycle 1	7.5	52.5	2	53	10
Cycle 2	5.5	72.0	2	2.9	4.6
Dolomite 1337	- Preattrited 6 hrs in glass column, V = 2.45 ft/sec, 26% loss overhead $[SO2]_{in}$= 6000 ppm				
Cycle 1	2	13.7	2.9	21.7	19.3
Cycle 2	2	18.1	2.9	3	15.2
Lime, 1343					
Cycle 1	8.5	22.8	2	7.5	15
Lime, 1359	- Exploratory experiments, $[SO_2]_{in}$ ~1%				
Cycle 1	5	Inappropriate Flue Gas	3.3	10	17
Cycle 2	2.5	27	3.3	1.7	15
Cycle 3	4	27	2.9	0	14

The data on the 1359 lime show its attrition to be small. Initial rounding of some sharp particles appears to have resulted in elutriation and loss of smaller particles, but this stone is basically quite stable.

The direct use of the attrition data generated in this laboratory system for the design of large systems is not recommended. It is known that attrition from particle collisions with walls is important and probably dominant in determining particle size. In laboratory equipment, such as the present apparatus, slugging occurs, causing particles to be carried into the top wall and to brush against the side walls. In large units slugging is impossible; instead bubbles break in the open disengaging sections. Attrition is then mainly due to particle-particle collisions. Wall interaction is less important as the surface wall/volume ratio is much smaller. Thus, attrition may be appreciably less in large systems, operating at the same velocity, than obtained in our experiments although qualitative rating of stones from the present data should be valid. Thus, the N-1337 dolomite would still be expected to attrit much more readily in a large commercial unit than would the N-1359 limestone. The amount of attrition obtained with the dolomite in the laboratory unit is unacceptably high. However, at this point it is not possible to completely rule out the commercial use of this sorbent, or other sorbents on physical grounds without additional testing in larger equipment.

6. PROCESS DESIGN CONSIDERATIONS

Of the various fluid bed processing alternatives that were researched in this program, only the use of coarse, untreated, sorbent particles, preferably with regeneration, was considered to offer potential application to commercial flue gas desulfurization. This section discusses the design of a coarse particle fluid bed desulfurization system.

6.1. Desulfurizer: Conventional Power Plant

6.1.1. Sizing: Reactor

In order to insure efficient desulfurization at low power loads, the design calls for a 1600°F bed at 90% boiler load. At 60% load, one could expect a temperature drop of about 100°F. Stone would need to be fed more rapidly to compensate for reactivity loss despite longer gas residence time.

Figure 29 shows the relationship between the reactor bed diameter and gas velocity at 1600°F for a system treating the flue gas from a 200 MW coal-burning power plant. The maximum diameter of a fluid bed at today's state-of-the-art is 55'-60'. Using present technology, a bed of 50 ft. diameter could be utilized in a desulfurization process. With such a bed, gas would flow through the reactor at a superficial velocity of 15 ft./sec at full load.

Figure 29

Reactor Size-Gas Velocity

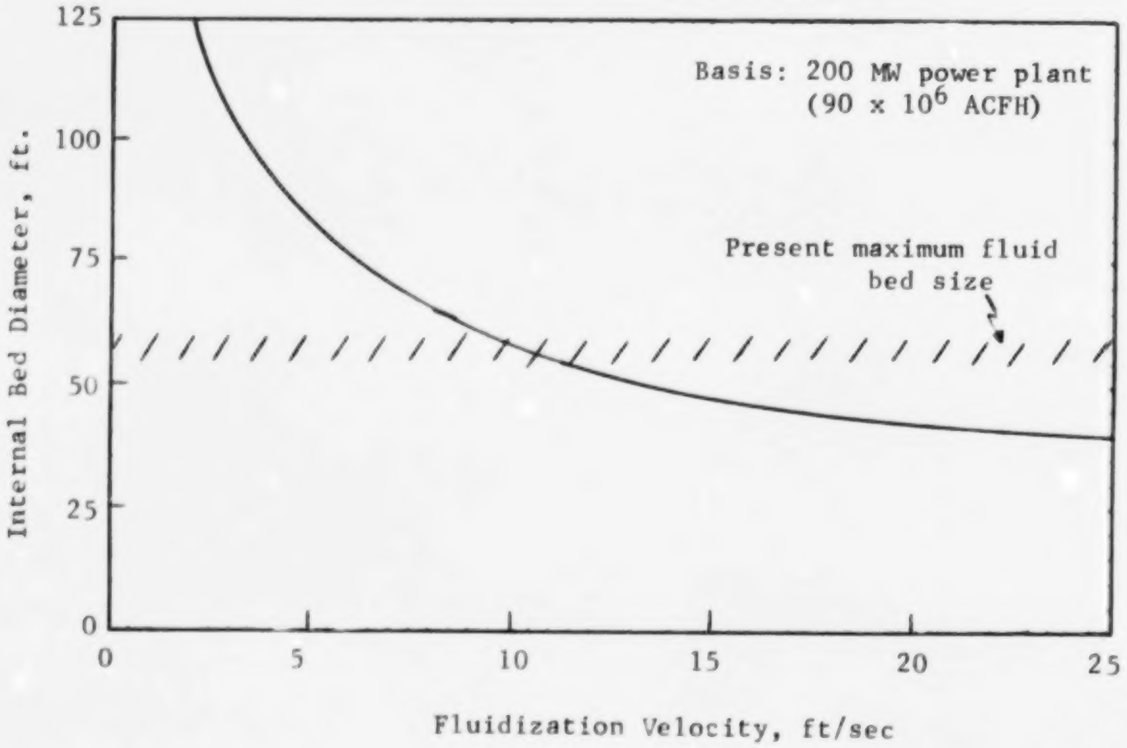

As the bed would operate near 1600°F, insulation would be required to limit heat loss. By using internal insulation, carbon steel would have enough structural strength to be used for the shell body.

Ducts to connect the required external desulfurizer and the boiler would be insulated to reduce heat loss. Erosion by fly-ash, accelerated by the gas, would be kept low by limiting the gas velocities to near 100 ft/sec. This means perhaps a 17' x 17' duct for a 200 MW boiler.

6.1.2. Sizing: Limestone Particles

For small particles the entrainment velocity is about 70 times the incipient fluidization velocity (3); however, as the particles become larger, different hydrodynamic effects occur and entrainment takes place at only 10 times the incipient fluidization velocity (13). A more severe restriction on velocity limitations and particle size distributions is encountered, then, with large particles.

Figure 30 presents a graph of the diameter of calcined limestone particles versus gas entrainment velocity. To avoid entrainment at the 15 ft/sec superficial velocity, a minimum particle diameter of 1100μ was specified. A maximum diameter of 5000μ was selected to obtain a range of sizes for good fluidization which could be obtained from a

Figure 30
Particle Entrainment Velocity

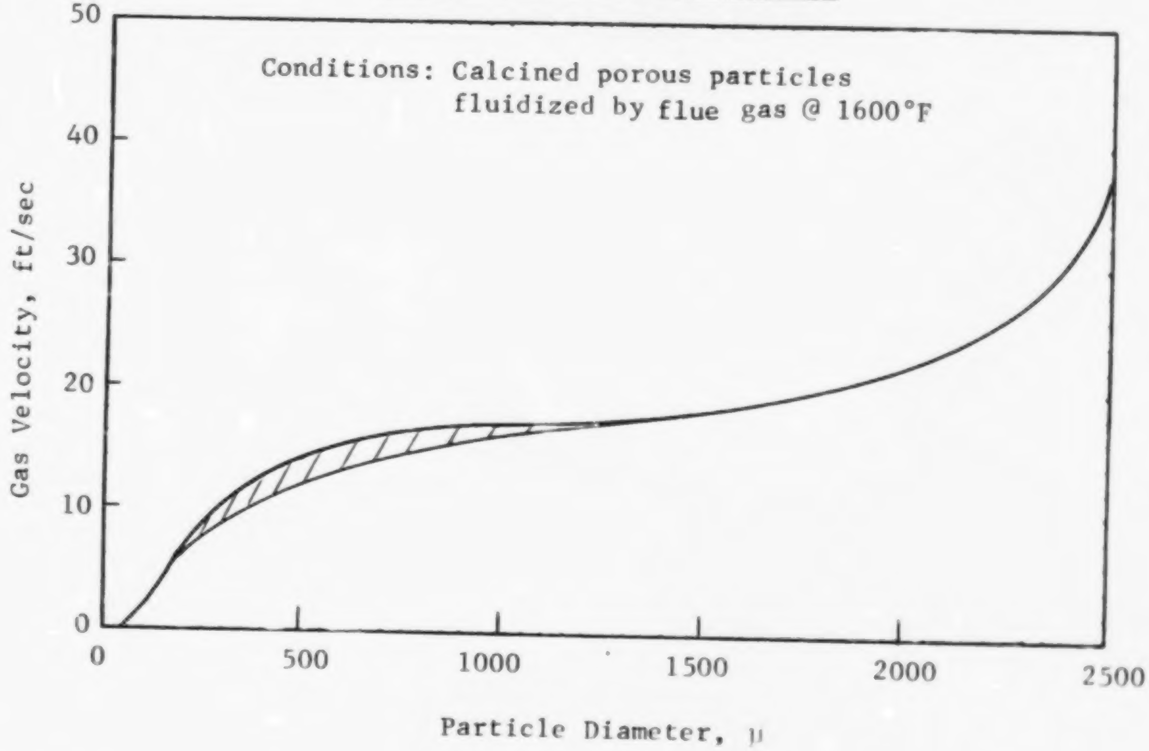

limestone supplier. Calculations for sulfated particles using the root-mean-squared average diameter of 2450µ give an incipient fluidization velocity of 4.3 ft/sec - using Leva's correlation (14). The range of particle sizes selected, 1100-5000µ , is a more narrow relative range of sizes than employed in fluidization processes such as catalytic cracking. A large range is normally necessary to provide good uniform fluidization; however, the above range should provide good characteristics for these larger particles. The reactor design calls for an enlarged-diameter, disengaging section to reduce the gas velocity by one-half, to ensure limitations on the carry-over of small particles.

6.1.3. Fluidization Requirements

Modern boilers use thin, flat-walled sides. With these walls, the pressure drop through the boiler is limited by the pressure differential that can be tolerated between the atmosphere and the inside of the boiler without the occurrence of an explosion or expensive reinforcement of the buck stays. The use of forced and induced draft fans can keep the average pressure inside the boiler near atmospheric; air is forced into the boiler at pressures above atmospheric and flue gas is drawn out below the outside pressure to reduce the maximum differential across the boiler walls. A maximum pressure drop of about 20" H_2O through the fluid bed might be tolerated in an integrated boiler-desulfurization system in such a balanced draft case. Depending on the sulfation level, which determines the density of the particles, a bed height of 15-24" might be tolerable.

To insure uniform gas distribution without channeling, a grid pressure drop of 30% of the bed pressure drop is needed (15). In addition, gas bubble sizes must be minimized to limit gas by-passing of the particles. Contacting efficiency would otherwise limit the desulfurization that could be obtained. Large grid openings lead to large bubbles according to the relation (3):

$$V_B \propto G^{6/5} \qquad (15)$$

Here V_B is the bubble volume and G is the volumetric gas flow rate through the opening above the minimum fluidization velocity. Now G is proportional to a grid design with numerous small holes as gas inlets.

A flat plate grid with 1" high imbedded buttons, containing small gas inlet holes, was assumed in this design. These buttons are similar to those being investigated by the Pope Evans and Robbins Co. for use in a fluid bed packaged boiler (16). Although the use of such a grid would insure the formation of only small bubbles initially, the bubbles could grow rapidly. The maximum bubble size is a function of particle size (3) and for the present large particles it is approximately the bed diameter. In even the shallow beds visualized, bubble growth is so rapid that bubbles could be several feet across at the top of the bed. To limit the bubble size, vertical pipes might be employed in a similar manner to that used in other large particle processes (17). The increase in vertical surface area would serve to reduce the equivalent effective bed diameter - and thus reduce bubble size, as bubbles only can grow to the containing vessel diameter.

6.1.4. Sorbent Selection

Obviously, a sorbent must be chosen for a fluid bed process which does not attrit too easily in a fluid bed. As shown in Section 4.4.1., the N-1359 limestone has good stability. Consequently, it was selected for the process designs even though its initial reactivity was lower than any of the other sorbents evaluated in this program (see Figure 10). It was felt that if the stone with the lowest rate constant measured from a variety of stones could desulfurize flue gas efficiently in the system as designed, then most other stones would also adequately desulfurize flue gas in this system. Naturally, the use of a more reactive stone, with comparable attrition characteristics would result in a lower process cost than that developed for the use of N-1359 sorbent.

The rate constant for 2380-3360 μ and 1000-1190μ particles of stone 1359 are given in Figures 9 and 10. The actual rate constant that should be used in calculating desulfurization is an average over the residence time distribution and particle size. An exponential residence time distribution has been used to calculate the effective rate constant for a given bed hold-up time (see Appendix VI for details).

A SO_2 removal of approximately 90% was chosen as the design criterion. For single-pass limestone use, a maximum of 87% of the SO_2 could be removed at rated load with 29% utilized particles. A 3/1 molar stoichiometric ratio of CaO to SO_2 would need to be added to a 2 ft. bed - assuming a rate constant average of 900 min^{-1} at the designated gas velocity of 15 ft/sec. The upper limit for desulfurization of 87% assumes ideality - gas plug flow with no gas by-passing in the fluidized bed. Real systems would have bubbles and some gas by-passing; desulfurization efficiency would thus be less than calculated.

In a regenerative process, approximately 92% desulfurization would be obtained in a 15 inch bed (settled depth) under ideal gas contacting and 17% average calcium oxide utilization. The average rate constant is 1800 min^{-1} for this case. The pressure drop through the 15 inch bed would be much lower than in the single-pass, 24 inch bed. The regenerative process would be more conservative, and fairly safe, with respect to structural boiler strength.

One might expect an incremental load on the boiler's cyclone-precipitator dust collection system due to attrited limestone. A nine to twenty-seven percent increase is estimated for the single-pass system using the data of Section 5.5.3. With the regenerative process, the dust loading increase in the boiler would depend on the limestone additive rate, which is determined by the length of time the sorbent effectively maintains its reactivity. Based on about a 1:3 CaO to SO_2 mole ratio make-up stone addition, a dust loading increase of 3% is estimated. It would be expected that the cyclones and electrostatic precipitators normally installed in a boiler should handle this limestone dust without modification.

6.2. Regenerator

The fluidized bed regenerator would be much smaller than the desulfurizer. A reducing gas with a $(CO_2 + H_2O):(CO + H_2)$ ratio of 2:1 would be used, as discussed in Section 5. This gas (at 2000°F) could be obtained by partially combusting coal or methane with air - pure, or diluted with flue gas. The cheaper coal should be used providing the resulting fly-ash proves no problem. An assumed gas velocity of 11 ft/sec at rated load sets the internal diameter of the regenerator at 10.8 ft. A high velocity is required to maintain agitation and decrease agglomeration problems.

Cyclones would be provided to capture and return any entrained or attrited particles. They would also serve to protect subsequent equipment from particle fouling. Pneumatic tubes would probably be used to transport the material to and from the desulfurizer downcomers to the regenerator since mechanical feeders would tend to attrite the particles.

The grid is assumed to be a firebrick arch as used in some present-day limestone kilns. The inlet openings could be straight through holes, as good contacting is not as necessary to obtain conversion in the regenerator as it is in the desulfurizer. This is because the reduction reaction is fast and at equilibrium. A bed depth of 3 feet is estimated to be sufficient for regeneration. The average composition of particles being returned to the desulfurizer would be about 5 mole % sulfate.

6.2.1. By-Product Processing

The nine percent sulfur dioxide concentration from the regenerator is high enough for use in a contact plant to produce sulfuric acid. Clean-up of the gas stream for use in a catalytic contacting plant would follow the outline presented by Wheelock and Boylan (18) for a process converting anhydrite to sulfuric acid. A standard sulfuric acid plant, except for the sulfur burning section, would be employed to obtain 98% sulfuric acid for by-product sale.

6.3. Schematic Design: Conventional Power Plant

The design considerations presented in Section 6.1. and 6.2. are incorporated into the schematic presented in Figure 31. This diagram presents the salient features in the integrated system but it is not drawn to scale.

Figure 31

Limestone Fluidized Bed Desulfurization Process-Conventional Power Plant

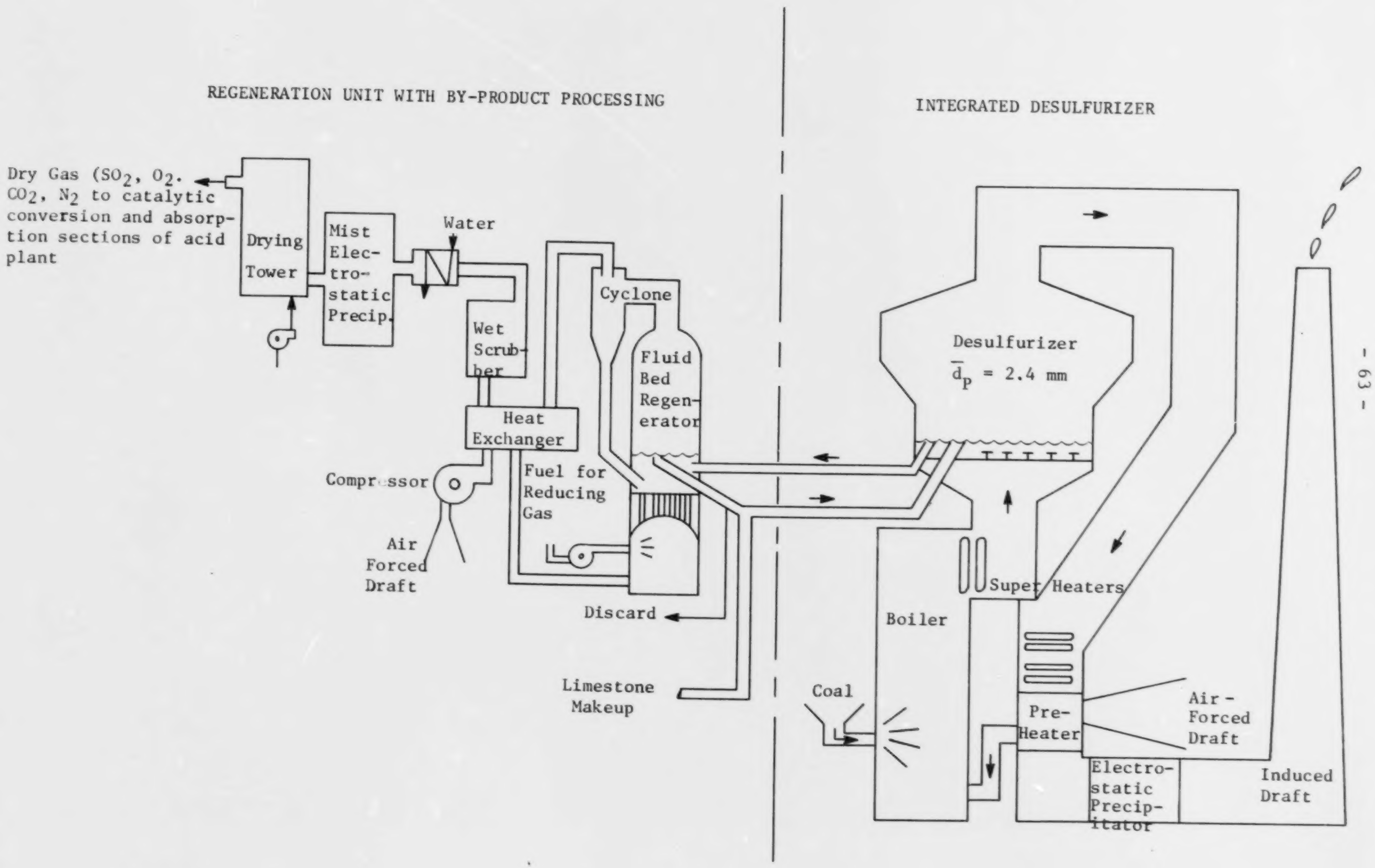
REGENERATION UNIT WITH BY-PRODUCT PROCESSING
INTEGRATED DESULFURIZER
Dry Gas (SO_2, O_2. CO_2, N_2 to catalytic conversion and absorption sections of acid plant
Drying Tower
Mist Electrostatic Precip.
Water
Wet Scrubber
Heat Exchanger
Cyclone
Fluid Bed Regenerator
Compressor
Air Forced Draft
Fuel for Reducing Gas
Discard
Limestone Makeup
Desulfurizer
$\overline{d}_p = 2.4$ mm
Super Heaters
Boiler
Coal
Pre-Heater
Air - Forced Draft
Electrostatic Precipitator
Induced Draft

6.4. Future Process Variation: Fluidized Bed Combustion

The use of fluidized bed combustion is currently being researched in the United States and in England as a means of raising steam in packaged and utility sized boilers. In fluidized bed combustion, advantage is taken of the excellent heat transfer coefficients obtainable in a fluid bed (i.e., 50 to 100 BTU/hr/ft^2/°F) to reduce high temperature boiler tube requirements (and costs) and to maintain bed temperature at about 1500 to 1800°F. Most of the fluidized bed consists of coarse inert material, with the fuel (usually coal) occupying only a small portion of the total bed.

Research has been directed at injecting finely pulverized limestones and dolomites into fluid bed combustor to effect desulfurization of the gases. With this type of system, sorbent utilizations have been low (i.e., 25-30%) and several times stoichiometric sorbent addition rates have been found to be required to provide high levels of SO_2 removal. An interesting variation of the fluid bed combustion process is to combust coal in a coarse lime particle bed. Fly ash would be entrained out of the bed by the gas, leaving the sulfated lime, which can be sent to a regenerator with less fear of agglomeration. Small diameter particles should be used because smaller particles and a wide size distribution offer better fluidization conditions, and thus less tendency to agglomerate (see Section 5.43). Present analysis indicates that gas velocities near 3 ft/sec would be used in the fluidized bed combustor for economic savings (19); then particles with d_{avg} = 1000 or smaller could possibly be used without entrainment difficulties. The Consolidated Coal Company has shown that such a coarse limestone fluid bed combustion system can work, that SO_2 capture is good, and that the sulfated sorbent can be reductively regenerated (20).

Design problems would be simplified in such a desulfurization scheme, compared to a conventional plant fluid bed desulfurizer, since the fluidized bed is also the combustion unit. Duct work and grid problems would be eliminated or substantially reduced. Stable stone particles would, of course, still be needed. As described for a conventional plant, high efficiency desulfurization should occur in a cyclic, regenerative scheme with the 2-3 foot bed height presently envisioned for fluidized bed combustion. The regenerator would be basically the same as that described for a conventional plant scheme.

Areas of potential problems, such as fly-ash separation and desulfurization efficiency, would need to be investigated. Combustion efficiency would be important. Low combustion might cause worse problems than with coarse particle combustion as the unburned carbon recycle load could increase; however, high combustion efficiency with fine pulverized coal might eliminate much of the costly cyclone system for carbon recycle presently expected to be needed in fluidized bed combustion.

6.5. Possible Process Innovations: Sulfur Production

Sulfur would be a more desirable by-product than sulfuric acid because of easier transportation, storage, and sales possibilities. It is therefore of interest to determine how the regeneration procedure might be modified to produce sulfur rather than sulfuric acid.

One method of producing sulfur might be to use a coke reduction process after concentration of the SO_2 from the regeneration by liquefaction. The COS formed over coke could be catalytically decomposed to sulfur. This mode of operation, however, appears too expensive and involved for a utility to operate. Sulfur could be produced by operating a modified Claus Process on the regenerator off-gas. In such a process, H_2S would be added to the regenerator off-gas in sufficient quantities to react with SO_2 according to the equation:

$$SO_2 + 2H_2S \longrightarrow 3S + 2H_2O \qquad (16)$$

The reaction could be operated at about 600°F over an alumina catalyst. The sulfur formed would be condensed downstream of the catalyst. Most of the sulfur would be collected as product with the remainder used to produce the H_2S added to the regenerator off-gas. This H_2S could be made by steam reforming natural gas together with S as proposed by Princeton Chemical Research (21).

An alternate route to sulfur might be to add CO or H_2 to the regenerator off-gas in sufficient quantities to reduce the SO_2 to sulfur:

$$SO_2 + 2CO \longrightarrow 2CO_2 + S \qquad (17)$$

CO and H_2 addition would have to be very carefully controlled; if too much were to be added, COS and H_2S would be produced:

$$S + CO \longrightarrow COS \qquad (18)$$

Ryason and Harkins (22) have researched a direct reduction technique for controlling SO_2 (and NO_x) emissions in flue gas. They found a copper oxide on Al_2O_3 catalyst to be very effective at temperatures near 1000°F for promoting the desired reactions.

Still another method would involve the lower temperature reduction of $CaSO_4$ to CaS instead of CaO and SO_2. The CaS might then be treated with steam and CO_2 as Squires (23) has suggested to yield H_2S:

$$CaS + CO_2 + H_2O \longrightarrow H_2S + CaCO_3 \qquad (19)$$

The H_2S could then be partially combusted to yield a 2:1 mixture of $H_2S:SO_2$ which would be converted to sulfur in a Claus Process.

7. ECONOMICS OF FLUID BED LIMESTONE DESULFURIZATION

The cost to desulfurize flue gas from fossil-fueled power plants with a limestone-based, fluidized-bed process has been estimated for a 200 MW plant using both the regenerative and the single-pass limestone processes and for a 1000 MW plant using the regenerative system. Comparable economics are also presented for direct injection techniques for desulfurization, and rough estimates of fluid bed combustion/desulfurization costs are given.

7.1. Basis for Cost Estimates

Details as to equipment size, material flow rates and costing are presented in Appendix VIII. Equipment was sized (Section 6) to handle full-rated capacity power loads. Summarized investment costs and operating charges are presented in the text. The base case is assumed to be a coal burning plant, using 3.5% S coal at the rate of 3000 ton coal/yr/MW capacity at 90% load or 8000 hrs/yr. Flue gas desulfurization in the fluid bed of 90% was designated at a 90% load factor. Eighty-five percent conversion of the sulfur in the coal to by-product H_2SO_4 was assumed in regenerative systems (1-2% loss in the sulfuric acid plant, 2-3% loss with limestone discard, and 90% actual desulfurization efficiency).

Costing procedures were standardized to insure valid economic comparisons and analyses for different processes. If they were available, equipment cost for heat exchangers, etc., were taken from Chemical Engineering Progress cost files and updated. Fans and electrostatic precipitator costs were obtained by manufacturer estimates. Installed costs of reactors were estimated from experience for construction of large scale equipment with the different materials specified. Limestone storage and feeder costs were taken from the experience of TVA (24). The sulfuric acid plant costs were taken from literature quotes, such as those by Connor (25). No cost was assumed for installation of the process into a new power plant designed to accommodate the desulfurization system. Costs for land for the regenerative-by-product sub-system were not included.

Total construction costs were obtained from these costs by the use of factors for electrical wiring, piping, buildings, etc. Lang's analysis (26) was followed closely for these factors. Purchased equipment costs served as a base factor. Installation costs for foundations and labor were 43% of purchase costs. Extra costs for foundations of the absorber and its flue gas duct work were assessed at 15% of installation costs. Piping costs ranged from 25%-60% of installed equipment costs for fluid-solid and fluid-fluid processes, respectively. Costs for instrumentation, utilities and electrical wiring, and building and land improvements ranged from 23% of piping-installation costs for the absorber to 50% for other parts of the process. A final direct cost was obtained for the process from the sum of these costs. An engineering, contingency, and construction fee of 35% of the direct cost was added to obtain the total construction cost. Working capital was estimated for 60 days operating supplies and labor.

In determining operating costs the following criteria were used: capital charges (taxes, interests, investment return) were 14% of investment (construction costs plus working capital), yearly maintenance is estimated at 5% of investment costs, power for operating induction fans, pumps, etc., should be available at 4 mils/kw. hr at the power station, limestone costs $2.05/ton delivered; coal costs $4.20/ton, labor is available at $3.00 hr/man and $12,000/yr supervision, and plant and payroll overhead are 50% x (maintenance + labor) and 40% of labor, respectively.

There would be a thermal effect on the boiler due to the need to heat-up limestone. At low stone addition rates, excess heat would be released from the exothermic reaction of sulfate formation and a small savings in fuel would result. At high addition rates, the endothermic heat of calcination would have to be made up by burning additional fuel in the furnace. In the cost estimates, these effects have been assessed at a cost or credit equivalent to $6.05/ton coal needed to make up power output variations.

The costs for a 200 MW plant, operating at a 60% and a 90% load factor, being desulfurized in turn by a direct injection process, a single-pass fluidization system, and a regenerative system producing sulfuric acid, are estimated. A scale-up to a 1000 MW plant regenerative desulfurization process was also performed. The costs at a 60% load factor may be the most significant, as the average power load on a grid, and thus on a single station averaged over its life, is 58-60%.

7.2. Process Installation in Existing Power Plants

The use of inexpensive limestone to eliminate sulfur dioxide pollutants from coal flue gas is very appealing. It would be desirable to install a process utilizing limestone in presently operating power plants. However, the cost of desulfurization must include modification costs to the boiler in addition to direct costs associated with the desulfurization process equipment. These costs for a fluidized bed desulfurization process operating at 1600°F would be quite prohibitive.

Present day boilers range in size, but a convenient typical size is a 200 MW unit. As will be shown later, a cost of $1-2/ton coal ($600,000-$1,200,000/yr) can be assessed to operate the process equipment for this size unit. To install this fluidized bed process, the boiler must be cut in the superheater region. Installation of duct work from the absorber to the boiler would necessitate moving half the boiler. As boilers and tubes are hung from the top, an almost complete reconstruction of half the boiler would be required. This might cost from $1-3 million. In addition the boiler would not be operating for a period of 6-18 months. A charge of $2.75 to $8.2 million would be assessed as the incremental price to keep customers supplied with purchased power while the plant is being modified. This figure is obtained by estimating a cost of $15,000/day to buy power at a premium rate over the internal cost of producing power. At a 14% yearly fixed charge rate on this total of %3.75-$11.2, an additional cost of $0.88-$2.60/ton coal would be levied on a fluidized bed process. Even the extremely optimistic case of $0.88/ton coal is excessive (the more realistic estimate is $1.65 ton/coal). These additional costs remove a fluidized bed desulfurization process from consideration for application to existing boilers.

7.3. Future Conventional Power-Plant Process Installation

7.3.1. Single Pass Desulfurization - 200 MW Plant

A single-pass process using stable limestone such as N-1359 to desulfurize the gas in a 200 MW plant would require a \$3,030,000 investment. The general outline of the process has been described and sized in Section 6 for a 200 MW unit. The construction cost breakdown is given in detail in Appendix VIII, including unit size specifications and flows. Capital costs are summarized in Table 16.

Table 16

200 MW Power Plants - Single Pass Fluidized Bed Desulfurization/Stable Limestone

Investment Costs

Item	Costs
Direct Costs:	
Desulfurizer	\$ 882,000
Ducts	314,000
Limestone Handling	566,000
Induction Fans and Motors, and **Desulfurizer-Power Plant**	430,000
Total	\$2,192,000
Engineering, Construction, Contingency Fee	758,000
Construction Costs	2,950,000
Working Capital	80,000
Total Investment	\$3,030,000 (\$15.15/kw)

Basis: 87% Desulfurization, 3:1 Limestone/SO_2 addition ratio, 3.5% S coal.

The yearly operating costs for 60% and 90% load factors for the single pass process are given in Tables 17 and 18. Power needs are fairly large because induction fans are needed to overcome a ΔP of about 26" H_2O through the fluidization absorber. Labor requirements are 2 operators/shift, plus a supervisor, plus one extra man for limestone handling.

Table 17

200 MW Power Plant - Single Pass Fluidized Bed Desulfurization/Stable Limestone

Yearly Operating Costs; 90% Load Factor

Item	Costs
Capital Charges (14% Investment)	\$425,000
Maintenance (5% Investment)	151,000
Power (4 mils/kw hr.)	140,000
Limestone (\$2.05/ton)	420,000
Labor	70,000
Payroll Overhead (40%)	28,000
Plant Overhead	110,500
Thermal Effect	72,000
Total	\$1,406,500
Cost/Ton Coal	\$2.35

Basis: 87% Desulfurization, 3:1 Limestone/SO_2 ratio, 3.5% S coal, 90% load factor, ideal gas contacting.

Table 18

200 MW Power Plant - Single Pass Fluidized Bed Desulfurization/Stable Limestone

Yearly Operating Costs; 60% Load Factor

Item	Cost
Capital Charges (14% Investment)	$425,000
Maintenance (5% Investment)	151,000
Power (4 mils/kw hr.)	93,500
Limestone ($2.05/ton)	322,000
Labor	70,000
Payroll Overhead (40%)	28,000
Plant Overhead	110,500
Thermal Effect	71,000
Total	$1,271,000
Cost/Ton Coal	$3.18

Basis. 87% Desulfurization, 3:45Limestone/SO_2 ratio, 3.5% S coal, 60% load factor, ideal gas contacting.

Lower operating costs would result if a more reactive material than N-1359 was available. If a physically stable material of reactivity similar to dolomite N-1337, could be found, the costs of operating a single-pass desulfurization process would be quite similar to that with 1359 limestone. However, only a 1.35:1 CaO (in dolomite)/SO_2 ratio would be required kineticly to obtain 89% flue gas desulfurization. The limestone handling costs would therefore be less, as less material is handled. However the desulfurizer costs and size would be about the same. About $160,000 would be saved in limestone handling investment costs (i.e., total investment = $2,870,000). The operating costs are summarized in Table 19. A net thermal credit is obtained at 90% load operation as less stone is calcined and heated up than with the N-1359 limestone, while the same heat release would be obtained from sulfate formation.

Table 19

200 MW Power Plant - Single Pass Fluidized Bed Desulfurization/Stable Dolomite

Yearly Operating Costs; 90% Load Factor

Item	Cost
Capital Charges (14% Investment)	$ 402,000
Maintenance (5% Investment)	143,000
Power (4 mils /kw hr)	140,000
Dolomite ($2.05/ton)	350,000
Labor	70,000
Payroll Overhead (40%)	28,000
Plant Overhead	106,500
Thermal Effect	Credit 6,000
Total	$1,228,000
Cost/ton coal	$2.05

Assumptions: 89% Desulfurization, 1.35:1 CaO-Dolomite/SO_2 ratio, 3.5% S coal, 90% load factor, ideal gas contacting.

Table 20

200 MW Power Plant - Single Pass Fluidized Bed Desulfurization/Stable Dolomite

Yearly Operating Costs; 60% Load Factor

Item	Cost
Capital Charges (14% Investment)	$ 402,000
Maintenance (5% Investment)	143,000
Power (4 mils/kw hr)	93,500
Dolomite ($2.05/ton)	295,000
Labor	70,000
Payroll Overhead	28,000
Plant Overhead	106,500
Thermal Effect	64,000
Total	$1,202,000
Cost/ton Coal	$3.00

Basis: 89% Desulfurization, 1.7:1 Limestone/SO_2 ratio, 3.5% S coal, 60% load factor, ideal gas contacting.

7.3.2. The Regenerative Process - 200 MW Plant

The desulfurizer costs in this case are the same as in the single-pass process. Limestone requirements would be less, so smaller facilities are needed to handle the stone. A 15 inch settled bed depth would be employed, as opposed to the 24 inch bed in the single-pass system. A shallower bed could be used since regeneration permits operation with a low sorbent utilization and high reactivity stone in the desulfurizer without increasing limestone requirements. The bed pressure drop would therefore be less than with a single pass system, and less powerful induction fan facilities are required. Capital costs are summarized in Table 21, including the costs for the regeneration sub-system. The acid plant includes a contacting-absorption section, but no sulfur burning equipment is needed. Off-site costs of 20% were included to obtain total construction costs for a working unit.

Table 21

200 MW Power Plant - Regenerative Fluidized Bed Desulfurization/Stable Limestone

Investment Costs

Item	Costs
Direct Costs:	
Desulfurizer	$ 882,000
Ducts	314,000
Limestone Receiving-Disposal	150,000
Limestone Recirculation	205,000
Fans & Motors, Desulfurizer-Power Plant	285,000
Regenerator	290,000
Regenerator Effluent Preparation for Acid Plant	300,000
Total	$2,426,00
Eng., Constr., Contigency Fees	848,000
Sulfuric Acid Plant, Constructed	1,185,000
Construction Costs	$4,459,000
Working Capital	126,000
Total Investment	$4,585,000 ($22.92/kw)

Basis: 90% Desulfurization; 1:3 Limestone/SO_2 addition rates, 3.5% S coal, 205 H_2SO_4 ton/day plant capacity.

Yearly operating costs are estimated for a 200 MW plant in Tables 22 and 23. The price of $14.00/ton H_2SO_4 is estimated return, exclusive of costs for transportation and marketing, on the product. The actual price will be set by outside competition, which will in turn be controlled by the sulfur prices prevalent. The above price is the sulfuric acid return price expected when sulfur prices are $30/ton. The sulfur price in the 70's is expected to be in the range, $25-35/ton (27). The personnel required to operate the desulfurization process should be sufficient to also operate the automated acid plant.

Table 22

200 MW Power Plant - Regenerative Fluidized Bed Desulfurization/Stable Limestone

Yearly Operating Costs; 90% Load Factor

Item	Cost
Capital Charges (14% Investment)	$ 643,000
Maintenance (5% Investment)	230,000
Power (4 mils/kw hr)	132,000
Limestone ($2.05/ton)	50,000
Labor	70,000
Plant Overhead	150,000
Payroll Overhead (40%)	28,000
Operating Water (50¢/M gal)	10,000
Reducing Coal ($4.20/ton)	118,000
Thermal Effect	Credit 57,000
Operating Cost	$1,374,000
Sulfuric Acid Return ($14.00/ton)	761,000
Net Desulfurization Cost	$ 613,000
Cost/ton coal	$1.02

Assumptions: 3.5% S coal, 8000 hr operation yearly, 90% load factor, 85% conversion of sulfur to sulfuric acid, 90% desulfurization in actual operation.

Table 23

200 MW Power Plant - Regenerative Fluidized Bed Desulfurization/Stable Limestone

Yearly Operating Costs; 60% Load Factor

Item	Cost
Capital Charges (14% Investment)	\$ 643,000
Maintenance (5% Investment)	230,000
Power	88,000
Limestone (\$2.05/ton)	42,000
Labor	70,000
Plant Overhead	150,000
Payroll Overhead	28,000
Operating Water (50¢/M gal)	7,000
Reducing Coal (\$4.20/ton)	80,000
Thermal Effect	Credit 29,000
Operating Cost	\$1,309,000
Sulfuric Acid Return (\$14.00/ton)	503,000
Net Desulfurization Cost	\$ 806,000
Cost/ton coal	\$2.01

Assumptions: 3.5% S coal, 8000 hr. operation yearly, 60% load factor, 85% conversion S $\longrightarrow$ H_2SO_4, 90% desulfurization in actual operation, 2.4:1 SO_2/limestone make-up ratio.

7.3.3. The Regenerative Process - 1000 MW Plant

Five desulfurization reactors of the size previously described would be used in this design, as larger diameter reactors are felt to be impractical. The flue gas must, therefore, be divided into five streams to be transported to the individual absorber. Thus, more duct work is required for this 1000 MW plant desulfurization unit than might be expected on scale-up from a 200 MW unit.

Costs for the 1000 MW system were calculated separately for each piece of equipment, where possible. If direct estimation could not be used, the 0.6 factor (26) was used for economic scale-up from a 200 MW unit. Other costing procedures followed the outline used for a 200 MW regenerative system.

Table 24

1000 MW - Regenerative Fluidized Bed Desulfurization/Stable Limestone

Investment Costs

Item	Costs	
Direct Costs		
Desulfurizers	$ 4,410,000	
Ducts	2,070,000	
Limestone Receiving-Disposal	350,000	
Limestone Recirculation	955,000	
Fans and Motors, Desulfurizers-Power Plant	740,000	
Regenerator	780,000	
Regenerator Effluent Preparation for Acid Plant	770,000	
Total	10,075,000	
Eng., Constr., Contigency Fees	3,525,000	
Sulfuric Acid Plant, Constructed	3,040,000	
Construction Costs	16,640,000	
Working Capital	310,000	
Total Investment	$16,950,000	($16.95/kw)

Basis: 92% peak desulfurization, 1:3 Limestone/SO_2 addition rates, 3.5% S coal, 1025 H_2SO_4 ton/day plant capacity.

The operating costs are given in Table 25 and 26 for two load factors. The same criteria were used for sulfuric acid credit, etc., as in the 200 MW unit case. Labor needs were estimated at 4 men/shift + 1 supervisor + 1 day time limestone disposal man.

Since the future value of sulfuric acid is uncertain, the effect of varying acid prices is graphed in Figure 32. The variations in sulfur content also affect desulfurization costs (Figure 33). In deriving the costs, it was assumed that the whole system was sized to be able to handle sulfur coals as high as 3.5-4%.

Table 25

1000 MW Regenerative Fluidized Bed Desulfurization/Stable Limestone

Yearly Operating Costs; 90% Load Factor

Item	Cost
Capital Charges (14% Investment)	$2,370,000
Maintenance (5% Investment)	848,000
Power (4 mils/kw hr)	660,000
Limestone ($2.05/ton)	250,000
Labor	118,000
Plant Overhead	483,000
Payroll Overhead (40%)	48,000
Operating Water (50¢/M gal)	50,000
Coal ($4.20/ton)	590,000
Thermal Effect	Credit 284,000
Operating Cost	5,133,000
Sulfuric Acid Return ($14.00/ton)	3,805,000
Desulfurization Cost	$1,328,000
Cost/ton coal	44¢

Assumptions: 3.5% S coal, 8000 hr operation yearly, 90% load factor, 1:3 limestone/SO_2 ratio, 85% conversion of sulfur to sulfuric acid, 90% desulfurization in actual operation

Table 26

1000 MW Regenerative Fluidized Bed Desulfurization/Stable Limestone

Yearly Operating Costs; 60% Load Factor

Item	Cost
Capital Charges (14% Investment)	$2,370,000
Maintenance (5% Investment)	848,000
Power (4 mils/kw hr)	440,000
Limestone ($2.05/ton)	210,000
Labor	118,000
Plant Overhead	483,000
Payroll Overhead	48,000
Operating Water (50¢/M gal)	33,000
Coal ($4.20/ton)	393,000
Thermal Effect	Credit 144,000
Operating Cost	$4,809,000
Sulfuric Acid Return ($14.00/ton)	2,535,000
Desulfurization Cost	$2,274,000
Cost/ton coal	$1.14

Assumptions: 3.5% S coal, 8000 hr operation yearly, 60% load factor, 1:2.4 limestone/SO_2 make-up ratio, 90% desulfurization in actual operation.

Figure 32

Net Desulfurization Costs as a Function of By-Product Credit

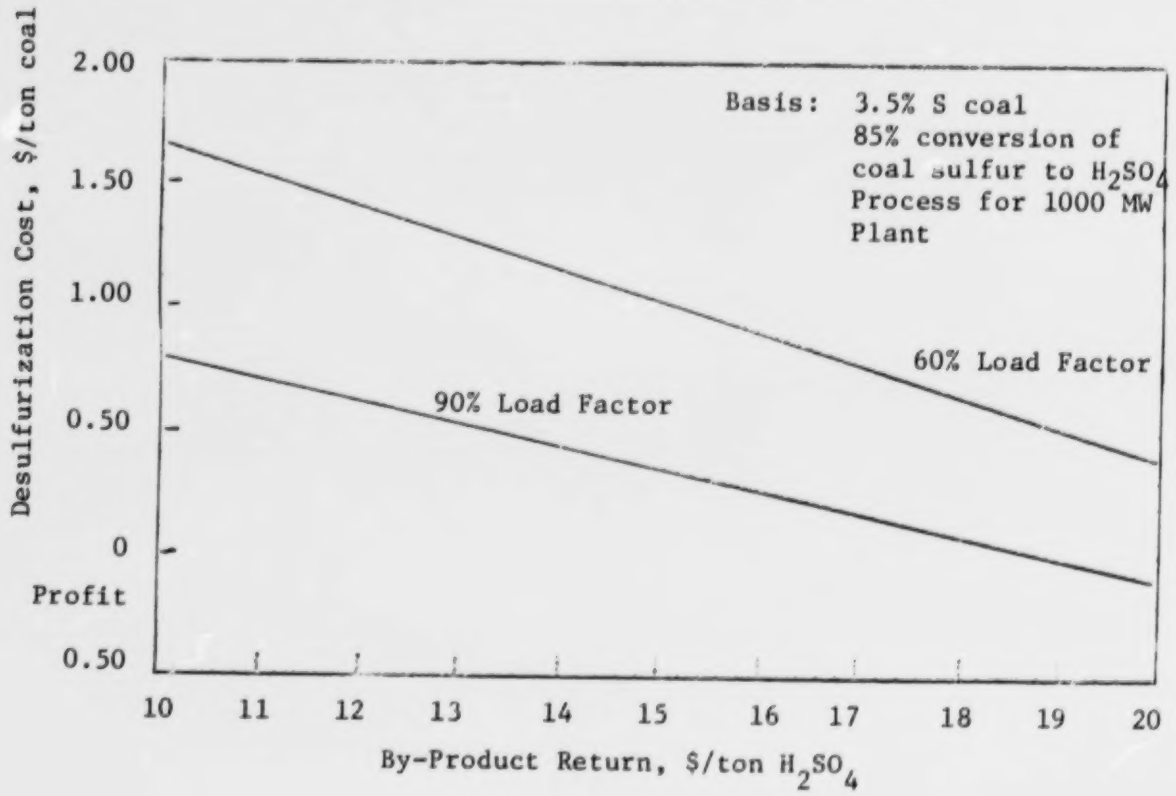

Figure 33

Net Desulfurization Costs as a Function of Sulfur Content

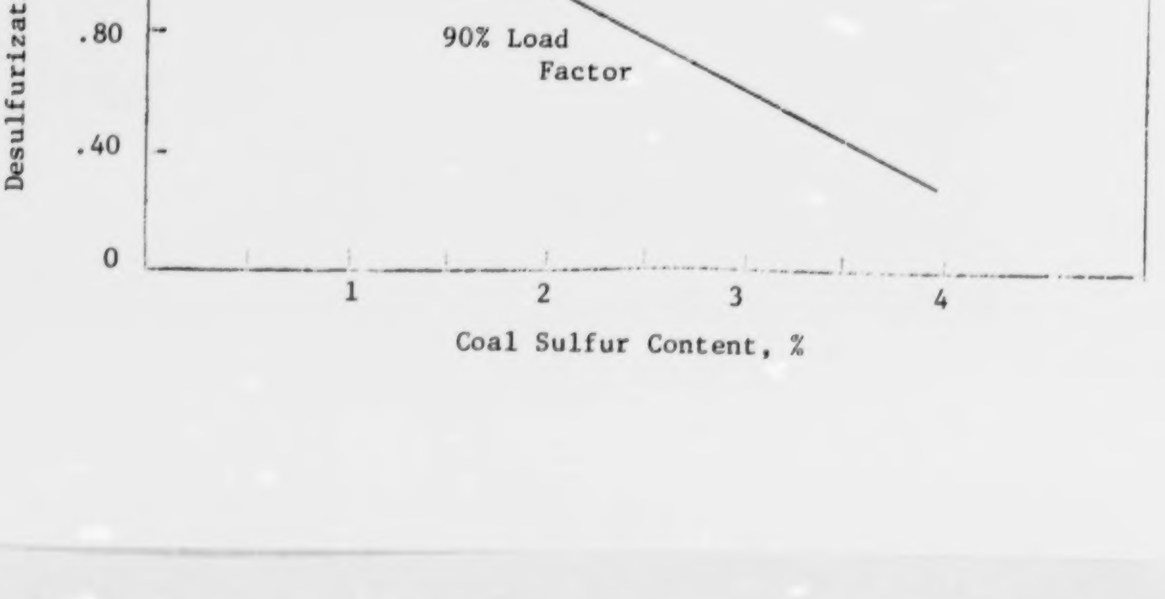

7.4. Direct Injection - 200 MW Plant

The capital investment required for a direct injection process using a 2:1 limestone/SO_2 mole ratio was taken directly from a TVA report (24). One could break down their direct costs into two major items: (1) \$569,000 is required to receive limestone, transport it to the boiler and cart it away; (2) \$581,000 is required to crush the limestone to fine particles and then collect the particles in cyclones and electrostatic precipitators so as not to contaminate the air. The engineering fees and working capital bring the investment to \$1.578 million.

It should be noted that the design specifications for this process call for 66% desulfurization, although only 40-50% SO_2 removal has been generally obtained with a 2:1 limestone to SO_2 ratio.

Yearly operating costs are given in the following table:

Table 27

200 MW Power Plant - Direct Injection Desulfurization Costs

Item	90% Load Factor Yearly Cost	60% Load Factor Yearly Cost
Capital Charges (14% Investment)	\$221,000	\$221,000
Maintenance (5% Investment)	29,000	29,000
Limestone (\$2.05/ton)	285,000	190,000
Power (4 mils/kw hr)	21,000	14,000
Labor	39,500	39,500
Payroll Overhead (40%)	16,000	16,000
Plant Overhead (50% Main. and Labor)	59,000	59,000
Thermal Effect	21,600	14,400
Total Cost	\$792,000	\$683,000
Cost/ton coal	\$1.24	\$1.71

Assumptions: 3.5% S coal, 8000 hr yearly operating time, a 2:1 limestone/SO_2 addition ratio.

7.5. Regenerative Desulfurization in a Fluidized-Bed-Combustion, 1000 MW Plant

Order of magnitude estimates of costs for desulfurization with limestone in the fluidized-bed-combustion system (FBC) described in Section 6.4. have been made, assuming favorable operating characteristics, which must still be demonstrated. The costs cited in this sub-section are therefore less firm than previous process estimates. Only the incremental costs for desulfurization above a non-desulfurizing FBC plant have been estimated.

The desulfurization reactor would be the fluidized-bed-combustion chamber. Since no modifications for the desulfurization scheme are required, no reactor costs have been assessed. No additional charge has been assessed for draft fans as they too are already required for the FBC scheme. The costs for the regenerative process are then as follows:

Table 28

Desulfurization in a 1000 MW - Regenerative Fluid Bed Combustion Plant With Stable Limestone

Incremental Investment Costs

Item	Costs
Direct Costs	
Limestone Receiving-Disposal	$ 350,000
Limestone Recirculation	540,000
Regenerator	780,000
Regenerator Effluent Preparation for Acid Plant	770,000
Total	$2,540,000
Eng., Constr. Contigency Fees	890,000
Sulfuric Acid Plant, Constructed	3,040,000
Construction Costs	$6,470,000
Working Capital	200,000
Total Incremental Investment	$6,670,000 ($6.67/kw)

Basis: 90% Desulfurization, 1:3 Limestone/SO_2 molar addition ratio, 3.5% S coal, 1600°F bed operating temperature.

Table 29

Desulfurization in a 1000 MW - Regenerative Fluid Bed Combustion Plant with Stable Limestone

Operating Costs

Item	Costs 60% Load Factor	 90% Load Factor
Capital Charges (14% Investment)	935,000	935,000
Maintenance (5% Investment)	334,000	334,000
Power (4 mils/kw hr)	40,000	60,000
Limestone @ 2.05/ton	167,000	250,000
Labor + Overhead	98,000	98,000
Plant Overhead	202,000	202,000
Water @ 10¢/M gal	33,000	50,000
Reducing Coal ($4.20/ton)	393,000	590,000
Thermal Effect	Credit 190,000	285,000
Total Cost	$2,012,000	$2,234,000
H_2SO_4 Return ($14/ton acid)	2,535,000	3,805,000
Net Profit	$ 523,000	$1,571,000
Profit/ton coal	17¢	52¢

Basis: 90% Desulfurization, 1:3 Limestone/SO_2 molar addition ratio, 3.5% S coal, 1600°F Bed opereating temperature

The incremental investment costs would be quite low, at $6.67/kw, in comparison with other desulfurization processes. Although a profit is estimated, operating problems could require additional investment to alleviate the difficulties, and costs could correspondingly increase.

7.6. Economics Summary

Table 30 summarizes the capital and operating costs developed for the different fluid bed limestone desulfurization cases. The high cost of modification to a power plant presently in operation would prohibit the process being used for this application. Instead, systems easily adapted to present plants, such as direct limestone injection, perhaps coupled with a wet scrubber, would be employed for desulfurization in these cases.

The ability to re-use limestone after regeneration cuts limestone costs significantly. The return from sale of a by-product (H_2SO_4) also reduces desulfurization costs. These factors give a significant advantage to a regenerative system as compared to a single-pass use of limestone.

Net operating costs of the external fluidized bed scheme appear competitive with other proposed processes. Most estimates for other processes are also in the range \$0.25-\$1.00/ton coal, for high load factors and 800-1000 MW plants. As expected, new (or large) plants operating at a 90% load factor are much more economical than those operating at 60% load, which is more nearly the average grid load factor. The quick estimate for fluidized-bed-combustion desulfurization shows greater economic long-term potential for this combined power-desulfurization scheme than the conventional power plant modified with a desulfurization unit.

Table 30

Cost Summary for the Limestone Fluid Bed Desulfurization Processes

Basis: About 90% Gas desulfurization, 3.5% S fuel
Limestone or dolomite at \$2.05/Ton,
H_2SO_4 return of \$14/ton.

Process	Plant Size MW	Plant Investment \$MM	Plant Investment \$/KW	Operating Costs - \$/Ton Coal 90% Load Factor	Operating Costs - \$/Ton Coal 60% Load Factor
Once-Through Limestone Process	200	3.03	15.15	2.35	3.18
Once-Through Dolomite Process	200	2.87	14.35	2.05	3.00
Regenerative Limestone Process	200	4.585	22.92	1.02	2.01
	1000	16.950	16.95	.44	1.14
Direct Injection Limestone Process	200	1.579	7.90	1.24	1.71
Regenerative Limestone Fluid Bed Combustion Process	1000	6.67(1)	6.67(1)	.52(2)	.17(2)

---

(1) Incremental investment over that required for a fluid bed combustion system without desulfurization.

(2) Net profit over the costs of operating a fluid bed combustion system without desulfurization

8. STATUS AND RECOMMENDATIONS

8.1. Present Status

The regenerative system provides considerable economic advantages over a process with single pass use of limestone and would be the preferred desulfurization system. The economics, necessarily preliminary at this stage, are competitive with other integrated power plant-desulfurization processes. Although this process would not be installed in presently operating power plants because of high boiler modification costs, it is a possibility to provide a relatively low cost SO_2 process for the large conventional plants of the future. The process, however, appears to have a much greater potential if fluidized bed combustion is developed commercially.

The process, as presented, yields the by-product, sulfuric acid. Modifications of the regenerative scheme might enable the process to produce the more versatile product, sulfur. The important points, however, are that a saleable by-product could be produced, and the regenerative system can work.

Another favorable aspect of this regenerative process is the relative insensitivity of the total cost on the use and price of limestone. Only 3% of the total costs are limestone purchase costs. Even if the price and life of limestone particles were in considerable error, the economics would not be significantly effected and the economic conclusions would not be changed.

8.2. Technical Problem Areas

Technical feasibility has been shown for a good part of the process. However, there are several potential problem areas in this process which would need to be more thoroughly investigated if the process were to be developed.

Bubble formation and growth in a large particle, shallow fluidized bed is difficult to predict from bench scale experiments. Fluid-solid contacting depends on bubble formation, as mentioned in the text. Poor contacting leads to low desulfurization efficiencies. The contacting factors, defined in Section 3.4., are difficult to predict and might range from 0.1 to 0.9. A contacting factor of 0.50 would mean a 70% SO_2 removal instead of 90%, and a reduction in the production of H_2SO_4 and subsequent sales credit. Costs would then increase by 25¢/ton coal. It is anticipated that engineering development on grid and bed design would be required to obtain high contacting factors by reducing bubble growth.

A probable grid-bed design has been mentioned in the text (Section 6.1.3). Grid materials of construction must retain sufficient tensile strength to support the weight of the bed at 1600°F. A supported stainless steel (310) plate was used in the design study although further study may indicate that a ceramic material is required. The gas inlet ports are small holes and are necessary to keep the initial bubble size small. Numerous vertical rods scattered throughout the bed hopefully would deter bubble growth.

In the assumed grid design, numerous small holes, drilled in grid buttons at right angles to the direction of gas flow through the bed, have been assumed to provide good fluidization, but the use of small gas-inlet holes presents a problem. It is known that fly ash (or any particle) will tend to follow straight paths when entrained by gas flow; they do not make sharp turns readily. Instead they tend to impinge against elbows, obstacles, or surfaces which force a turn. The possibility of compaction and clogging of the gas inlet orifices by fly ash thus exists. Fly ash clogging or impingement wear of the button must be demonstrated to be small before complete technical feasibility of our fluid bed process has been shown.

Fly-ash impingement in the grid would not be present in a fluidized bed combustion process, since the coal would be fed above the grid. The grid itself would be cooled by inlet air, and materials for construction would be easily obtainable.

Means to prevent agglomeration of the lime particles in the regenertor still need to be definitely established to insure a viable cyclic process. Possibly, bed agitation and correct particle size distribution will suffice, as described in the text. If not, reducing gas would have to be made by the partial combustion of oil or gas. Other reducing gases (e.g., reformer gas) would not be able to satisfy the thermal requirements of the system.

8.3. Other Process Considerations

The process equipment is quite large. The desulfurizers are 50 feet high with large duct work into the 50 foot diameter beds. As a comparison, a conventional 1000 MW power plant burns coal in perhaps a 50' x 70' chamber and extends upward 180' (plus 80' for support girders) before returning through the superheater tubes, etc.

The operating temperature of 1600°F requires the placement of the desulfurizers in the secondary superheater region. Even in a specially designed system, the economics of power operation would be affected by this placement. At very low power loads, the temperature in the superheater region might decrease down to 1400°F. This would adversely affect reaction rate although balanced to some extent by the lower gas velocities and consequently longer gas residence times. Lower reaction rates would necessitate higher relative addition rates of limestone for the same desulfurization efficiency. Thus, the large power units, which are favored economically in this process, should be operated at high loads for economy with the smaller units in the power grid used to accomodate the daily changes in power consumption.

The regenerator itself is not large. However, as in all desulfurization processes which produce a by-product, considerable land is needed to accomodate the by-product plant. The cost of land must be included as added investment for all such processes and this may rule out their use in some cases.

The 90-odd new fossil fueled plants over 500 MW capacity projected for construction by 1990 by the Federal Power Commission (28) will be built mostly in the central part of the U.S. Easy access to limestone deposits is thus foreseen. The highly congested Northeast with its higher land costs in the big cities but great need of ambient sulfur dioxide control will not have many new fossil-fueled plants, and thus little need for the present regenerative desulfurization process.

8.4. Commercialization Lead Time

To carry the development of the present conventional process through to commercial status, several steps must be taken. The fly-ash and the contacting problems must be investigated. Preliminary information could be gained on the compaction problem in present laboratory size equipment. Further answers must await the construction of a 1 to 2 foot diameter semi-works fluid bed. To minimize scale-up problems, a proto-type unit of the order of 20 feet in diameter would be needed. As the power industry demands high reliability, a complete commercial size 200 MW integrated power plant-process would need to be financed and demonstrated for reliability before the industry would accept it for use. The time scale for this development under a crash program might be 4 years until commercial plant construction, followed by several years of demonstration of the reliability of the process in a power plant.

8.5. Recommendations

Adaption of the present process to fluidized bed combustion power cycle, presently being developed, is potentially quite attractive. Fly ash compaction problems should not occur; gas-solid contacting problems would be reduced; and the economics predict a possible profit, assuming favorable operating conditions on this first analysis. The future of this process is therefore judged to lie with development of fluidized bed combustion. Such development is estimated to be at the commercial plant demonstration state in the mid 1970's. If a concurrent program on regenerative limestone desulfurization with fluid bed combustion is carried on, an integrated fluid bed combustion desulfurization system could be developed almost as rapidly as other fluid bed combustion systems. Consequently, we recommend that future development on limestone-based fluid bed desulfurization be directed at adapting the process to fluidized bed combustion schemes.

NOMENCLATURE

C_H = Concentration of SO_2 exiting from a fluidized bed.

C_o = Initial concentration of SO_2 into a fluidized bed.

d = Limestone particles average "diameter" as measured by passage through given mesh sizes.

D = Reactor diameter.

k = Psuedo first order rate constant on SO_2 concentration for sulfation reaction

G = Volumetric gas flow rate.

H_o = Initial settled bed height

R = Psuedo rate coefficient for sulfation reaction at specified conditions in a fluidized bed.

T = Temperature

U = Superficial gas velocity in a fluidized bed.

U_o = Superficial gas velocity at incipient fluidization.

V_B = Volume of gas bubbles in a fluidized bed.

X = Fraction of CaO in limestone particles that has apparently reacted to form $CaSO_4$.

Y = Contacting factor, essentially the efficiency of contact between solids and gas in a fluidized bed.

ΔG_f° = Gibbs free energy of formation of a compound

ΔP = Pressure drop through a given system, usually the fluidized bed and grid combined.

REFERENCES

(1) Harvey, R. D., "The Mineralogy and Petrography of Carbonate Rocks Related to Sulfur Dioxide Reactivity," NAPCA sponsored 3rd Limestone Symposium, St. Petersburg, Florida, December 1, 1967.

(2) "Status Report of Alkaline Additive In-House Research," Prepared for the National Center for Air Pollution Control, Cincinnati, Ohio, Process Control Engineering Section by Bituminous Coal Research.

(3) Davidson, J. F. and Harrison, D., "Fluidized Particles," Cambridge University Press, 1963.

(4) Matsen, J. M. and Tarmy, B. L., "Scale-up of Laboratory Fluid Bed Data: The Significance of Slug Flow," AIChE Meeting, Tampa, Florida, May 1968.

(5) Hovmand, S. and Davidson, J. F., "Chemical Conversion in a Slugging Fluidized Bed," Trans. Inst. Chem. Eng., 46(6):T190-T203, 1968.

(6) Coutant, R. W., et al., "Investigation of the Reactivity of Limestone and Dolomite for Capturing SO_2 from Flue Gas," Battelle Memorial Institute, Summary Report, 1968.

(7) Glasson, D. R., "Reactivity of Lime and Related Oxides. VII. Crystal Size Variations in Calcium Oxide Produced from Limestone," J. Appl. Chem., 11:201-6, June 1961.

(8) Levenspiel, O., "Chemical Reaction Engineering," J. Wiley and Sons, Inc., 1962, pp. 346-367.

(9) Wheelock, T. D. and Boylan, D. R., "Production of Sulfur Dioxide and Lime from Calcium Sulphate," The Ind. Chem., 36(430):590-4, 1960.

(10) White, S. B., Johnson, S. M. and Dantzig, G. B., "Chemical Equilibrium in Complex Mixtures," Rand Corp. Bulletin, P-1059.

(11) Clasen, R. J., "The Linear Logarithmic Programming Problem," Rand Corp. Bulletin, RM-3707.

(12) Boynton, R. S., "Technology of Lime and Limestone," Interscience Publishers, New York, 1966.

(13) Bourgeois, P. and Grenier, P., "The Ratio of Terminal Velocity to Minimum Fluidizing Velocity for Spherical Particles," Candian J. Chem. Eng., 46:325-8, Oct. 1968.

(14) Leva, M., "Fluidization," McGraw-Hill, New York, 1959.

(15) Zenz, F. A. and Othmer, D. F., "Fluidization and Fluid-Solids System," Rheinhold Publishing Corp., New York, 1960.

(16) Visits to and discussion with the Pope Evans and Robbins Co., Alexandria, Virginia.

(17) Volk, W., Johnson, C. A. and Statler, H. H., "Effect of Reactor Internals on Quality of Fluidization," Chem. Eng. Prog., 58(3):44-7, 1962.

(18) Wheelock, T. D. and Boylan, D. R., "Sulfuric Acid from Calcium Sulfate," Chem. Eng. Prog., 64(11):87-92, 1968.

(19) Williams, D. F., "Power Station Boilers: Preliminary Costing and Design Considerations," First International Conference on Fluidized Bed Combution, sponsored by NAPCA. Hueston Wood, Ohio, 1968.

(20) Zielki, C. W., Lebowitz, H. E., Struck, R. T. and Gorin, E., "Sulfur Removal During Combustion of Solid Fuels in a Fluidized Bed of Dolomite," Div. of Fuel Chemistry of ACS, 13(4):13-29, 1969.

(21) "SO_2 Removal: Cheaper Process Piloted," C&EN, 46(34):22, 1968.

(22) Ryasan, P. P. and Harkins, J., "Studies on a New Method of Simultaneously Removing SO_2 and NO_x from Combustion Gases," J. Air Pollution Control Assoc., 17(12):796-99, 1967.

(23) Squires, A. M., "Cyclic Use of Calcined Dolomite to Disulfurize Fuels Undergoing Gasification," Advances in Chemistry, Series No. 69, p. 205-229, 1967.

(24) "Sulfur Oxide Removal from Power Plant Stack Gas: Conceptual Design and Cost Study; Sorption by Limestone or Lime; Dry Process," Prepared for NAPCA by TVA. CFSTI:PB-168-972, 1968.

(25) Connor, J. M., "Economics of Sulfuric Acid Manufacture," Chem. Eng. Prog., 64(11):59-65, 1968.

(26) Lang, H. J., "Cost Engineering in the Process Industries," C. H. Chilton, Ed., McGraw-Hill, New York, 1960.

(27) Manderson, M. C., "The Sulfur Outlook," Chem. Eng. Prog., 64(11);47-53, 1968.

(28) "Electric Power: Environment Counts," C&EN, 47(2):12, 1969.

APPENDICES

APPENDIX I

DESULFURIZATION KINETICS, BASIC DATA

Standard Conditions: Bed Temperature, 1600°F; SO_2 inlet conc.,
2700 ppm. Calcination of stones: 6-7 hrs @ 1700°F
Studies Performed in Unit Described in Section 3,
Figure 1

Run	N-	U.S. Mesh	U (ft/sec)	H_o (in.)	Fraction SO_2 in Effluent at Utilization, X, of 0.05	0.10	0.15	0.2	0.25	0.3	0.35	0.4	0.45	0.5	0.6	0.7	0.8	0.9
A - Standard Conditions																		
R-17	1337	16/18	3.2	2				.01		.04		.12		.21	.33	.46	.62	
R-18	1337	16/18	2.1	2								.04		.12	.22	.36	.53	.77
R-23	1337	16/18	3.2	2				.02		.09		.19		.29	.40	.54	.72	.95
R-30	1337	12/14	3.2	2				.17		.34		.46		.565	.66	.76		
R-31	1337	12/14	1.1	2										.03	.15	.31	.50	.71
R-34	1337	16/18	1.9	2				.01		.08		.19		.31	.42	.52	.61	.70
R-35	1337	16/18	1.3	2				.03		.15		.32		.46	.58	.70	.83	
R-36	1337	16/18	6.2	2				.30		.54		.73		.90				
R-38	1337	16/18	2.6	2						.01		.05		.12	.22	.35	.51	.70
R-39	1337	16/18	4.2	2				.03		.10		.19		.29	.39	.50	.62	.73
R-40	1337	16/18	5.1	2				.05		.14		.24		.30	.44	.54	.64	.73
R-41	1337	16/18	6.2	2				.13		.31		.48		.60	.72	.83	.93	
R-46	1359	16/18	1.6	2					.005	.11	.57	.81						
R-47	1359	16/18	2.1	2			.01	.02	.09	.29	.54	.73						
R-48	1359	16/18	3.2	2			.03	.10	.25	.58	.80							
R-49	1359	16/18	4.2	2		.01	.06	.13	.25	.46	.74							
R-50	1359	16/18	5.3	2		.01	.07	.17	.34	.59	.89							
R-51	1359	16/18	6.2	2	.01	.06	.14	.26	.40	.58	.77	.91						
R-52	1359	16/18	3.1	2		.01	.07	.18	.33	.65	.86							
R-54	1359	16/18	4.2	4		.04	.25	.69	.92									
R-61	1359	16/18	4.2	4		.08	.32	.85										
R-62	1359	16/18	4.2	8		.40	.92											
R-63	1359	16/18	4.2	2		.04	.15	.57	.81									
R-64	1359	16/18	4.2	1	.01	.06	.13	.23	.35	.49	.62	.72	.78					
R-65	1359	16/18	4.2	2		.02	.09	.22	.48	.74								
R-66	1359	16/18	4.2	1	.04	.10	.17	.28	.42	.56	.68	.78	.86					

APPENDIX I (Cont'd)

Run	N-	U.S. Mesh	U (ft/sec)	H_o (in.)	Fraction SO_2 in Effluent at Utilization, X, of													
					0.05	0.10	0.15	0.2	0.25	0.3	0.35	0.4	0.45	0.5	0.6	0.7	0.8	0.9
R-67	1337	16/18	4.2	4				.05	.14	.23	.39	.46	.51					
R-68	1337	16/18	4.2	1	.01	.04	.07	.11	.15	.20	.25	.31	.37					
R-72	1359	6/8	4.2	2	.05	.17	.39	.62	.79									
R-73	1359	16/18	4.2	2		.04	.17	.61	.90									
R-74	1359	6/8	4.2				.69	.85										
R-76	1359	6/8	4.2	1	.44	.48	.66	.83										
R-77	1351	6/8	4.2	1	.18	.27	.36	.45	.54	.60	.66	.71	.76					
R-78	1360	6/8	4.2	1	.26	.41	.51	.58	.65	.71	.76	.79						
R-79	1363	6/8	4.2	1	.28	.46	.61	.71	.79	.87	.94							
R-80	1351	6/8	4.2	1	.15	.29	.41	.51	.60	.66	.72	.77	.82					
								Modifications										
B - T=1200°F (Half-Calcined Stone)																		
R-60	1337	14/16	1.7	2	.20	.25	.30	.34	.38	.42	.46	.51	.56					
								(Copper Modified)										
R-44	1337	14/16	1.7	2	.14	.29	.42	.53	.64	.75	.87							
C - T=1600°F (Metal-Doped)								(Nickel)										
R-20	1359	18/25	1.1	2				.40	.95									
								(Aluminum)										
R-26	1359	16/25	1.1	2		.20	.70											
								(Cobalt)										
R-22	1359	18/25	1.1	2			.36	.82										
R-27	1359	16/25	1.1	2		.32	.76											
								(Iron)										
R-25	1359	16/25	1.1	2			.40	.82										
								(Copper)										
R-21	1359	18/25	1.1	2			.04	.26	.68									
R-28	1359	16/25	1.1	2		.01	.13	.53										

APPENDIX I (Cont'd)

Run	N-	U.S. Mesh	U (ft/sec)	H_o (in.)	Fraction SO_2 in Effluent at Utilization, X, of 0.05	0.10	0.15	0.2	0.25	0.3	0.35	0.4	0.45	0.5	0.6	0.7	0.8	0.9
D - Temperature Effects				T=1500°F														
R-45	1359	4/10	4.0	2	.32	.77	.93											
J-129	1359	25/50	2.0	3.2					.01	.34	.74							
				T=1413°F														
J-122	1359	25/50	2.0	3.2				.03	.12	.32								
				T=1400°F														
R-81	1359	6/8	3.8	1	.52	.61	.70	.80										
				T=1250°F														
R-82	1359	6/8	3.5	1	.66	.75	.87											
E - Particle Size																		
R-14	1337	16/25	1.1	2											.15	.51	.79	
R-29	1337	20/25	1.1	2								.08		.24	.43	.67		
A-37	1337	40/50	0.5	4											.02			
A-38	1337	70/100	0.5	4													.02	
A-39	1337	140/170	0.5	3													.00	.10
A-47	1359	50/100	0.5	3											.15			

APPENDIX II

REDUCTIVE REGENERATION BASIC DATA

Basic representative data on reduction of sulfated particles, followed by absorption of SO_2 from flue gas, are presented in this section.

A. Desulfurization in unit described in Section 3(D)
Regeneration in unit described in Section 5 (R)
Material: $MgSO_4$, 50/100 Mesh, H_o = 6 in.

Run	Temperature (°F)	Gas Composition	$[SO_2]_{(Max)}$ %	X $(20\% SO_2 \frac{Out}{In})$
A-15R	1600	10% H_2/90% N_2	7.6	
A-16R	1600	10% CO/90% N_2	8.9	
A-17R	1400	10% CO/90% N_2	11.3	
D	1350	Simulated Flue Gas		0
A-18R	1300	10% CO/90% N_2	8.3	
D	1350	Simulated Flue Gas		0
A-21R-1	1500	10% H_2/20% H_2O/70% N_2	9.1	
R-2	1500	20% CO/20% CO_2/60% N_2	17.3	
A-23R-1	1700	5% H2/95% N2	6.8	
R-2	1700	10% H_2/90% N_2	10.0	
R-3	1700	10% H_2/5% CO/15% N_2	11.9	
D	1350	Simulated Flue Gas		0.005

B. Desulfurization in unit described in Section 3(D)
Regeneration in unit described in Section 5 (R)
25/50 Mesh $CaSO_4$ (anhydrite) particles
Fluidizing Gas 2/1 CO_2/CO or H_2O/H_2; bal. N_2; H_o = 6" in Reg., 3" in Desulf. (initially).

Run	Cycle	Temperature (°F)	Gas Composition	$[SO_2]_{(Max)}$ %	X $(20\% SO_2 \frac{Out}{In})$
A-37R-1		2060	10% CO	7.3	
R-2		2060	20% CO	9.3	
A-38R-1		2060	10% H_2	8.7	
R-2		2060	15% H_2	10.3	
D		1600	Flue Gas		0.55
A-39R-1		2160	10% CO	6.6-7.3	
R-2		2160	15% CO	8.6-9.5	
D		1600	Flue Gas		0.31
A-40R-1		1960	10% CO	6.3-7.3	
R-2		1960	15% CO	8.1-9.6	
D		1600	Flue Gas		0.44
A-41R-1		1960	10% H2	8.4-8.7	
R-2		1960	15% H_2	9.9-10.2	
D		1600	Flue Gas		0.47

APPENDIX II (Cont'd)

Run	Cycle	Temperature (°F)	Gas Composition	$[SO_2]_{(Max)}$ %	$X\left(20\%\ SO_2\ \frac{Out}{In}\right)$
A-43R-1		1860	10% H_2	5.2-6.0	
R-2		1860	15% H_2	6.6-6.9	
D		1600	Flue Gas		0.42
A-44R-1		1960	10% CO	5.7-6.7	
R-2		1960	15% CO	8.0-9.6	
A-45R-1	1	2060	10% H_2	8.6	
R-2		2060	15% CO	9.3	
D-1		1600	Flue Gas		0.48
R-2	2	2060	10% CO	8.0	
D-2		1600	Flue Gas		0.20
R-3	3	2060	10% CO	8.3	
D-3		1600	Flue Gas		0.17
R-4	4	2060	10% CO	8.4	
D-4		1600	Flue Gas		0.127
R-5	5	2000	10% CO	8.6	
D-5		1600	Flue Gas		0.114
R-6	6	2000	10% CO	8.2	

C. Desulfurization in unit described in Section 3 (D)
Regeneration in unit described in Section 5 (R)
U = 2 ft/sec, H_o = 8 in; 2/1 CO_2/CO; Material 25/50 Mesh N-1337

Run	Cycle	Temperature (°F)	Gas Composition	$[SO_2]_{(Max)}$ %	$X\left(20\%\ SO_2\ \frac{Out}{In}\right)$
J-58D	1	1600	Flue Gas		0.45
R		2000	8.1% CO	8.2	
J-59D	2	1600	Flue Gas		0.212
R		2000	8.1% CO	7.6	
J-62D	3	1600	Flue Gas		0.154
R		2000	8.1% CO	8.0	
J-68D	4	1600	Flue Gas		0.175
R		2000	10% CO	9.1	

D. Desulfurization, Regeneration in one unit;
U = 3 ft/sec; Material 25/50 N-1337,
Preattrited at U = 6 ft/sec for 6 hr.

Run	Cycle	Temperature (°F)	Gas Composition	$[SO_2]$ (Max) %	$X\left(20\%\ SO_2\ \frac{Out}{In}\right)$
J-60D	1	1600	Flue Gas		0.35
R		2000	8.1% CO	7.8	
J-61D	2	1600	Flue Gas		0.151
R		2000	8.1% CO	8.1	
U = 2 ft/sec H_o = 6 in, Calcined Dolomite, N-1337					
J-74D	1	1600	Flue Gas		0.525
R		2000	10% CO	8.7	
J-75D	2	1600	Flue Gas		0.720
R		2000	10% CO	8.8	

APPENDIX II (Cont'd)

E. Desulfurization, Regeneration in unit described in Section 5.
$U = 2$ ft/sec, $H_o = 8.1$ in, 2/1 CO_2/CO,
Material 25/50 lime (N-1359)

F. Regeneration of particles with pure H_2/N_2 feed mixtures, followed by N_2/O_2 mixtures to oxidize CaS. 25/50 Mesh, N-1359 Lime.

Run	Temperature (°F)	Feed Gas Composition (excluding N_2)	$[SO_2]_{(Max)}$% (Minus H_2O), Effluent
Fluidized Bed			
J-131R-1	2000	25% H_2	7.2
		(with O_2 overhead to react with H_2S	10.1
R-2	2000	15.5% O_2	8.2
Packed Bed			
J-135R-1	2000	10% H_2	3.5 (includes oxidized H_2S)
R-2	2000	16% O_2	4.8
J-136R-1	2000	9.2% H_2	2.8
			3.6 (includes oxidized H_2S)
R-2	2000	9.2% H_2, 2.3% SO_2	0
R-3	2000	16% O_2	7.0

APPENDIX III

ERROR ANALYSIS - DESULFURIZATION TO $CaSO_4$ FORMATION

The amount of SO_2 sorbed by the lime particles from the flue gas was calculated from infrared detector monitoring and from weight gain of the particles. The following runs were chosen to determine any difference between the methods.

SUMMARY, WEIGHT DIFFERENCE DEPENDENCE ON ANALYSIS PROCEDURE

Run	Z, Chart - Weight (gms SO_3/155 gm bed)	Z^2
R-18	+4.6	21.2
-23	+2.2	4.4
-30	-0.6	0.4
-31	-2.7	7.3
-34	+4.2	17.7
-35	+7.0	49.0
-36	-10.5	111.0
-38	+9.2	84.7
-39	+13.3	177.5
-41	-8.2	67.2
-46	+5.3	28.2
-47	+11.6	135.0
-48	+5.4	29.2
-49	+12.7	162.0
-50	+9.5	90.5
-51	+3.0	9.0
-52	+5.5	30.3
-54	+9.4	88.5
-61	+5.7	32.6
-62	+4.5	20.3
-63	+6.8	46.3
-65	+10.6	112.5
-66	+9.8	96.0
-67	+10.8	117.0
-68	+15.0	225.0
-72	-8.5	72.2
-73	+1.5	2.2
-77	+11.4	130.6
-79	-5.8	33.7
-80	+8.0	64.0
n=30	+150.7	2,165.0

Then a statistical analysis gives:

$\bar{Z} = +5.02,$

$\%\bar{Z} = 3.2,$

Standard Deviation, $S = \sqrt{\frac{\Sigma Z^2}{n} - (\bar{Z})^2} = 6.85$

$\%S = 4.5$

This difference is significant, as at 95% confidence limits (using Studentized statistics):

$$\text{Deviation} = Z \pm t_{.05} \frac{S}{\sqrt{n-1}} = 3.2 \pm 1.7\%$$

APPENDIX IV

EQUILIBRIUM PREDICTIONS OF POSSIBLE REACTIONS IN DESULFURIZATION

A typical flue gas contains about 15 vol. % CO_2, 1-10% H_2O, (for coal, oil), 3% O_2 and 0.15 to 0.30% SO_2. Possible reactions that might occur can be obtained from equilibrium calculations. Here we shall only consider whether an individual reaction should proceed or not.

IV-1. Hydroxide Formation

Displacement of carbonate by water vapor to form hydroxides should not occur as the amount of CO_2 in the flue gas is large enough to prevent displacement by H_2O at all temperatures up to the carbonate dissociation temperatures, i.e., reaction 1, is always displaced to the left.

$$CaCO_{3(s)} + H_2O_{(g)} \rightleftharpoons Ca(OH)_{2(s)} + CO_{2(g)} \qquad (1)$$

IV-2. Carbonate Dissociation

The carbonates dissociate as follows:

$$CaCO_{3(s)} \overset{\Delta}{\rightleftharpoons} CaO_{(s)} + CO_{2(g)} \qquad (2)$$

The dissociation pressure, P_{CO_2}, will increase with temperature as shown in Figure A-1. Whenever the prevailing flue gas partial pressure of CO_2 is greater than the equilibrium P_{CO_2}, CaO formation will be inhibited. At approximately 1450°F for $CaCO_3$ and 680°F for $MgCO_3$, the P_{CO_2} will equal the partial pressure of CO_2 in the flue gas. Further heating will liberate CO_2 with the attendant oxide formation. It was noted by Battelle (6) that the dissociation temperature of the magnesium carbonate constituent of the dolomite was slightly higher than that of pure magnesium carbonate (730°F vs. 680°F). This temperature difference is caused by the weak chemical bonding of the carbonates in the dolomite as illustrated by Equation 3:

$$CaCO_3 \cdot MgCO_{3(s)} \rightleftharpoons CaCO_3 \cdot MgO_{(s)} + CO_{2(g)} \qquad (3)$$

Such bonding will also affect the magnesium carbonate reactions described in later sections. Since these predictions are based on a pure magnesium carbonate reactant, it should be recognized that the results will be slightly modified for bonded magnesium carbonates.

Figure A-1

Equilibrium CO_2 Pressures for $MgCO_3$ and $CaCO_3$ Dissociation

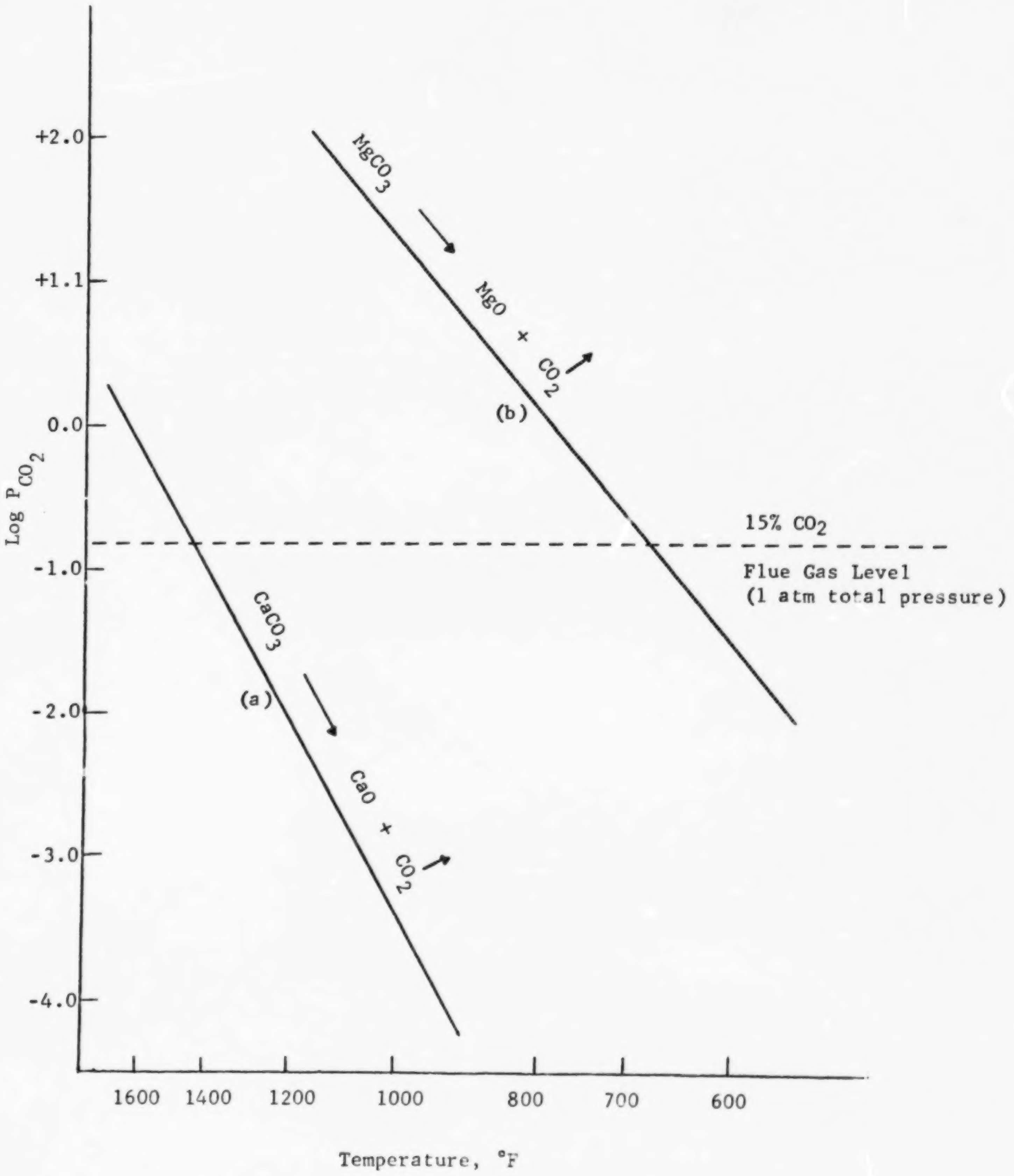

Once the oxides are formed from the carbonates, they will not react with the water vapor in the flue gas according to Equation (4). The hydroxide dissociation temperature is 400°F for $Mg(OH)_2$ and 720°F for $Ca(OH)_2$. Below these temperatures, the results of Section IV-1 are applicable, and Equation (1) is driven to the left.

$$CaO_{(s)} + H_2O_{(g)} \rightleftharpoons Ca(OH)_{2(s)} \tag{4}$$

From these observations, it is apparent that the CO_2 and H_2O levels present in flue gases permit dolomite materials to exist only as carbonates or as oxides. Magnesium and calcium carbonates dissociate at approximately 680°F and 1450°F respectively, under a "usual" flue gas CO_2 partial pressure equal to 0.15 atmospheres.

IV-3. SO_2 Reactions in the Carbonate Phases

Magnesium and calcium carbonates are each capable of forming sulphites and sulphates with the SO_2 in the flue gas below their dissociation temperatures.

IV-3.1. Sulphite Formation

SO_2 can directly displace the CO_2 in the carbonates to form the sulphites.

$$CaCO_{3(s)} + SO_{2(g)} \rightleftharpoons CaSO_{3(s)} + CO_{2(g)} \tag{5}$$

Figure A-2 indicates that these displacement reactions will proceed at temperatures less than 840°F for the $CaCO_3$ and 460°F for the $MgCO_3$ when the SO_2 concentration is at a 0.25% level. However, with 90% of the SO_2 removed from the flue gas, the maximum allowable temperatures for these reactions become 570°F and 320°F, respectively.

Equation 5 moves to the right even though the CO_2 concentration in the flue gas is assumed to be 600 times greater than the SO_2 concentration (15 vol. % CO_2, .025% SO_2). This occurs because SO_2 is far more acidic than CO_2. Since the displacement of a weak acid with a strong acid can be expected to be exothermic, the reaction should proceed at low SO_2 concentrations at lower temperatures. Figure A-2 shows that this expectation is correct.

Once the sulphites are formed they have a strong tendency to become oxidized to the sulphates by the low (0.1 - 5%) oxygen concentration in the flue gas as shown in Figure A-3. However, at relatively low temperatures their reaction rates could be relatively slow.

IV-3.2. Sulphate Formation

The SO_2 and O_2 concentrations in the flue gas can jointly displace the CO_2 in the carbonates to form directly the sulphates according to the equation:

$$CaCO_{3(s)} + SO_{2(g)} + 1/2\ O_2 \rightleftharpoons CaSO_{4(s)} + CO_{2(g)} \tag{6}$$

Figure A-2

CONVERSION OF CALCIUM AND MAGNESIUM CARBONATES TO THEIR SULPHITES AT A CO_2 PARTIAL PRESSURE EQUAL TO 0.15 ATMOSPHERES*

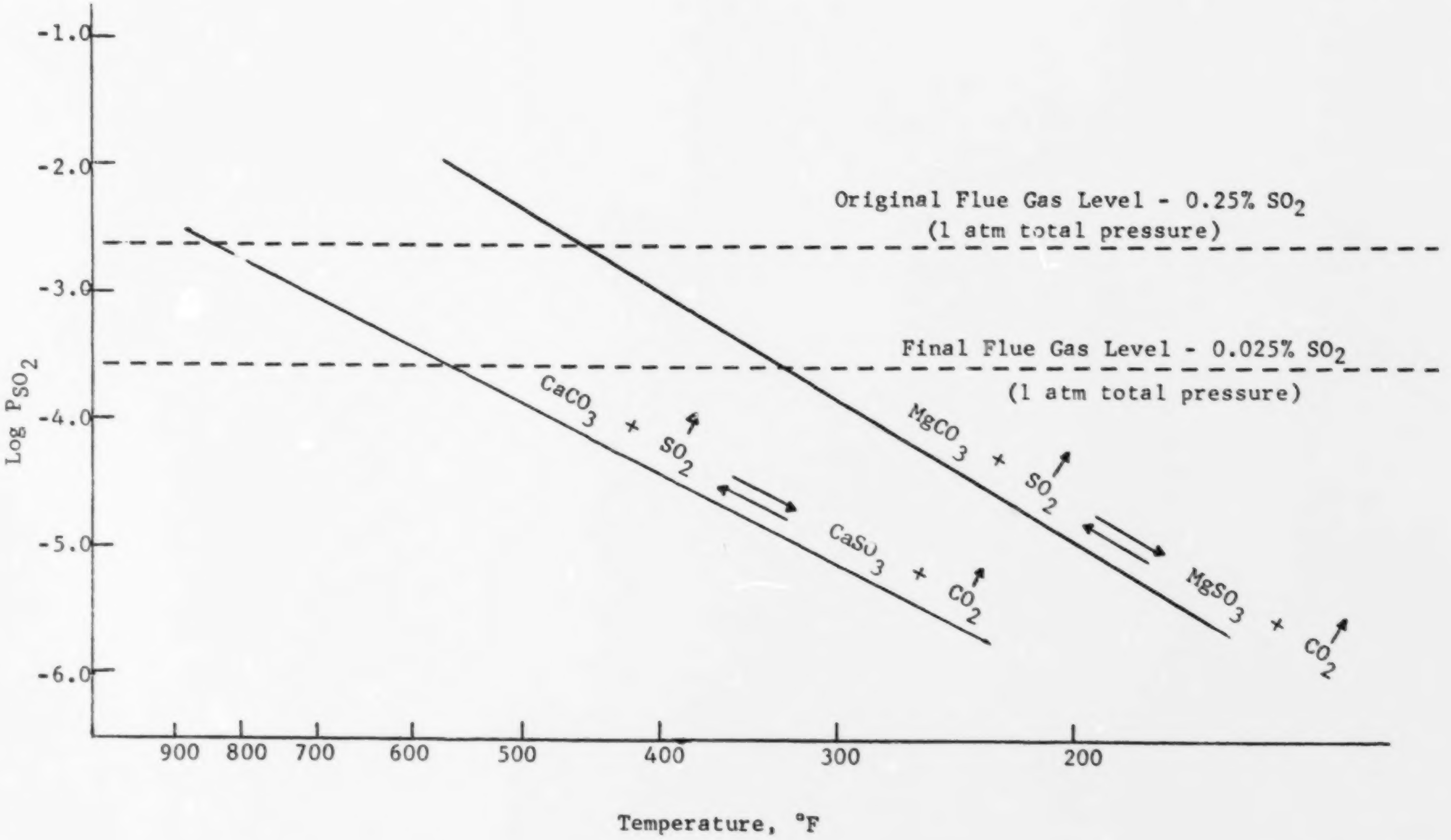

---

*Calculations given by Erdos, E., Collection Czechoslov. Chem. Commun, 27, 2152 (1962).

Figure A-3

Equilibrium O_2 Pressures Required for the Oxidation of Sulfites to Sulfates

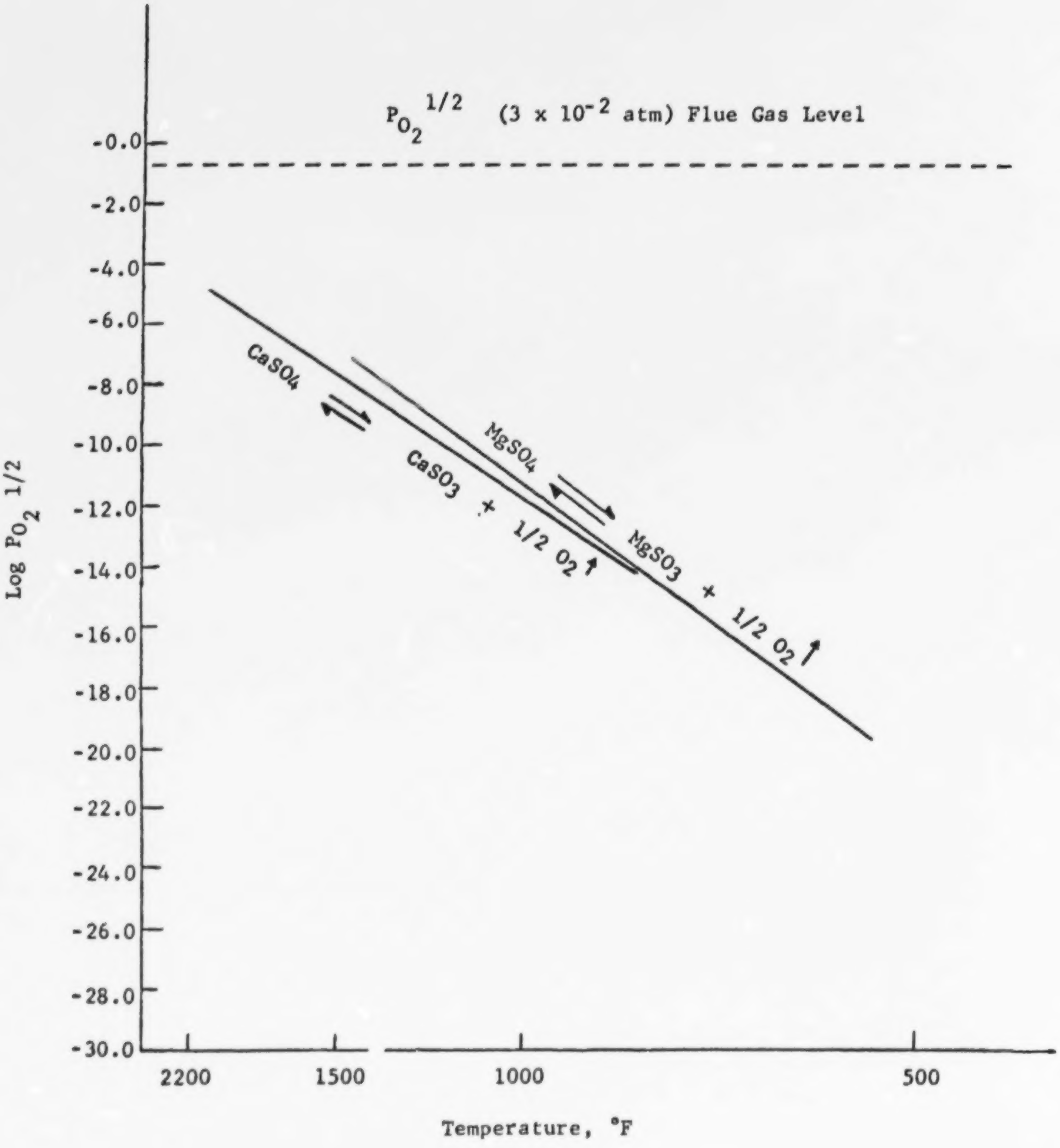

Figure A-4

THE EQUILIBRIUM PARTIAL PRESSURES OF SO_2 AND O_2 FOR SULFATE FORMATION FROM MAGNESIUM AND CALCIUM CARBONATES

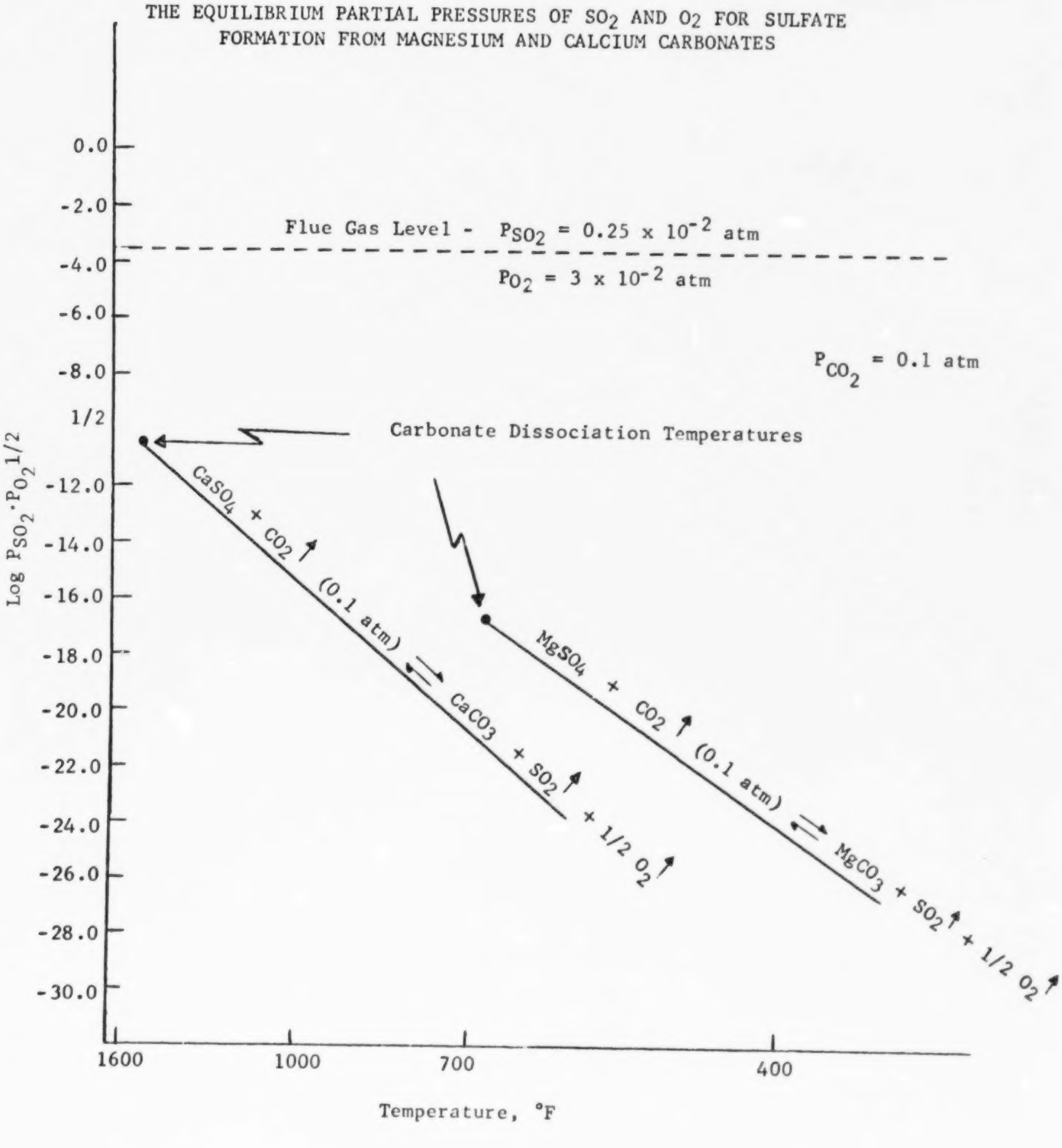

Figure A-5

THE EQUILIBRIUM PARTIAL PRESSURES OF SO_2 AND O_2 FOR MAGNESIUM AND CALCIUM SULFATE DECOMPOSITION REACTIONS*

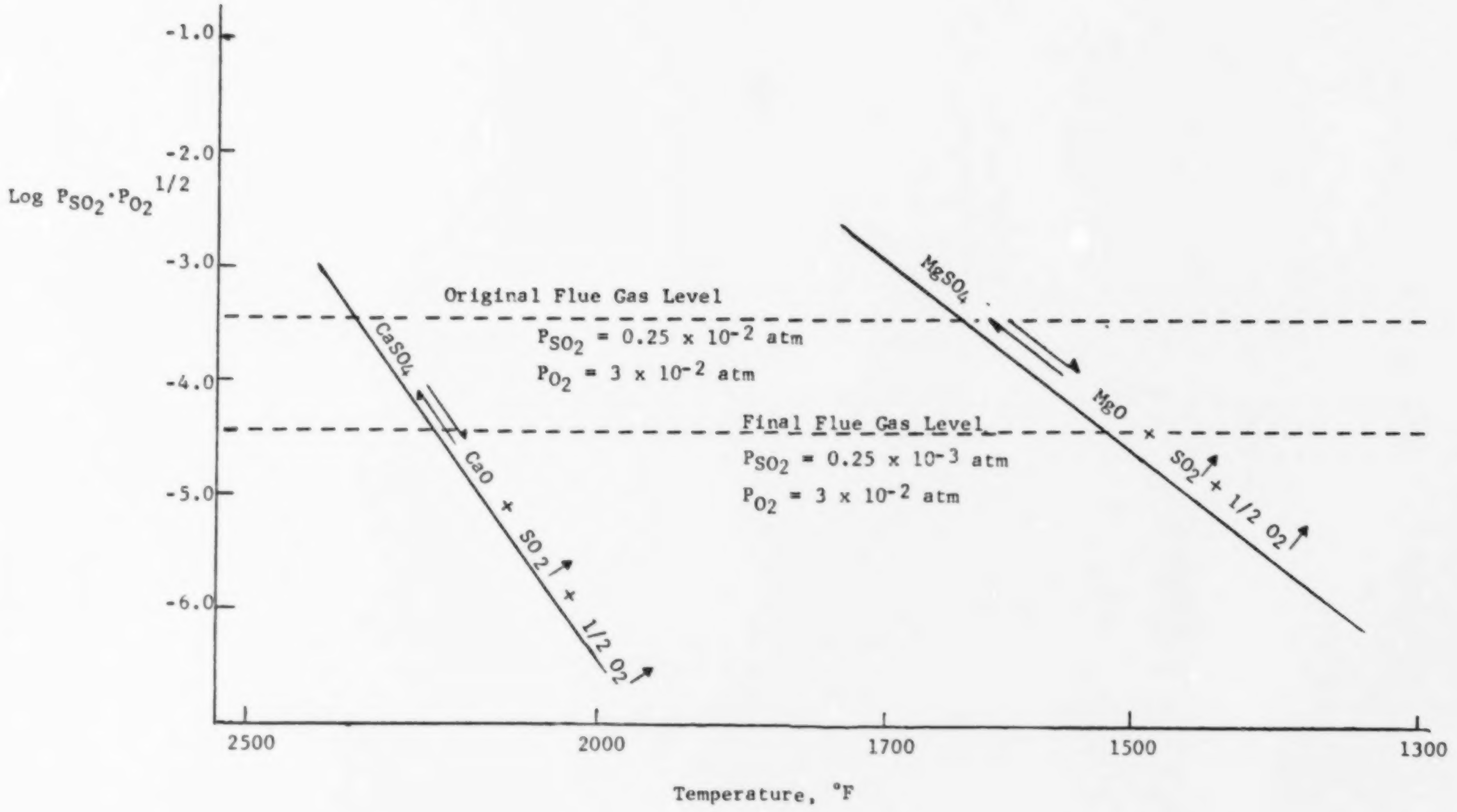

---

*Data taken from Dewing, E. W., and Richardson, F. D., Trans Faraday Soc. 55, 611-15 (1959).

As indicated in Figure A-4, the partial pressure product $P_{SO_2} \cdot P_{O_2}^{1/2}$ is sufficiently high in the furnace to permit these conversions to occur at temperatures up to the dissociation temperatures of the carbonates.

IV-4. SO_2 Reaction in the Oxide Phase

SO_2 and O_2 can similarly react with the oxides to form the sulphates according to the equation:

$$CaO_{(s)} + SO_{2(g)} + 1/2\ O_{2(g)} \rightleftharpoons CaSO_{4(s)} \qquad (7)$$

Figure A-5 shows that when 90% of the SO_2 has been removed the partial pressure product $P_{SO_2} \cdot P_{O_2}^{1/2}$ in the flue gas is still sufficiently high to cause sulphate formation at temperatures up to 2200°F for CaO and 1500°F for MgO. At temperatures lower than the carbonate dissociation temperatures (680°F for $MgCO_3$ and 1450°F for $CaCO_3$) some of the oxides would form intermediate carbonates and sulfites which would then be converted to sulphates as described in Section IV-3.

IV-5. Summary of Reaction Regions

Table A-1 lists possible reactions which could take place in desulfurization over the various temperature ranges from 200°F to 2000°F.

TABLE A-1

POSSIBLE REACTIONS FOR THE OXIDES AND CARBONATES OF MAGNESIUM AND CALCIUM IN FLUE GASES FROM 200°F TO 2000°F

Possible Reaction	Temperature Range
$CaCO_3 + SO_2 \longrightarrow CaSO_3 + CO_2$	200°F - 570°F
$CaSO_3 + 1/2\ O_2 \longrightarrow CaSO_4$	200°F - 2000°F+
$CaCO_3 + SO_2 + 1/2\ O_2 \longrightarrow CaSO_4 + CO_2$	200°F - 1450°F
$CaO + SO_2 + 1/2\ O_2 \longrightarrow CaSO_4$	1450°F - 2000°F
$MgCO_3 + SO_2 \longrightarrow MgSO_3 + CO_2$	200°F - 320°F
$MgSO_3 + 1/2\ O_2 \longrightarrow MgSO_4$	200°F - 2000°F+
$MgCO_3 + SO_2 + 1/2\ O_2 \longrightarrow MgSO_4 + CO_2$	200°F - 680°F
$MgO + SO_2 + 1/2\ O_2 \longrightarrow MgSO_4$	680°F - 1500°F

APPENDIX V

GIBBS FREE ENERGY OF FORMATION OF RELEVANT SPECIES

The free energies used in calculating equilibria constants and compositions in Section 4.1 and Appendix V are listed below. The basic reference for this data is "JANAF Thermochemical Data," Dow Chemical Co., Midland, Michigan, supplemented by Wheelock and Boylan (see Reference 9).

FREE ENERGY OF FORMATION VARIATION WITH TEMPERATURE

ΔG_f° (kcal/mole)

Compound @ °K	500	600	700	800	900	1000	1100	1200	1300	1400	1500	1600
°F	440	620	800	980	1160	1340	1520	1700	1880	2060	2240	2420
CO	-37.14	-39.31	-41.47	-43.61	-45.74	-47.96	-49.96	-52.05	-54.13	-56.19	-58.24	-60.28
CO_2	-94.40	-94.46	-94.51	-94.56	-94.60	-94.63	-94.66	-94.68	-94.70	-94.72	-94.73	-94.74
CS	34.60	30.79	27.07	22.12	19.95	17.79	15.64	13.50	11.37	9.25	7.14	5.04
CS_2	8.41	5.04	1.84	-3.85	-4.01	-4.16	-4.33	-4.48	-4.64	-4.80	-4.96	-5.11
COS	-43.73	-45.59	-47.36	-50.37	-50.62	-50.86	-51.10	-51.35	-51.59	-51.83	-52.07	-52.30
CH_4	-7.85	-5.49	-3.05	-0.53	2.03	4.63	7.25	9.89	12.54	15.20	17.86	20.52
H_2O	-52.36	-51.16	-49.92	-48.65	-47.35	-46.04	-44.71	-43.37	-42.02	-40.66	-39.38	-37.93
H_2S	-9.60	-10.13	-10.54	-12.16	-11.01	-9.84	-8.67	-7.49	-6.31	-5.13	-3.95	-2.77
S_2	11.81	8.58	5.53	----------	----------	----------	----------	0	----------	----------	----------	----------
SO_2	-71.92	-71.79	-71.56	-72.57	-70.82	-69.07	-67.33	-65.58	-63.84	-62.10	-60.37	-58.64
SO_3	-84.31	-81.92	-79.44	-78.41	-74.23	-70.26	-66.31	-62.36	-54.43	-54.50	-50.59	-46.69
S_2O	-24.90	-26.59	-28.10	-32.09	-30.55	-29.02	-27.50	-25.97	-24.45	-22.93	-21.41	-19.89
MgO	-130.76	-218.19	-125.62	-123.06	-120.51	-117.78	-115.00	-112.22	-109.44	-106.18	-101.20	-96.25
$MgCO_3$	-232.28	-235.68	-219.14	-212.66	-206.25	-199.72						
$Mg(OH)_2$	-184.53	-177.30	-170.12	-163.02	-155.99	-148.86						
MgS	-80.48	-79.68	-78.78	-79.13	-76.70	-74.08	-71.41	-68.73	-66.05	-62.89	-58.01	-53.15
$MgSO_3$		-201.07	-194.33									
$MgSO_4$	-255.506	-246.09	-236.65	-228.52	-217.69	-206.76	-195.85	-185.01	-174.24	-163.06	-150.24	-137.52
CaO	-138.25	-135.80	-133.35	-130.90	-128.50	-126.05	-123.60	-121.05	-118.45	-115.05	-113.30	-110.70
$CaCO_3$		-249.96	-243.96	-238.01	-232.16	-226.18	-220.36	-214.36	-208.45	-201.77	-196.73	-190.84
$Ca(OH)_2$		-191.76	-184.77	-177.85								
CaS		-115.00	-112.54	-110.01	-107.60	-105.30	-102.00	-100.50	-98.00	-94.00	-93.00	-89.60
$CaSO_3$		-238.79	-231.51	-225.47	-216.72	-207.97	-199.63	-191.18	-182.64	-173.35		
$CaSO_4$		-291.00	-280.10	-269.10	-258.50	-248.00	-236.60	-227.05	-216.75	-205.05	-199.90	-186.30

APPENDIX VI

RESIDENCE TIME AVERAGING FOR THE EFFECTIVE RATE CONSTANT IN A FLUIDIZED BED

The analysis of the reaction of SO_2/O_2 with limestone in the fluid bed reactor has thus far been limited to consideration of a very specific idealized flow pattern, namely plug flow. Real reactors never fully satisfy the flow requirements of such idealized models. Deviations from ideality can be caused by channeling of the fluid through the vessel, by recycling of fluid within the vessel, or by the existence of stagnant regions of fluids in the vessel. The experimental data obtained in our laboratory data showed evidence of a large deviation from ideality, which was treated by assigning a contacting factor which related the actual performance of the reactor to that which would have been expected under conditions of ideal flow of the fluid.

The prediction of the performance of the commercial desulfurization reactor will also be very dependent on how ideal the flow distribution is at the velocity and bed height used. Lacking sufficient information to estimate the ideality of flow in the commercial unit, the following prediction of the commercial unit performance will be limited to considering the maximum performance that can be expected. This assumes ideal flow conditions and the applicability of the plug flow model used in analysis of the laboratory reactor data. This approach is equivalent to setting the contacting factor used in analyzing the laboratory reactor data at unit value. This assumption is clearly incorrect, but does serve to establish the limiting case for performance of the commercial unit.

Since it is not possible to attain complete knowledge about the commercial reactor system, let us be less ambitious and ask how we can at least describe the system adequately enough to yield information useful in the design of the unit. The commercial unit, unlike the laboratory reactor, will be in a dynamic state as far as solids entering and leaving the reactor.

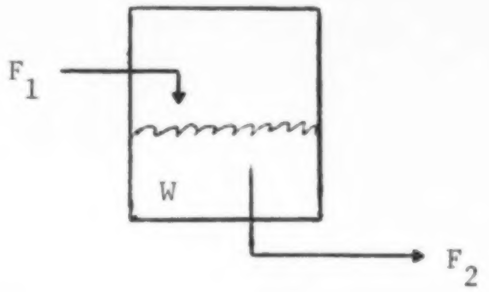

Where F_1 = feed rate of uncalcined stone to the reactor - lb moles/hr

F_2 = removal rate of sulfated product - lb moles/hr

W = bed hold up - lb/moles

The feed and removal rates, F_1 and F_2, are adjusted to maintain a uniform quantity of material, W, in the fluidized bed. The backmixing of solids which occurs in the fluid bed results in an age distribution for the solids, i.e., the solid particles being removed from the bed in the overflow stream F_2 have been in the bed for various lengths of time. This variation in the residence time of the solids is of course reflected in their degree of CaO utilization.

The kinetic data obtained in Section 3.3. presented the reaction rate constant as a function of particle utilization, X. In order to use this rate information it is necessary to know how the utilization of the particle changes with the time the particles are in the bed, (the particle age or particle residence time θ).

Assume an increment of fresh particles of weight, W, added to this fluid bed at time $\theta = 0$. The rate of SO_2 uptake by these particles is

$$+\frac{dN_{SO_2}}{d\theta} = r \cdot W \cdot C_{SO_2} \qquad (8)$$

Where N_{SO_2} = amount of SO_2 (mass)

θ = time particle is in bed

r = rate of SO_2 uptake per unit mass of particles

C_{SO_2} = average SO_2 concentration seen by particles.

At steady state, C_{SO_2} is constant during the residence time of the particles at some average between SO_2 in and SO_2 out.

Expressing equation (8) in terms of the rate constant **k**

$$+\frac{dN_{SO_2}}{d\theta} = \frac{k(X)}{\rho_s} \; W \cdot C_{SO_2} \qquad (9)$$

Here ρ_s = bulk density of solid and k has been written k(X) to indicate that it is a part of the particle utilization (X).

The particle utilization X is the fraction of SO_2 uptake compared to the SO_2 capacity of the charge.

$$X = \frac{\text{wt } SO_2 \text{ uptake}}{\text{capacity for } SO_2} = \frac{N_{SO_2}}{W \cdot \alpha} \qquad (10)$$

where α = mass capacity of SO_2 per unit mass of stone.

Differentiating equation (10)

$$dX_B = \frac{dN_{SO_2}}{W \cdot \alpha} \qquad (11)$$

Substituting eq. (11) into eq. (9) and separating variables,

$$\frac{dX}{k(X)} = \frac{\overline{C}_{SO_2}}{\rho_s \alpha} \cdot d\theta \qquad (12)$$

On integration between X=0 and X at time θ, we obtain after rearrangement:

$$\int_0^X \frac{dX}{k(X)} = \frac{C_{SO_2}}{\rho_s \cdot \alpha} \theta \qquad (13)$$

The integral in eq. (13) is done numerically to various values of X and the particle residence time to obtain that X given by:

$$\theta = \frac{\text{(area under the curve from } X=0 \text{ to } X) \cdot \rho_s \cdot \alpha}{\overline{C}_{SO_2}} \qquad (14)$$

A logarithmic mean concentration for C_{SO_2} is the appropriate averaged concentration.

In order to predict the limiting performance of the commercial unit it is necessary to know the age distribution of the reacting solids. It has been found that the following particle age distribution function, I(θ), is quite accurate for perfectly mixed solids*.

$$I(\theta) = \frac{1}{\overline{\theta}} \exp(-\theta/\overline{\theta}) \qquad (15)$$

Here $\overline{\theta}$ is the average particle residence time defined as

$$\overline{\theta} = \frac{W}{F} \qquad (16)$$

and θ is the particle residence time.

---

*E. B. Nauman and C. N. Collinge, Chem. Eng. Sci. 23, 1317 (1968).

The analysis of the reaction rate constant presented earlier showed that the rate constant, $k(X)$, depended on the degree of CaO utilization, X. The degree of CaO utilization, X, for a particle injected into the fluid bed reactor was shown above to depend on the length of time the particle was in the reactor, θ. These considerations suggest that the reaction constant, $k(X)$ for a given sorbent particle will depend on the time that this particle has been in the reactor. The expression for this dependence of the rate constant on the particle residence time, $k(\theta)$, can readily be obtained from the expressions previously determined for the dependence of the rate constant on the degree of CaO utilization, $k(X)$, and the dependence of the degree of CaO utilization on the particle residence time $X(\theta)$.

The desulfurization performance for the commercial reactor will be made up of the contribution of all the particles in the fluid bed, each with its own particular residence time. The average rate constant for the commercial reactor, k, is obtained by integrating the product of the expressions for the variation of rate constant with particle residence time, $k(\underline{\theta})$, and the age distribution for the particles, $I(\underline{\theta})$ over all values of particle residence time, θ.

$$\overline{k} = \int_0^\infty k(\theta)\cdot I(\theta)\, d\theta \qquad (17)$$

This expression is solved numerically.

The desulfurization performance can now be calculated, using the rate expression previously described for the plug flow reactor model, by specifying the operating parameters

$$C' = \frac{C_H}{C_O} = \exp\left(-\overline{k}\cdot Y\cdot \frac{H_\Omega}{U}\right) \qquad (18)$$

where the contacting factor, Y, is the factor representing the departure from ideal flow conditions in the commercial reactor.

The overflow stream from the fluid bed, F_2, contains, as mentioned earlier, a wide distribution of particle ages, each with a degree of CaO utilization dependent on its history in the bed. An analysis similar to that used above leads to an expression for the average CaO utilization, X, in the commercial reactor.

$$\overline{X} = \int_0^\infty X(\theta)\cdot I(\theta)d\theta \qquad (19)$$

APPENDIX VII

ECONOMIC EVALUATION FOR A ONCE THROUGH FLUID BED LIMESTONE DESULFURIZATION PROCESS USING SMALL PARTICLES

A coal-fired, 800 MW power plant burning a 3% sulfur fuel was selected as the basis for evaluating a fine particle fluid bed desulfurization process. Process designs were based on experimental data obtained with the N-1337 dolomite. The designs call for operating the bed at about 1600°F and fine-grinding the dolomite before charging it to the fluid bed. Under these conditions, our experiments show that calcination will be rapid and active sorbent will be produced. The use of fines necessitates a once through system, as fly ash could not be separated from the sulfated dolomite, which would render a regenerative system inoperable.

Economic evaluations have been made for several cases designed to remove 80% of the SO_2 from the flue gas while utilizing about 85% of the CaO portion of the dolomite (the CaO represents about 28 wt% of the uncalcined dolomite for N-1337).

The best design from a combined engineering and cost standpoint consisted of a 73 foot diameter bed operating at a 24 ft/sec superficial velocity and using 60 to 100μ particles. Four stages of cyclones are used; pressure drop through the system is estimated at 48" H_2O.

A high superficial gas velocity was chosen to keep bed size down. Nevertheless, a large fluid bed must be used to handle the huge volume of flue gas generated by the 800 MW plant (85 x 10^6 SCFH). At these high velocities, there would be virtually total solids entrainment by the gas passing through the reactor. A minimum of three, preferably four, stages of cyclones would be required to collect these solids and return them to the bed. These cyclones are necessarily quite large to handle the huge volume of flue gas. The designs call for eight primary cyclones (each of which is 22 ft in diameter) discharging into 24-secondary cyclones (each of which is 12 ft in diameter) which in turn discharge into 72 tertiary cyclones (each of which is 8 ft in diameter). Taken together, the investment for these cyclones constitutes about 45% of the total investment.

Four large induced draft fans are needed to overcome the added pressure drop of the desulfurization system. With these fans discharging into the bottom of the stack at a positive pressure, the pressure in the fluid bed itself would be lower than atmospheric.

TABLE A-2

ECONOMIC EVALUATION OF FINE PARTICLE FLUIDIZED BED DESULFURIZER FOR 800 MW POWER PLANT

Investment	Cost
Desulfurizer (includes Foundation)	$ 7,722,000
Ducts	400,000
Induced Draft Fans, Buck Stags	1,270,000
Feed and Disposal System	770,000
Limestone Crusher	300,000
Total	$10,462,000
Contigency Fees	3,650,000
Working Capital	529,000
Total	$14,641,000

Yearly Operating Costs	60% Load Factor	90% Load Factor
Capital Charges (14% Investment)	$2,050,000	$2,050,000
Plant Maintenance	732,000	732,000
Labor and Supervision	80,000	83,100
Payroll Overhead	32,000	33,000
Plant Overhead	407,000	407,000
Power	603,000	905,000
Fuel	7,000	10,000
Limestone	657,000	980,000
Thermal Effect	0	-10,000
Total	$4,624,000	$5,273,000
$/Ton coal	$2.90	$2.20

For the hetero-reactor system, assuming a one-foot settled bed height can achieve 90% desulfurization with stoichiometric sorbent addition, the cost savings shown below would be obtained for a 800 MW plant.

	Total Annual Cost Savings, $ With a 90% Load Factor
Capital Charges (fans and drives)	41,000
Power Cost (to overcome ΔP)	140,000
Maintenance Charge	14,000
	$195,000 (8¢/Ton Coal Burned)

APPENDIX VIII

FLUIDIZED BED DESULFURIZATION PROCESS DETAILS

VIII-1. Costing Procedures

Criteria used to estimate purchase prices or on-site construction costs of special process equipment are listed below. Using Lang's factors as outlined in the text section 6, the final direct cost of construction was obtained from these prices.

TABLE A-3

PURCHASE PRICE ESTIMATION PROCEDURES

Item	Method
Process Equipment-Installed Costs	
1. Steel Shells	a. $1.00/lb carbon steel
	b. $1.80/lb stainless steel
2. Insulation	a. $20/ft² for 9" thick insulation - 6" firebrick, 3" ceramic
	b. $15/ft³ firebrick
3. Grid	a. 25¢/stamped, snap-in gas inlet button
	b. $27/ft² grid surface area - for vertical rods to deter bubble growth
Process Equipment-Purchase Price	
1. Electrostatic Precipitator	$1.50/CFM gas throughput
2. Heat Exchangers	Chem. Eng. News Cost Files, Jan '58
3. Compressors, Pumps, Fans	
a. Small Units	Chem Eng News Cost Files, Jan '61
b. Large Fans	Direct Manufacturer Estimates

VIII-2. Unusual Equipment - Details, 200 MW Plant, Regenerative Process

VIII-2.1. Desulfurizer

Specifications: 3/8" thick steel shell, 50' overall height; insulation protection of shell and grid underside against fly-ash impingement - 6" firebrick, 3" ceramic undercoating; 48.5 ft I.D. fluid bed x 15' shell height; 70' ft I.D. disengaging section x 12' shell height; tapered body to duct work; 1" thick stainless steel grid, with 750 gas inlet buttons (appr. 1" dia)/ft^2 grid surface area, supported by girders for strength.

Maximum Flow Conditions: Limestone particles, 1000-5000μ fed at 3 tons/hr; 90 x 10^6 ACFH flue gas @ 1600°F; U superficial = 15 ft/sec in bed, $U_{superficial}$ = 7.2 ft/sec in disengagement section, U = 150 ft/sec in inlet ports; $H_o \sim 15$ inches; $\Delta P \sim 20$ inches H_2O.

VIII-2.2. Ducts

Specifications: 3/8" thick steel shell with insulation protection, 17' x 17' square ducts connecting boiler with the absorber; length 150'.

Maximum Flow Conditions: U_{gas} =100 ft/sec @ 1600°F.

VIII-2.3. Regenerator

Specifications: 3/8" thick steel shell, 35' overall height, 10.5' I.D.; insulation protection of shell as in absorber; 3' firebrick arch grid perforated with straight bore holes; 6.2 ft diameter cyclones with return tubes (design, 20-86 in Perry's Chem. Eng. Handbook). Multiple particle downcomers, 1 ft^2 flow area

Maximum Flow Conditions: 6.6×10^5 SCFH @ 2000°F, reducing gas, $U \doteq 11$ ft/sec; 3.8 tons coal/hr partially combusted with air to yield 10% CO/H_2, 20% CO_2/H_2O gas; $H_o = 3$ feet; $\Delta P = 42$ inches H_2O; recirculate 0.17 $CaSO_4/CaO$ into bed at 42 tons/hr, send out 0.05 $CaSO_4$-CaO (for 3.5% sulfur coal boiler feed).

VIII-2.4. Induction Fans

Specifications: 2 fans to overcome pressure drop through desulfurization reactor, handling 34×10^6 ACFH gas. At 65% machine efficiency, 2600 horsepower to the motors is required.

VIII-3. Unusual Equipment - Details, 1000 MW Plant, Regenerative Process

VIII-3.1. Desulfurizers

Five units, each of specifications and flows described in VIII-2.1.

VIII-3.2. Ducts

Specifications: One conduit, 38' x 38', insulated, 3/8" thick shell, to connect to boiler at each end of absorbers; five ducts, 17' x 17', split from this conduit to carry flue gas to the absorbers; total length of small ducts, 900 ft.

Maximum flow conditions: $U_{gas} \sim 100$ ft/sec @ 1600°F.

VIII-3.3. Regenerator

Specifications: 3/8" thick steel shell, 24' I.D., 40' overall length; 4' firebrick arch grid, perforated with gas inlet holes, 8' diameter cyclones.

Maximum flow conditions: 33×10^5 SCFH @ 2000°F reducing gas, $U \doteq 11$ ft/sec, 19 tons coal/hr partially combusted with air to yield 10% CO/H_2, 20% CO_2/H_2O gas; $H_o = 3$ feet, $\Delta P = 42$ inches H_2O; recirculate 210 tons/hr of $CaSO_4$-CaO.

VIII-3.4 Induction Fans

Specifications: 2 fans to overcome pressure drop, handling 170×10^6 AFCH gas.

Unclassified

Security Classification - This Page

DOCUMENT CONTROL DATA - R & D

(Security classification of title, body of abstract and indexing annotation must be entered when the overall report is classified)

1. ORIGINATING ACTIVITY *(Corporate author)* Esso Research & Engineering Company P.O. Box 8 Linden, New Jersey 07036	2a. REPORT SECURITY CLASSIFICATION Unclassified 2b. GROUP

3. REPORT TITLE
Fluidized Bed Studies of the Limestone-Based Flue Gas Desulfurization Process

4. DESCRIPTIVE NOTES *(Type of report and inclusive dates)*
Summary Report - May 15, 1967 - August 27, 1969

5. AUTHOR(S) *(First name, middle initial, last name)*
Alvin Skopp, John T. Sears, Rene R. Bertrand

6. REPORT DATE August, 1969	7a. TOTAL NO. OF PAGES 114	7b. NO. OF REFS 28
8a. CONTRACT OR GRANT NO. PH 86-67-130 b. PROJECT NO. c. d.	9a. ORIGINATOR'S REPORT NUMBER(S) GR-9-FGS-69 9b. OTHER REPORT NO(S) *(Any other numbers that may be assigned this report)*	

10. DISTRIBUTION STATEMENT
Distribution of this report requires prior approval of the National Air Pollution Control Administration

11. SUPPLEMENTARY NOTES	12. Sponsoring Activity Process Control Engineering Program National Air Pollution Control Administration

13. ABSTRACT

A conceptual design of a fluidized bed flue gas desulfurization process has been developed based on the ability of coarse lime particles to react with and remove SO_2 from combustion flue gases in a fluidized bed. Reduction of the sulfated lime particles formed in such a process has been demonstrated to provide reactivated particles. These particles can again react with the sulfur dioxide in a flue gas to form sulfates. The effluent from reduction has a high SO_2 concentration and is suitable for the production of sulfuric acid. Thus, a cyclic, regenerative flue gas desulfurization process can be envisioned that produces a saleable by-product to offset processing costs.

Experiments were performed to determine and improve the reactivity of different limestone and dolomitic sorbents in a fluidized bed, and to define conditions for regeneration of the sorbents. A conceptual design of a system was formulated from these data. A coarse particle, high-gas-velocity fluidized bed operating at 1600°F was the basis of the best design. Regeneration was carried out with a producer-type gas at about 2000°F. Preliminary economics indicated that the system was not applicable in presently operating boilers but a grass-roots power plant might operate competitively. However, other general considerations, such as the large size and location of the equipment in the boiler train, make a commercial process appear unlikely in its present form. Adaption of this process to fluidized bed combustion schemes is quite promising, and future process development should proceed in this direction.

ESSO **1473**

Unclassified

Security Classification - This Page